

CRANFIELD UNIVERSITY

Sotiria D. Psoma

**A proof of concept of a BioMEMS glucose biosensor
using microfabricated SU-8 films**

CRANFIELD HEALTH

MSc by Research Thesis

Academic year: 2009 - 2010

Supervisor: Prof. A.P.F. Turner

December 2009

CRANFIELD UNIVERSITY

CRANFIELD HEALTH

MSc by Research Thesis

Academic Year: 2009 - 2010

Sotiria D. Psoma

**A proof of concept of a BioMEMS glucose biosensor
using microfabricated SU-8 films**

Supervisor: Prof. A.P.F. Turner

December 2009

This thesis is submitted in partial fulfillment of the requirements
for the degree of Master of Science by Research

© Cranfield University 2009. All rights reserved. No part of this publication may be
reproduced without the written permission of the copyright owner.

ABSTRACT

The present project investigated and proved the concept of developing a novel BioMEMS glucose micro-biosensor using a simple one-step microfabrication process of the widely used SU-8 polymer. More specifically, the study focused on the investigation of the suitability of the SU-8 polymer as a matrix for enzyme immobilisation that is carried out during the microfabrication process. A comparative study between commercially available SU-8 and “customised” SU-8 solutions showed that the optimum concentration of photo-initiator for stress reduction can be achieved easier with “customised” SU-8 solutions. The most appropriate type of microstructure for the SU-8 matrix and the corresponding required microfabrication process were defined and encapsulation of the enzyme GOx in the SU-8 solution was accomplished. A detailed experimental investigation of the immobilised enzyme’s activity inside the SU-8 matrix, was carried out using amperometric detection of hydrogen peroxide in a 3-electrode set-up. SU-8 films were immersed in a buffer solution and the platinum working electrode was brought in close contact with the film. Films without enzyme showed negligible variation in current upon the addition of glucose, as opposed to films with encapsulated enzyme which showed a very clear increase in current. Experiments using films of increased thickness or enzyme concentration, showed a higher response, thus proving that the enzyme remained active not only on the film’s surface, but inside the matrix as well. In the fluorescence spectroscopy experiments, the utilisation of the tris (4,7-diphenyl-1,10-phenanthroline) ruthenium(II) dichloride oxygen indicator, which was also captured in the polymer matrix during the microfabrication process, was proven to be very sensitive to glucose concentration changes during the glucose oxidation and there was no photo-bleaching.

The experimental investigations proved that the proposed concept of using SU-8 matrices for the immobilisation of biomolecules, is a valid proposal for the construction of a BioMEMS glucose biosensor. An important outcome was the successful immobilisation of glucose oxidase in SU-8 microfabricated structures. The enzyme still showed activity despite the “hostile” conditions during microfabrication. The proof of principle of enzyme immobilisation in SU-8 films opens up new possibilities for combining BioMEMS with biosensors and organic electronics.

“Προς ζωήν αγαθήν, ή παιδεία και ή αρετή μάλιστα άγουσιν”

“The education and the exercise of virtue, above all, lead to an honest life”

Aristotle (384 BC – 322 BC)

Dedicated to my husband Antonios and to my daughter Anna.

ACKNOWLEDGMENTS

I would like to express my sincerest gratitude to my supervisor Professor Anthony P.F. Turner for his invaluable suggestions, personal interest, encouragement and support throughout all stages of this research programme. Without his guidance, this research programme would not have reached its final form.

I wish to acknowledge the support that I have received from Mr Gareth Derbyshire from Rutherford Appleton Laboratory for providing me with the opportunity to use the clean room facilities for part of my experimental work.

I am grateful to Professor Nico F. de Rooij from IMT, EPFL, in Switzerland, for his generosity of offering to me access to all necessary facilities of his Laboratory in Neuchatel, his advice, full support and constant interest for this project.

A special thank goes to Dr Peter van der Wal from IMT, EPFL, for his constant assistance, support, advice, and his tireless discussions on the project.

I acknowledge the Swiss National Science Foundation (SNF) for the financial support of part of the experimental work of this project (International Exchange Programme - IZK0Z2-124260).

Finally, this work is dedicated to my husband Antonios and my daughter Anna, as an expression of my deep gratitude for their constant support, love, encouragement, patience and for sharing all the hard times with me throughout the period of this study.

TABLE OF CONTENTS

	Page Number
ABSTRACT	i
ACKNOWLEDGEMENTS	iii
TABLE OF CONTENTS	iv
LIST OF FIGURES	vii
LIST OF TABLES	x
GLOSSARY	xi
CHAPTER 1 – INTRODUCTION	1
1.1 Background	1
1.2 Fabrication and structure of BioMEMS	3
1.3 BioMEMS and biosensors	4
1.4 Motivations and objectives of the current research project	7
1.5 Structure of the thesis	10
CHAPTER 2 - LITERATURE REVIEW	11
2.1 SU-8 polymer	11
2.1.1 General	11
2.1.2 Properties of SU-8	12
2.1.3 SU-8 biocompatibility	16
2.2 BioMEMS applications using SU-8 polymer	16
2.3 BioMEMS / Biosensors	21
2.3.1 General	21
2.3.2 Problems with biosensors	24
2.3.3 BioMEMS/glucose biosensors: recent developments	25
2.4 BioMEMS/biosensors using SU-8 polymer: recent developments	30
2.5 BioMEMS/biosensors using SU-8 polymer: latest immobilisation techniques	35
2.6 Outline summary of the literature review	38

	Page Number
CHAPTER 3 – GENERAL MATERIALS AND INSTRUMENTATION	40
3.1 Materials	40
3.2 Instrumentation	41
3.3 Properties of SU-8 polymer	42
3.3.1 Commercially available SU-8 composition	42
3.3.2 Chemical properties	43
3.3.3 Physical properties	44
3.3.3.1 Mechanical properties	44
3.3.3.2 Optical properties	46
3.3.3.3 Electrical properties	46
3.3.4 Preparation of “customised” SU-8 solutions	47
3.4 Outline of the experimental work	48
CHAPTER 4 – INVESTIGATION INTO THE MICROFABRICATION PROCESS OF “CUSTOMISED” SU-8 FILMS	50
4.1 SU-8 microfabrication processing	50
4.1.1 Introduction	50
4.1.2 Microfabrication steps	51
4.1.3 Pretreatment of the silicon wafers – sacrificial layers	52
4.1.4 Spin-coating of SU-8	52
4.1.5 Soft bake – prebake	53
4.1.6 UV – exposure	54
4.1.7 Post-exposure bake	55
4.1.8 Development	56
4.2 Influence of photo-initiator concentration on residual mechanical stress in SU-8 films	57
4.2.1 Introduction	57
4.2.2 Experimental setup	57
4.2.3 Influence on the SU-8 films due to soft-bake temperature	58

	Page Number
4.2.4 Influence on the SU-8 films due to UV-exposure	59
4.2.5 Influence of the percentage of the photo-initiator on SU-8 films	61
4.2.6 Influence on the SU-8 films due to post-baking process	62
4.2.7 Influence of the addition of nanoparticles on the SU-8 films	62
4.2.8 Sacrificial layers for releasing SU-8 films	64
4.2.9 Conclusions from the SU-8 stress experiments	66
4.3 Experimental procedures for the preparation and microfabrication of SU-8 films for glucose biosensor application	67
4.3.1 Specific SU-8 composition	67
4.3.2 Specific microfabrication process of optimum SU-8 films	69
4.3.3 Enzyme and fluorescent indicator immobilisation in SU-8 films	72
CHAPTER 5 – EXPERIMENTAL INVESTIGATION FOR THE PROOF OF CONCEPT OF THE SU-8 GLUCOSE BIOSENSOR	74
5.1 Introduction	74
5.2 Characterisation of SU-8 films with immobilised enzyme GOx	75
5.3 Amperometric measurements of SU-8 films with immobilised enzyme	80
5.3.1 Enzymatic Reaction	80
5.3.2 First Experimental Set-up	81
5.3.3 Second Experimental Set-up	86
5.4 Fluorescence intensity measurements of SU-8 films with immobilised enzyme and fluorescent indicator	89
CHAPTER 6 – GENERAL CONCLUSIONS AND SUGGESTIONS FOR FUTURE WORK	97
6.1 Conclusions	97
6.2 Suggestions for future work	100
REFERENCES	102

LIST OF FIGURES

	Page Number
Figure 1.1	Research areas of BioMEMS applications. 2
Figure 1.2	Diagram of the biosensor principle. 6
Figure 1.3	Key detection modalities used in BioMEMS and biochips sensors. 6
Figure 2.1	Molecular structure of EPON SU-8. Monomer and monomer unit in the cross linked polymer (<i>Genolet, 2001</i>). 12
Figure 2.2	Microfabrication process steps of SU-8 (<i>source: http://www2.mic.dtu.dk/research/bioprobes/SU8/SU8-Material.htm</i>). 14
Figure 2.3	Conceptual diagram of the biosensors/biochips principle. 23
Figure 3.1	(a) Protolysis of the triaryl sulfonium hexafluorantimonium which generates an acid that induces the cross linking. (b) Opening of the epoxy group and reaction propagation (<i>Genolet, 2001</i>). 43
Figure 3.2	Young's modulus against temperature for a model polymer. Tg is the glass transition temperature (<i>Bower, 2002</i>). 45
Figure 4.1	Schematic diagram of the processing steps for SU-8. 51
Figure 4.2	Selective SU-8 spin-speed versus film thickness curves. 53
Figure 4.3	Calibration curves of exposure dosage versus film thickness of SU-8 films. 55
Figure 4.4	Variations of the measured stress as a function of the exposure time for different thickness of 40/60 SU-8 with 10% photoinitiator UV1. 59
Figure 4.5	Variations of the measured stress as a function of the exposure time for different thickness of 40/60 SU-8 with 5% photoinitiator UV1. 60
Figure 4.6	Interferometer images of the surface topology for 40/60 SU-8 film with 2.5% photo-initiator (a) after the softbake at 75 °C (compressive stress) and (b) after the exposure time of 40s (tensile stress). 60
Figure 4.7	Variations of the measured stress as a function of the exposure time for three different concentrations photo-initiator UV1 of the 40/60 SU-8 resist. 61
Figure 4.8	Variations of the measured stress as a function of the postbaking temperature for four different concentrations of the photo-initiator

UV1 of the 40/60 SU-8 resist.	62
Figure 4.9 Interferometer images of surface topology of the 40/60 SU-8 film (a) Film thickness map, (b) planar and 3-D surface topology	63
Figure 4.10 Undercutting of SU-8 structures using as sacrificial layer with: (a) dextran solution 5%, (b) PMMA, (c) Polystyrene, (d) Al, (e) Cr and (f) Cu.	65
Figure 4.11 (a) “Customised” SU-8 solutions without adding the photoinitiator, (b) resulted SU-8 films/structures.	69
Figure 4.12 Basic microfabrication process of “customised” SU-8.	70
Figure 4.13 Temperature profile of prebake and post-exposure microfabrication steps of SU-8 films (aprox. 5.5 μ m) (40/60 SU-8 film with 2.5% photo-initiator).	71
Figure 4.14 Final SU-8 films/structures.	71
Figure 5.1 Interferometer images of plain SU-8 films (prepared from one week matured solution prior to film microfabrication) (a) 3-D image, and (b) planar image.	76
Figure 5.2 Interferometer 3-D images of two different plain SU-8 films (prepared from two weeks matured solution prior to film microfabrication).	76
Figure 5.3 Interferometer images of surface topography of SU-8 films: (a) 3-D view, and (b) planar view of plain SU-8 film; (c) 3-D view, and (d) planar view of GOx (5mg) loaded SU-8 film; (f) 3-D view, and (e) planar view of GOx (10mg) loaded SU-8 film.	77
Figure 5.4 Comparison of SEM pictures of surface topography of (a) plain SU-8 films (magnification: 2313x) and (b) SU-8 films with immobilised enzyme (magnification: 1920x).	78
Figure 5.5 SEM pictures of surface topography of (a) plain SU-8 films (magnification: 18502x); (b) SU-8 films with immobilised enzyme (magnification: 30720x).	79
Figure 5.6 SEM pictures of surface topography of SU-8 films with immobilised GOx in two different regions (magnification: 30720x).	79
Figure 5.7 Amperometric experimental set-up.	81

Figure 5.8	Measurement glass cell for the first experimental set-up.	82
Figure 5.9	SU-8 films without immobilised GOx with added glucose.	83
Figure 5.10	SU-8 films with immobilised GOx during oxidation (average film thickness 5.7 μ m).	84
Figure 5.11	SU-8 films with immobilised GOx during oxidation after 1 week from the first measurement (average film thickness 5.7 μ m).	84
Figure 5.12	SU-8 films (2.4 μ m) with immobilised GOx.	85
Figure 5.13	SU-8 films (4,2 μ m) with immobilised GOx.	85
Figure 5.14	SU-8 films (8.8 μ m) with immobilised GOx.	86
Figure 5.15	Measurement glass cell for the second experimental set-up.	87
Figure 5.16	Amperometric measurements using SU-8 films with similar thickness and different GOx concentrations. Glucose concentration is increased from 0 to 10 mM in the first part of the graph. Stirring is stopped every 6 minutes.	88
Figure 5.17	Amperometric measurements using SU-8 films with stirring-independent values, effect of SU-8 film's thickness (similar GOx). At t=0, 10mM glucose is added.	89
Figure 5.18	Fluorescence spectra using SU-8 films with immobilised GOx only.	92
Figure 5.19	Fluorescence spectra using SU-8 films with immobilised GOx and oxygen sensitive fluorescent indicator.	92
Figure 5.20	Fluorescence spectra using SU-8 films with immobilised GOx and pH indicator.	93
Figure 5.21	Fluorescence spectra using SU-8 films (thickness: 2.4 μ m) with immobilised GOx and Oxygen indicator.	94
Figure 5.22	Fluorescence spectra using SU-8 films (thickness: 5.5 μ m) with immobilised GOx and Oxygen indicator.	95
Figure 5.23	Fluorescence spectra using SU-8 films (thickness: 8.8 μ m) with immobilised GOx and Oxygen indicator.	95

LIST OF TABLES

Page Number

Table 3.1	Physical Properties of SU-8 Photoresist	45
Table 3.2	Chemical compositions for preparing SU-8 resists with different percentages of photo-initiator.	48
Table 4.1	Sacrificial materials used and their etchants.	64

GLOSSARY

BioMEMS	Biomedical or Biological Micro-Electro-Mechanical Systems
CAD	Computer-Aided Design
CNTs	Carbon NanoTubes
CV	Cyclic Voltammetry
DI	DeIonised water
DNA	DeoxyriboNucleic Acid
DPV	Differential Pulse Voltammetry
DWCNT	Double Wall Carbon NanoTubes
EDX	Electron Diffraction X-ray
ELISA	Enzyme Linked Immunosorbent Assay
FeLV	Feline Leukemia Virus
FIV	Feline Immunodeficiency Virus
GBL	γ -butyrolactone
GOx	Glucose Oxidase
HBM	Human Breast Milk
HPTS	8-HydroxyPyrene-1,3,6-TriSulfonic acid trisodium salt
IPA	IsoPropyl Alcohol
LOC	Lab-On-Chip
MZI	Mach-Zehnder Interferometer
MEMS	Micro-Electro-Mechanical Systems
MWCNT	Multi-Wall Carbon NanoTubes
MWNTs	Multi-Walled Carbon NanoTubes
PANI	Polyaniline
PBS	Phosphate Buffer Solution
PDMS	PolyDiMethylSiloxane
PEGDA	PolyEthylene Glycol DiAcrylate
PGMEA	Propylene Glycol Methyl Ether Acetate
PMMA	PolyMethylMethAcrylate (Acrylic)
PPy	Polymer Polypyrrole
RF	Radio Frequency

RLS	Resonance Light Scattering
SAMs	Self-Assembled Monolayers
SEM	Scanning Electron Microscope
TEM	Transmission Electron Microscopy
UV	Ultra Violet
VLSI	Very-Large-Scale Integration
XPS	X-ray Photoelectron Spectroscopy
μ TAS	micro-Total Analysis Systems

CHAPTER 1

INTRODUCTION

1.1 Background

Researchers and scientists working in the fields of Micro-Electro-Mechanical Systems (MEMS) and microfabrication technologies have experienced an exciting and productive period during the last decade. Starting from the earliest devices in electromechanical transducers, such as pressure sensors and accelerometers, which are among the most commercially successful MEMS devices and systems, the technologies have undergone a very fast expansion into many different fields of engineering, physical sciences and biomedicine.

In recent years, one of the most exciting progresses in MEMS technology is the rapid evolution of Biomedical or Biological Micro-Electro-Mechanical Systems (BioMEMS). In general, BioMEMS are defined as systems or devices which are constructed using nano- or microfabrication methods, and are used for the analysis, delivery, processing, or for the development and construction of chemical and biological entities (Bashir, 2004). This is a scientific area that has attracted significant research interest and has found a broad spectrum of biomedical applications. In addition to basic components for flow management at microscopic volumes, such as microchannels,

micropumps, microvalves, micromixers and microreactors, various novel sensor and detection platforms have been published in the fields of microfluidics and Bio-MEMS. Many lab-on-a-chip systems or micro-total analysis systems (μ TAS) have been proposed, and these offer new paradigms in biomedicine and biology, in particular the capability of performing point-of-care measurements. The word BioMEMS is currently used in a very wide manner and also incorporates other devices without any electro-mechanical parts, such as protein and DNA arrays.

A graphical representation of the key research areas evolving from the combination of life sciences and biomedical specialities with nano- and microsystems, is illustrated in Figure 1.1. The research fields appearing on the left are application areas of nano- and microsystems to biochemical and biomedical problems and the research areas on the right are biological applications to nano- and microsystems.

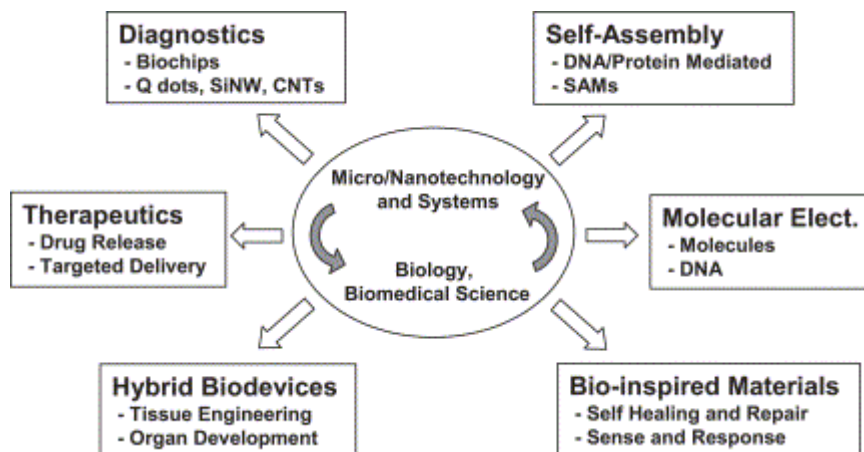


Figure 1.1 Research areas of BioMEMS applications (Bashir, 2004)

The advantages of such systems are the micro-volumes of biological or biomedical samples that can be delivered, processed and analysed in an integrated fashion, the dramatic reduction of the required human involvement in sample handling and processing, and the improvement of data quality. This format also facilitates the reduction of overall cost and measurement time and in parallel it improves the sensitivity and specificity of the analysis.

Consequently, Bio-MEMS is a technological field which includes more than simply developing new biomedical or biochemical applications for existing or new MEMS systems. It constitutes a new platform for an expansion into new polymer materials, microfluidic physics, surface chemistry and modification, “soft” fabrication techniques (including polymers and biological components), biocompatibility and cost-effective solutions to biomedical problems. It brings together the expertise and creativity of most engineering disciplines such as mechanical, electrical, materials and optical, with the experience of physicians and clinical laboratory scientists. BioMEMS devices are the platform upon which nano-medicine will be delivered for the improvement of the human condition. It is also the quintessential science for genomics, the study of sets of genes, gene products and their interactions, and proteomics, the study of proteins, the expression of genes in health and disease.

1.2 Fabrication and Structure of BioMEMS

Traditional fabrication techniques previously transferred from the manufacturing of integrated circuits to MEMS devices underwent yet another transition when they were applied to BioMEMS devices, with an improved physical understanding of microfluidics and of the surface science of silicon, polymers, glass and ceramics. Surface modification for biochemical or biomedical assays and biocompatibility has emerged as a complex science, with abundant opportunities for creating novel techniques and applications. New micro-manufacturing processes are evolving for moulding, replication, casting and bonding that are essential for mass production with reproducibility and functional reliability at low cost, both of which are crucial to the market of medical disposables.

Fabrication process steps are becoming more complex as integrated electronics, or recently developed organic electronics, are now becoming intergrated with microreactor chambers in monolithic devices. In addition, packaging for safety and biocompatibility poses a significant challenge for the BioMEMS engineer.

Three types of materials can be used for the fabrication of BioMEMS devices. These are: firstly, materials which are used in microelectronics and MEMS such as silicon, glass etc.; secondly, polymeric and plastic materials such as SU-8, PDMS, etc.; and, finally, biological materials such as cells, tissues and proteins.

In terms of size, BioMEMS devices typically have at least one or more of their dimensions in the range of microns or submicrons (about 100 nm to 200 μm), and the remaining dimensions in the range of several millimeters. On one end of the application scale they may be the platform for nanotechnologies, while on the other end they may be the key component in a much larger device, such as a medical imaging machine. They may have external or self-contained power supplies and operate *in vitro* or *in vivo* (outside or inside a living system). They may have integrated microprocessors (*smart systems*), and operate as either an open-ended (biosensor, sensor or actuator) or a closed-loop system (autoregulators). More typically they are integrated with other components (biochips) and perform one or more functions in a chain of operations connected by tubing or other conduits, or they may be all encompassing devices. Implanted devices may be part of a distributed system that provides continuous information from various parts of the body to a central medical device.

Among the main advantages of biochip miniaturisation are small size, reagent use, reproducibility and lower cost of manufacturing as compared to conventional bioelectronics devices. Additional advantages of miniaturised biochips are improved response time and signal-to-noise ratio, accurate mixing control, reacting and discarding of waste products, in-line or embedded detection methods and high throughput.

1.3 BioMEMS and Biosensors

The largest segment of BioMEMS which has attracted the highest level of research is represented by diagnostic applications. In the last decade, a significant and continuously growing number of publications related to newly developed BioMEMS devices have

appeared in the literature covering a wide range of design and fabrication approaches and also areas of application. “Biochips” are usually BioMEMS devices aimed for use in diagnostic applications. Combinations of biochips and biosensors were developed for biochemical and medical applications in parallel with significant progress in these technological areas during the last two decades.

In terms of definition, biosensors are analytical devices which incorporate either: a biological material such as a tissue, microorganism, organelle, cell receptor, enzyme, antibody or nucleic acid; a biologically derived material, for example recombinant antibody, engineered protein or aptamer; a biomimic such as a synthetic catalyst, combinatorial ligand or imprinted polymer. Furthermore, the recognition element should be intimately associated with, or integrated within, a physicochemical transducer or transducing microsystem, which may be electrochemical, optical, thermometric, piezoelectric, magnetic or micromechanical (Turner *et al.*, 1989; Turner, 2005). Biosensors usually produce a digital electronic signal which can be related to the concentration of a specific analyte or group of analytes. In Figure 1.2, a schematic layout of the basic principles of a biosensor is illustrated. Biosensors have been developed for utilisation in a wide variety of sectors including drug discovery, medicine, food, environment, process industries, defence and security.

During the last decade, BioMEMS and devices have been used as biosensors and the resulting biochips can allow sensitive, rapid and real time measurements. These BioMEMS type of biosensors can be employed in order to detect cells, proteins, DNA, or small molecules such as lactate, glucose, glutamate, etc. (Ainslie & Desai, 2008, Giouroudi *et al.*, 2008). Many detection methods are employed in BioMEMS biochips and biosensors, including electrical, optical, mechanical, etc. A detailed diagram of these detection methods is presented in Figure 1.3.

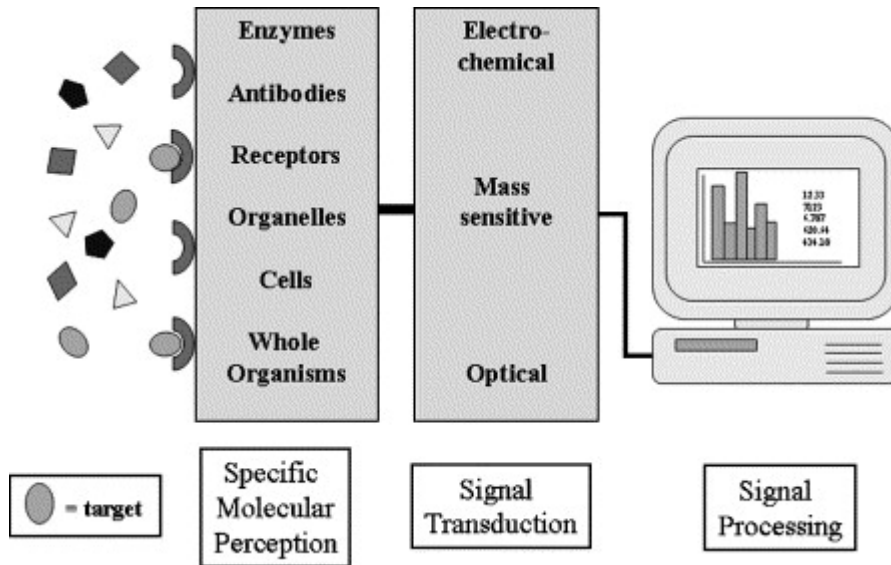


Figure 1.2 Diagram of the biosensor principle (Nakamura & Karube, 2003)

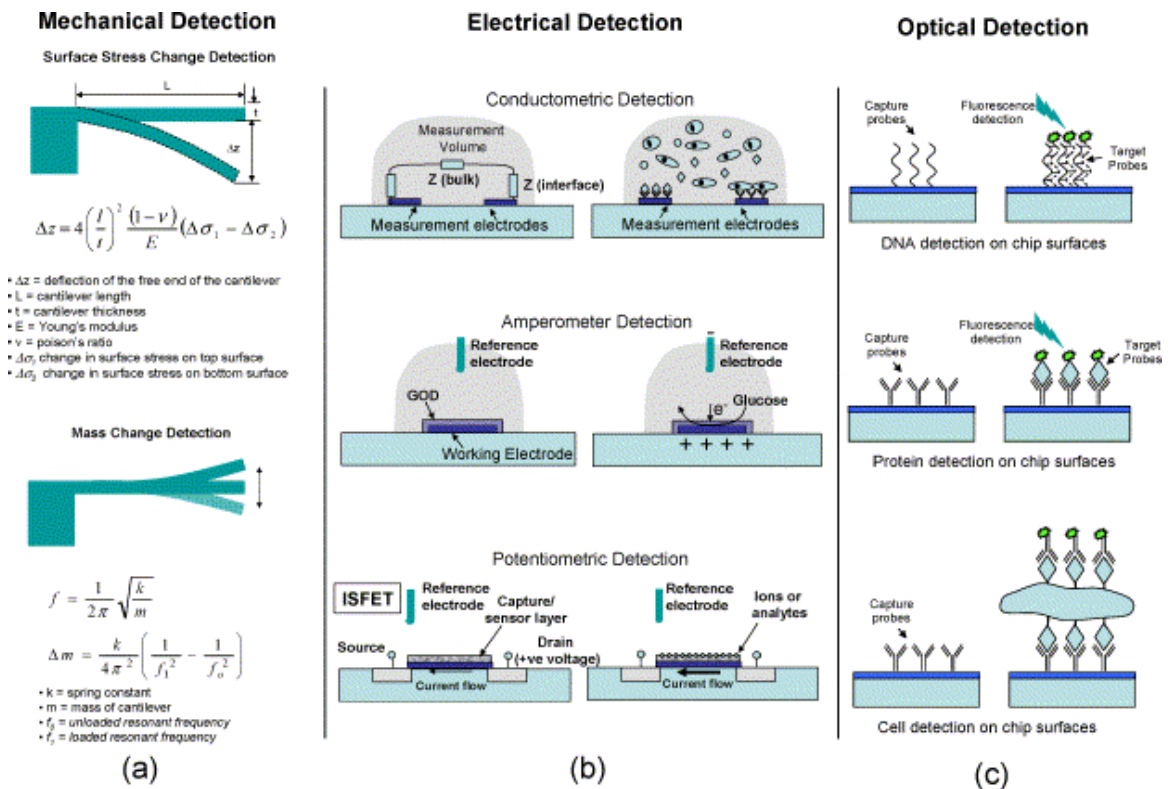


Figure 1.3 Key detection methods of BioMEMS and biochips sensors (Bashir, 2004).

It is well established that continuous monitoring of the levels of specific analytes can have an impact on an improved treatment of both acute incidents and chronic diseases. Glucose is the analyte which has attracted the largest number of developed biosensors (Henry, 1998; Wang, 1999) and this is due to the importance of glucose monitoring in order to avoid hyper- and hypoglycaemic incidents in patients who suffer from diabetes mellitus (Reach and Wilson, 1992). Close glucose control is often required in diabetes mellitus management in order to limit the effects of the disease including retinopathy, nephropathy, and vascular disease. Moreover, infections and short-term treatment with corticosteroids may adversely raise glucose levels. Diabetic patients should be among the largest group to directly benefit from new BioMEMS drug delivery systems with embedded glucose monitoring.

The immobilisation of a biological active species comprises the crucial step for the fabrication of bio/chemical microelectromechanical systems (BioMEMS). Several fields are involved including biological analysis, chemical microreactors, environmental investigations and clinical diagnosis. The fixation of biomolecules through a covalent bound and intermediate linker is one of the most interesting methods which allows a more stable linkage than that through adsorption phenomena, and offers the best access to the active site of the molecule.

1.4 Motivation and Objectives of the Current Research Project

One of the most urgent needs for the application of BioMEMS is the development of new biomaterials for the design of micro-nano sensors. The advanced preparation of biosensor and biomaterial surfaces, by constructing surface patterns with customised topographic and chemical properties, is one of the most important current research directions. Among other polymers, SU-8 has found a large number of attractive applications as a fundamental building material in the construction of various analytical tools. A literature survey can easily reveal that SU-8 is one of the most promising materials with biomedical and technological applications because of its biocompatibility, stability under varying environmental conditions, and low cost (Saliterman, 2006; Liu,

2007). The SU-8 photoresist is extensively utilised in the design and manufacturing of micro- and nano- mechanical structures for MEMS and BioMEMS applications such as actuators and electrostatic sensors, biosensors, micromoulds, microfluidic devices or packing applications.

SU-8 is a negative tone epoxy, based on the Epikote resin which is dissolved in an organic solvent and photoinitiator. The SU-8 resin layer presents good bonding and adhesion features that are superior compared to conventional thick resins. The cured layer of SU-8 forms a highly cross-linked matrix of covalent bonds, which results in a hard glass-like coating. This material constitutes a cost-effective solution for the production of fine-patterned, mechanical resistant structures for a variety of MEMS applications because of its compatibility with different types of standard X-ray and UV lithography techniques and with different coating processes.

While several researchers evaluated the frictional properties of nanocomposite materials and nanomaterials based on the SU-8 polymer, no attempts have been reported to investigate the performance and suitability of SU-8 photoepoxies to act as an immobilisation matrix in the field of biosensors.

The present project investigated the concept of developing a novel BioMEMS micro-biosensor using a simple one-step microfabrication process of new polymer matrices with immobilised biomolecules. More specifically, the study aims to investigate the suitability of the widely used SU-8 polymer as a matrix for enzyme immobilisation carried out simultaneously with the microfabrication process. SU-8 is of particular technological interest for BioMEMS applications including glucose micro-biosensors. The ultimate objective could be the utilisation of the above immobilisation matrix for the development of an integrated optical micro-biosensor.

During the present research project, the following aspects were investigated:

- Detailed experiments were carried out in order to define the optimum composition of the SU-8 films. Subsequently, a study for the control and reduction of the internal

mechanical stresses through modification of the chemical composition of the “customised” SU-8 resist, without deterioration of its lithographic properties as compared to conventional SU-8, was carried out. More specifically, the influence of different concentrations of photo-initiator on the residual stresses was studied. In addition, it was concluded that a distribution of nanoparticles in the low stress SU-8 films dramatically improved the strength and flexibility of the films with considerably fewer cracked features.

- A specific microfabrication process with detailed steps appropriate for the current project was established. In addition, an investigation was carried out for the selection of a sacrificial layer for the removal of the final SU-8 structures from the silicon wafers in the final step of the microfabrication process.
- The suitability of the SU-8 polymer as a biocompatible matrix capable of encapsulating biomolecules such as enzymes was thoroughly assessed and compared with the available biocompatible nanoporous matrices, such as porous silicon, using microfabrication techniques.
- The enzyme glucose oxidase (GOx) was immobilised in the characterised matrices. Different immobilisation techniques were attempted. Testing of immobilised enzyme activity inside the SU-8 matrix, was carried out using an amperometric method for the detection of hydrogen peroxide in a 3-electrode setup. SU-8 films were immersed in buffer solutions and the platinum working electrode was brought in close contact with the film.
- Optical fluorescent indicators (e.g. an oxygen-sensitive ruthenium complex) were included in the matrices and tests (fluorescence spectrophotometer, scanning electron microscope etc.) were performed on the optimum matrices. The optical properties of the SU-8 materials were studied such as transparency, photobleaching, luminescence and stability that are important parameters in optical biosensor design.

1.5 Structure of the Thesis

This thesis is divided into six chapters.

Chapter 2 provides a literature review which covers the utilisation of polymers in BioMEMS with an emphasis on the characteristics of the SU-8 polymer and its application in the field of Biosensors. The main areas that are addressed are related to the SU-8 polymer which is utilised in the present study, the required microfabrication process steps and the field of glucose biosensors.

Chapter 3 describes the general materials and instrumentation that were employed in the various aspects of the experimental work. In addition, an outline of the experimental programme is mentioned.

Chapter 4 includes a review of microfabrication methods for SU-8 and also reports on the results of the experimental investigation that was carried out in order to define the optimum procedure for obtaining the SU-8 microstructure for the purpose of the present investigation. The influence of the photoinitiator concentration on the residual stresses is experimentally defined and the optimum sacrificial layer is selected. The immobilisation of glucose oxidase in the SU-8 polymer is described.

Chapter 5 describes the results from the experimental investigation of the enzyme's catalytic activity in the microstructure when the latter is used as the sensing element of a glucose biosensor. Firstly, surface characterisation experiments are carried out. An electrochemical method is utilised for the assessment of the activity of glucose oxidase and also the performance of the biosensor. Finally, fluorescence spectra are obtained and compared.

Chapter 6 describes the main conclusions from the present research project. A number of recommendations and directions for carrying out potential further work are also suggested, which are expected to improve and strengthen a relevant future study.

CHAPTER 2

LITERATURE REVIEW

2.1 SU-8 Polymer

2.1.1 General

The introduction of polymers in BioMEMS has constituted one of the latest key developments in this field. In terms of definition, polymers are a class of macromolecules that consist of regular repeating chemical units joined to form a chain. Monomers refer to either the repeating chemical unit or the small molecule that polymerises to give the polymer, though the atomic structures may be different. Homopolymers consist of the same type of repeating unit, while copolymers consist of two (typically) or more types. The structure of polymers may be linear, branched or a network, resulting in 3-D shapes. Combinations of linear chains and/or cyclic polymer molecules (two ends are connected) may result in a number of molecular architectures. They are divided in two categories, the synthetic and the natural polymer materials. Biopolymers, including DNA and proteins (Saliterman, 2006) are natural polymers, SU-8 is a synthetic polymer (Wang & Soper, 2007). Suitable polymers are attractive for BioMEMS because they are lightweight, inexpensive, easily mass produced, fracture tolerant, pliable and flexible.

2.1.2 Properties of SU-8

Although the traditional use of photoresists has been the transfer of a pattern in a thin film during photolithography, a recent development has been their utilisation as structural materials in micro- and nanotechnology. A typical example is the SU-8 polymer which is a negative-tone, epoxy-type, near-UV, thick-film photoresist which was patented by IBM in 1989 (US Patent 4882245, Gelorme *et al.*, 1989) (Lee *et al.*, 1995; Lorenz *et al.*, 1996; Shaw *et al.*, 1997; LaBianca & Delorme, 1998; Lorenz *et al.*, 1998). Commercially available components are used for its preparation by dissolving an EPON[®] SU-8 resin (from Shell Chemicals) in an organic solvent such as γ -butyrolactone (GBL). The resin is photosensitised with triaryl sulfonium salts (e.g. CYRACURE[®] UVI from Union Carbide, 10% of the EPON SU-8 weight). The SU-8 is the photoresist with the highest commercially available epoxide functionality per molecule, it has eight epoxy sites per monomer, Figure 2.1 (Genolet, 2001).

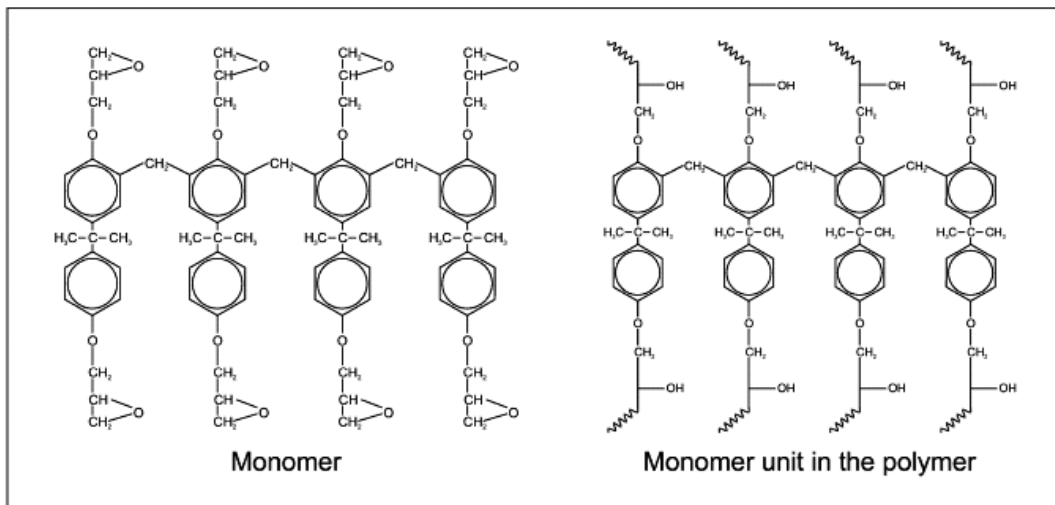


Figure 2.1: Molecular structure of EPON SU-8. Monomer and monomer unit in the cross-linked polymer (Genolet, 2001).

The ultraviolet (UV) exposure induces a highly cross-linked structure which provides SU-8 with good chemical resistance and high thermal stability. During the process of crosslinking, the epoxide monomers are transformed from a melt with low-molecular

weight to a highly cross-linked network due to the stimulation caused by the curing agent.

Microfabrication is the process for the production of devices in the submicron to millimeter range. Often the fabrication techniques are divided into “hard” and “soft” manufacturing methods to describe the differences in materials and procedures (Gad-El-Hak, 2006; Saliterman, 2006). Many of the “hard” fabrication techniques for silicon and other ceramics are similar to the ones that are used for the fabrication of intergrated circuits. “Soft” fabrication techniques are used for BioMEMS devices (e.g. biosensors) that incorporate synthetic polymers, natural polymers such as DNA (deoxyribonucleic acid) and proteins, self-assembled monolayers (SAMs) and biological materials.

Prior to fabrication, the device needs to be designed and modeled. The design process may be a team approach, using the skills of mechanical, electrical, optical, and biochemical engineers, and assisted with computer-aided design (CAD) and mathematical modeling tools. Another important issue is linked to the capabilities and limitations of the fabrication facility. There are differences in research, prototype and commercial application techniques based on equipment availability, cleanliness of the fabrication facility, ability for mass production and quality control.

The effects of the main process parameters such as exposure dose, postexposure bake, development time and packing density of the microfabricated features on the development depth and increase in feature size at the upper portion of the resist (as compared to that in a mask) were investigated by Vora *et al.* (2004) and (2006). As test samples, they fabricated 1mm high, densely-packed SU-8 structures and dissolution rates were found to be longer for densely packed structures than predicted by simple physical models based on isolated structures. Vora *et al.* (2007) found that lower postexposure bake and exposure dose minimises dimensional errors. Using overdevelopment, they demonstrated an improvement in dimensional error for a given structure.

The standard soft-fabrication of UV-lithography processing procedures of SU-8 include: (1) pretreatment of the substrate and spin-coating of SU-8 solution; (2) pre-exposure baking, UV exposure (320 to 450 nm); (3) post-exposure baking; and (4) development. The process parameters determine the final quality of the microstructures. Figure 2.2 illustrates the microfabrication process steps for SU-8 photoresist.

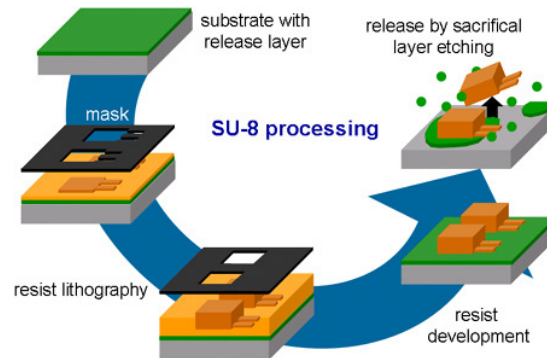


Figure 2.2 Microfabrication process steps of SU-8

(source: <http://www2.mic.dtu.dk/research/bioprobes/SU8/SU8-Material.htm>)

Ultraviolet (UV) lithography of ultrathick photoresist with good dimensional control, high-aspect ratio and high sidewall quality is very important for microelectromechanical systems (MEMS) and micro-optoelectromechanical systems (MOEMS). Although these requirements can be met by X-ray lithography of methyl methacrylate (PMMA), many researchers do not have direct access to the expensive beamlines. The X-ray lithography is impractical for many applications because of its high cost.

As a cheaper alternative, UV lithography of SU-8 has attracted a wide interest in the last few years. As the results which are obtained with UV lithography of SU-8 are improved with time, ever more applications have been found for the technology in MEMS and BioMEMS. In microtechnology, this unique feature was exploited for first time in the LIGA technique (German acronym for Lithographie, Galvanoformung und Abformung) through the replacement of the expensive X-ray lithography process by a conventional UV lithography process (Lorenz *et al.*, 1997; Cremers *et al.*, 2001). This process is known as “UV-LIGA” or “poor man’s LIGA”, allows mass fabrication of metallic microparts at a low cost and can be also applied for mould fabrication used in

thermoplastics for replication. The SU-8 polymer is particularly appropriate for thick-film applications because it can be dissolved at high concentrations and has a low absorbance in the near-UV range (Lee *et al.*, 1995). As a result, SU-8 layers of a few hundred of microns can be easily produced through spin-coating and use of standard UV exposure systems (Behringer & Uttamchandani, 2001; Abgrall *et al.*, 2007).

The utilisation of photoresists as structural materials also offers new development opportunities in the field of system integration. A resist has the ability to planarise previous layers and can be aligned very accurately allowing both hybrid and 3-D stacking integration with devices based on silicon. These unique features of photoresists can be exploited for complete integration of silicon-sensors and polymeric microchannels in a complex Lab-on-Chip (LOC) (Abgrall *et al.*, 2006; Abgrall *et al.*, 2008).

Cross-linked SU-8 has also good physical and chemical properties and can be used in many applications as high quality structural material (Konaka & Allen, 1996; Dellmann *et al.*, 1998; Lee *et al.*, 2003). For SU-8s near-UV contact printing, normally broadband near UV light, with a wavelength between 320 nm and approximately 450 nm, is utilised for the exposure. Cross-linked polymer microstructures with high aspect ratios could be obtained at heights of more than 1000 micrometers using controlled lithography conditions, pressure or vacuum contact exposure (Chang & Kim, 2000; O'Brien *et al.*, 2001; Zhang *et al.*, 2001; Lin *et al.*, 2002).

Chang and Kim obtained a 1 μm feature size with 25 μm thickness (Chang & Kim, 2000). Ling *et al.* reported 360 μm -thick structures with a 14 μm feature size (Ling *et al.*, 2000). Using a well-collimated proximity ultraviolet source, aspect ratios of more than 20:1 for film thicknesses between 200 to approximately 700 μm , were obtained (Dentinger *et al.*, 2002). Yang and Wang (2005) reported both numerical simulations and an experimental study of the air gap effect and compensation, with optimal wavelengths of the light source for UV lithography of ultrathick SU-8 resist for high-aspect-ratio microstructures with an aspect ratio higher than 100 and resist thickness of more than 2 μm .

The stripping of SU-8 is considered to be a cumbersome process, but efficient strippers were reported by Kim *et al.* (2006). High-pressure water jets (MIMOTEC process) or the previous deposition of sacrificial layers (Omniccoat™ from Microchem, <http://www.microchem.com/>) are common alternative techniques for removing SU-8.

2.1.3 SU-8 Biocompatibility

Kotzar *et al.* (2002) studied the biocompatibility of common MEMS materials, including single-crystal silicon (Si), silicon dioxide (SiO₂), silicon nitride (Si₃N₄), polysilicon, single-crystal cubic-silicon carbide (3C-SiC), titanium and SU-8. The authors performed five of the ISO 10993 physiochemical and biocompatibility tests. All materials, except the SU-8 photoresist and the silicon nitride, fell below detectable limits in four test categories (residue on ignition, nonvolatile residues, UV absorption and turbidity) that can be extracted in water. Silicon nitride and SU-8 showed only nonvolatile residues above detection limits, and SU-8 also produced detectable buffering capacity. For all materials, cytotoxicity studies showed a mild reactivity. All above materials were classified as nonirritants.

In addition, the biocompatibility and biofouling of metallic gold, silicon nitride, silicon dioxide, silicon, and SU-8 photoresist were studied as potential materials for an implanted drug-delivery system (Voskerician *et al.*, 2003). The biocompatibility and good chemical compatibility renders SU-8 a very attractive material for microfluidic applications (Weisenberg & Mooradian, 2002).

2.2 BioMEMS Applications Using SU-8 Polymer

Several fabrication techniques for making complex three-dimensional arrays of micro-wells for biological cell patterning and single-neuron guidance were presented by Griscom *et al.* (2001). In this work, inductively coupled plasma reactive ion etching (ICP-RIE) was used to construct three-dimensional micro-moulds directly on silicon

wafers, and also using SU-8 negative photoresist. Cell placement was achieved through an array of 50- μm square holes in a 150-100 μm thick PDMS membrane, which was placed on a glass substrate.

Weisenberg and Mooradian (2002) carried out a study for the materials selection to be used in blood-contacting MEMS. The hemocompatibility of silicon (Si), silicon dioxide (SiO_2), silicon nitride (Si_3N_4), low-stress silicon nitride ($\text{Si}_{1.0}\text{N}_{1.1}$), parylene and SU-8 photoresist thin films was studied through an *in vitro* assessment. Experiments were performed in order to assess the platelet adhesion or morphology after contacting these materials under static conditions.

The commercial formulation of Nano(TM) SU-8 2075 and process limitations were investigated by Rabarot and his colleagues in 2003. Good layer uniformity for single layers were obtained in a spin coater, but for ultra-thick microstructures it was also possible to cast on the wafer a volume controlled of resist up to 1.5 μm without barrier. Long baking times were necessary for a well process control. The layout of the photomask design and process parameters had great impact on residual stress effects and adhesion failures, especially for dense SU-8 patterns on metallic under-layer deposited on silicon wafers. Bio-fluidic applications of on-wafer direct prototyping (silicon, glass, plastics) were presented. An example was given on prototyping dielectrophoretic micro-cell manipulation component. The SU-8 fluidic structure was made by a self planarised multi-level process. The authors reported that biotechnology applications of integrated micro-cells could be considered because of the SU-8 good resistance to PCR (Polymerase Chain Reaction).

Lian *et al.* (2003) investigated the thermal stability of the SU-8 resist structures as a function of exposure doses and changes in photoinitiator concentration. The results showed that the relative mass loss is inversely proportional to the exposure dose as well as the post-baking time, which also directly affects the thermal stability of SU-8 components.

The effects of main plasma etching parameters such as RF power, gas flow rate, chamber pressure and time, on SU-8 resist structures were systematically studied by Vora *et al.* (2004). Results indicated that with the increase of RF power, etch rate and roughness increases almost linearly. With increase in gas flow rate, etch rate increased while roughness decreased in a non-linear fashion.

In 2005, Choi and his co-workers presented a simplified microfabrication process for the constructing electrical signal lines which were highly elevated (at a height of up to 700 μm) from the substrates, for use in a BioMEMS device where high aspect ratio three-dimensional (3-D) multi-electrode arrays (MEA) are engaged in order to detect signals from neuron networks.

Velten *et al.* (2005) provided an overview of packaging strategies and technologies for Bio-MEMS. They covered partitioning of subsystems within integrated microsystems for (bio)chemical synthesis or analysis; microassembly methods; bonding techniques for polymer Bio-MEMS; packaging of miniaturised medical devices; packaging of *in vitro* biosensors; micropumps' packaging .

Powers *et al.* (2005) presented a new platform for the optical analysis of biomolecules based upon the polysaccharide chitosan. This work demonstrated the spatially selective assembly of a fluorescent molecule on chitosan and its applicability to microscale optical transducers. Fluidic channels and multimode waveguides were manufactured on a wafer from Pyrex using a single SU-8 layer. The implementation of sidewall patterning of transparent electrodes (indium tin oxide) on SU-8 structures was demonstrated and was highly beneficial to fluorescent signal transduction.

Two MEMS devices for lab-on-a-chip bio-applications were reported (Feng *et al.*, 2005). The first one was used in cell secretion studies allowing electrochemical detection with high temporal resolution. Prototypes of micro-arrays were fabricated using Cr/Au microelectrodes on a number of different substrates such as SU-8, polyimide and SiO₂. The design of the second device aimed for the 3-D transportation of living cells on chips. Initial prototypes of micro-arrays were fabricated with SU-8

channels buried on a silicon substrate. SU-8 buried channels of both single or double layer were utilised enabling 2-D and 3-D transportation of cells.

Kentsch *et al.* (2006) proposed a novel adhesive bonding technique through the preparation of ultra-thin adhesive layers between high precision cylinders and roll-to-surface print transfer onto micro-machined substrates. The procedure was initially proposed for bonding of glass/SU-8 structures to glass cover plates for the fabrication of micro-fluidic devices with integrated 3-D arrays of micro-electrodes.

Addae-Mensah *et al.* (2007) presented fabrication steps that enable the utilisation of poly (vinyl alcohol) as an agent for release of structures in microfabrication of BioMEMS. This technique was utilised to release SU-8 discs which were attached to a vertically placed array of cylindrical microcantilevers which were moulded from polydimethylsiloxane (PDMS). The proposed method may be utilised in for release of structures made from various materials that are not compatible with standard lift-off chemistries.

Rowe and his coworkers (2007) demonstrated a microscaffold system which was fully functional, packaged active, with fluid perfusion and electrical stimulation/recording functionalities for 3-D neuronal culture studies. The fluid perfusion capabilities of the active microscaffold serve as an artificial circulatory system to facilitate 3-D growth and proliferation of re-aggregate neuronal cultures.

Cohen *et al.* (2007) reported a novel polymeric BioMEMS device for the invasive detection of Feline Immunodeficiency Virus (FIV). The device was constructed upon a silicon substrate with gold microelectrodes coated with polypyrrole (PPy), an electrically conducting and biocompatible polymer. Microfluidic channels were fabricated using SU-8.

Pai *et al.* (2007) investigated photoresists composed of resins with epoxide side groups and photoacids, for their ability to act as low-fluorescence photoresists with satisfactory resolution to generate microstructures. The structures formed from the 1002F

photoresist were approximately 10 times less fluorescent than similar SU-8 microstructures and their absorbance was substantially lower than that of SU-8 in the visible wavelengths. When the 1002F photoresist is compared with SU-8, it presents significant improvements as a substrate in bioanalytical devices and is likely to find widespread use in BioMEMS.

The process of chemical-mechanical polishing of SU-8, polycarbonate and poly(methyl methacrylate) polymers was examined by Zhong *et al.* (2005). Experiments were designed and carried out in order to quantify the effects of two important process parameters. The process of chemical-mechanical polishing is well suited for SU-8 structures with high aspect ratios.

Elbunken *et al.* (2008) published a paper on the modelling, simulation and characterisation of a bent-beam microactuator which was actuated photo-thermally. The microactuator consists of a single SU-8 layer and the principle of operation was relied on the thermal expansion of the beams from the absorption of the required heat by laser illumination.

Perera and Nikolau (2007) and his team published an article showing the realisation of an electro magnetic micro pump. The basic build-up consisted of a polymer magnet integrated into a pump chamber of a fluidic PDMS device, which was located above a double layer micro coil. The microfabrication process included UV depth lithography, electroforming of copper for the double layer spiral coil and Epon SU-8 for embedding, insulating and manufacturing of the valve seat. The fluidic devices were realised by replica moulding of PDMS using a multilayer SU-8 master.

Desai *et al.* (2008) demonstrated the application of a commercially available photopatternable silicone (PPS) that combines the advantageous features of both PDMS and SU-8 to address a critical BioMEMS materials deficiency. PPS readily integrates with many cell-based bioMEMS since it exhibits low autofluorescence and cells easily attach and proliferate on PPS-coated substrates.

Rahman *et al.* (2009) presented the design, microfabrication, packaging, surface functionalisation and *in vitro* testing of an electrochemical cell-on-a-chip (ECC) which used a microdisc electrode array (MDEA). The device was intended for intramuscular implantation as an electrochemical biotransducer for the continuous amperometric monitoring of lactate and glucose in a vertebrate animal trauma model.

Mata *et al.* (2009) reported work on a 3-D structure comprising precisely defined micro-architecture and surface microtextures, designed to present specific physical cues to tissues and cells, which may act as an efficient scaffold in a variety of regenerative medicine and tissue engineering applications. The proposed manufacturing technique was based on microfabrication and soft lithography of SU-8 which allowed the building of 3D scaffolds with both precisely engineered architecture and customised surface topography.

Despite its advantages, the potential toxicity of SU-8 2000 may be a limitation in its utilisation in cell-based applications. Vernekar *et al.* (2009) showed that when a population of primary neurons was cultured adjacent to or on top of untreated SU-8 2000, less than 10% of the population survived. They evaluated the performance of various surface treatments and detoxification for SU-8 2000 in neuronal cultures after 7-21 days *in vitro*. A 3-day heat treatment (150 °C) under vacuum improved viability to 45.8%, while UV exposure and CO₂ supercritical extraction did not influence the survival rate.

2.3 BioMEMS / Biosensors

2.3.1 General

In the last decade, the biological and medical fields have experienced significant advances in the development of biosensors and biochips capable of characterising and quantifying biomolecules. A variety of biosensors and biochips types have been developed for biological applications, along with significant progress in these technologies over the last several years (Moser *et al.*, 2002; Moser 2003; Ozkan *et al.*,

2009). A biosensor should be clearly distinguished from a bioanalytical system, which requires additional processing steps, such as reagent addition.

Sensitivity and specificity are the main properties of any proposed biosensor. The first depends on both the nature of the biological element and the type of transducer used to detect this reaction whereas specificity depends entirely on the inherent binding capabilities of the bioreceptor molecule (Byfield & Abuknesha, 1994). While much current research attempts to improve biosensor sensitivity, other sensor characteristics are also important (Fan *et al.*, 2008). The ideal biosensor would satisfy the following requirements:

- (i) be sensitive and non-invasive to permit use in a wide range of applications,
- (ii) allow real-time, label-free measurements to provide kinetic data for interaction mapping,
- (iii) be small and integrated with microfluidics to reduce reagent usage, making analyses quick, inexpensive, and accurate,
- (iv) integrated into 2-D (possibly 3-D) arrays to provide the high throughput drug discovery and interactomics mapping require,
- (v) be easy and inexpensive to manufacture,
- (vi) be highly reproducible sensor-to-sensor and chip-to-chip, and
- (vii) allow a simple, inexpensive, and robust instrument design to read the sensors and analyse the data.

In general, two major biosensor classes are recognised depending on the recognition properties of most biological components, (Mehrvar *et al.*, 2000; Hillberg *et al.*, 2005). The first category of biosensors is the catalytic biosensor. These are also known as metabolism sensors and are kinetic devices based on the accomplishment of a steady-state concentration of a detectable species by the transducer. The progress of the biocatalysed reaction is related to the analyte concentration, which in turn can be measured by monitoring the rate of a product formation, the reduction in a reactant concentration or the inhibition of the reaction. The biocatalyst can be a microorganism, an isolated enzyme, a tissue slice or a sub-cellular organelle. The second category of biosensors is the affinity biosensor. In these biosensors, the receptor molecule binds the

analyte non-catalytically and irreversibly. The binding incident between the target molecule and the bioreceptor, for instance a nucleic acid, an antibody, or a hormone receptor, constitutes the origin of a physicochemical change which will be detected by the transducer. Biosensor development is driven by the continuous requirement for simple, rapid, and continuous *in-situ* monitoring techniques that can be implemented in a broad range of areas.

Biosensors can also be classified according to either the principle of transducer operation or the nature of the bioreceptor element. The main types of transducer utilised in the development of biosensors were divided into four groups by Hulanicki *et al.* (1991): (i) optical (Hsieh *et al.*, 2007; McDonagh *et al.*, 2008), (ii) electrochemical (Wu *et al.*, 2008), (iii) mass-sensitive, and (iv) thermometric. More recent work suggests that the categories of micromechanical and magnetic should be added to this list (Turner, 2005). Each of the aforementioned groups can be further subdivided into different classes, because of the broad range of techniques that are used to monitor analyte–receptor interactions as can be seen in Figure 2.3.

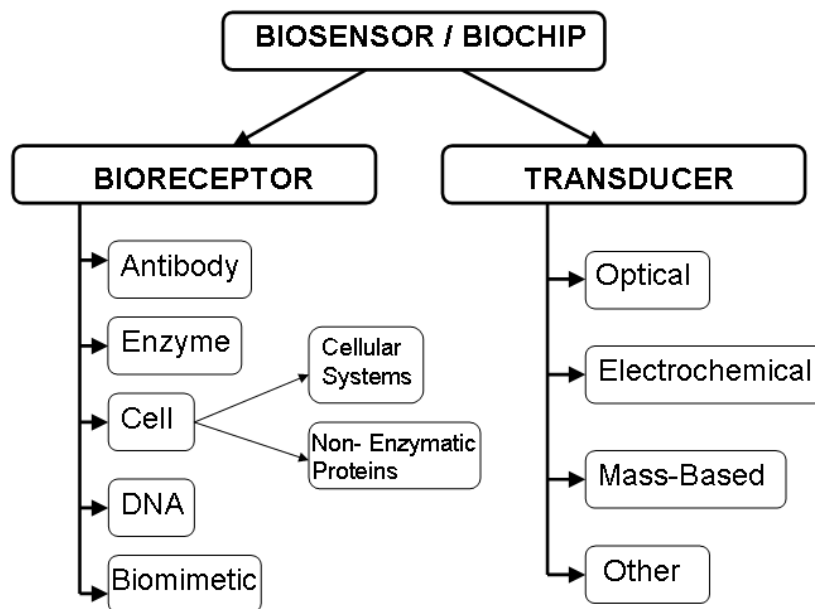


Figure 2.3: Conceptual diagram of the biosensors/biochips principle.

The component of bioreceptor can be categorised into five groups (Rogers & Mascini, 1998):

- (I) Enzymes, proteins that catalyse specific chemical reactions; and, can be utilised either in a purified form or be present in a slice of intact tissue or in a microorganism.
- (II) Antibodies and antigens.
- (III) Nucleic acids. The complementary nature of the base pairs (adenine and thymine or cytosine and guanine) of adjacent strands in the double helix of DNA, determine the recognition process.
- (IV) Cellular structures or whole cells. The whole microorganism or a specific cellular component, for example a non-catalytic receptor protein, is used as the biorecognition element.
- (V) Biomimetic receptors. Recognition is accomplished through the use of receptors, for instance, artificial membranes, genetically engineered molecules, or molecularly imprinted polymers (MIP), which mimic a bioreceptor.

BioMEMS / biosensors are characterised by two intriguing features. Firstly, the biosensor recognition elements are required to make use of sensing elements that have a naturally evolved selectivity to biological or biologically active analytes. Secondly, biosensors need to be capable of responding to analytes in a physiologically relevant manner. Biosensors have the potential of providing sensitive, rapid, low-cost measurement technology for detection and monitoring of bioavailable analyte concentrations.

2.3.2 Problems with biosensors

Although in the 1980s it seemed that the biosensor concept was likely to revolutionise 'point-of-sample' analysis, the evolution of biosensor technology has been rather slow and covered only a very small proportion of the perceived market. Nearly 90% of the current biosensor market is accounted for by just one biosensor: the glucose biosensor (Newman & Turner, 2005; Newman & Turner, 2008.)

Modern approaches to biosensor design can offer detection of a wide variety of analytes over a broad spectrum of concentrations. However, the current methods employed in assessing risks to human life in areas contaminated with pathogens, pollutants, or other agents are lacking technology.

Many of the key problems are directly linked to physical and chemical properties of the biological macromolecule at the heart of the biosensor. Particularly important are issues of unpredictable stability and shelf-life, poor inter-batch reproducibility and availability, difficulties in incorporating biomolecules into sensor platforms, environmental intolerance (e.g. temperature, pH, ionic strength, organic solvents) and poor engineering characteristics (Hillberg *et al.*, 2005).

2.3.3 BioMEMS / Glucose Biosensors: Recent Developments

Diabetes mellitus management often requires close glucose control to limit the effects of the disease, which include retinopathy, nephropathy and vascular disease. Pregnant patients especially need fine adjustments of their insulin therapy and commonly must measure their glucose levels several times a day. Moreover, infections and short-term treatment with corticosteroids may adversely raise glucose levels. Diabetic patients should be among the largest group to directly benefit from new bioMEMS drug delivery systems with embedded glucose monitoring. For this reason, a large number of elaborate research efforts have been devoted to the development of a glucose sensor for the continuous *in vivo* monitoring of glucose (Abel & von Woedtke, 2002; Petrou *et al.*, 2003). Among the variety of the established glucose sensing strategies, methods which are based on the enzyme glucose oxidase (GOx) are most widespread.

Schaffer and Wolfbeis (1990) reported a fast responding miniaturised glucose biosensor for the continuous measurement of glucose concentration. The proposed biosensor was based on an oxygen optrode, which measured the oxygen consumption via dynamic quenching of the fluorescence of an indicator by molecular oxygen. Glucose oxidase (GOx) was immobilised onto the surface of the oxygen optrode by adsorption to carbon

black and by crosslinking with glutaraldehyde. The measurements were obtained in a flow through cell with air-saturated glucose standard solutions. The effect of four different qualities of GOx in relation to response times, the linear analytical range and the long-term stability were investigated. A resulted simple device was developed that was capable of extending the analytical range up to 200 mM glucose concentration.

As early as 1994, Weigl *et al.* (1994) demonstrated a triple sensor unit consisting of opto-chemical sensors for simultaneous measurement oxygen, pH and carbon dioxide in bioreactors. The colour change of a pH-sensitive dye immobilised on a polymeric support was utilised as the basic principle of operation in the pH and the CO₂ sensors. Optical fibres were used to monitor the resulting changes in absorption. The oxygen sensor was based on the quenching of the fluorescence of a metal-organic dye. All three sensors were fully LED compatible and the sensitive membranes consisted of plastic films and could be stored and replaced in a convenient manner.

The Stern–Volmer equation can be used as a practical calibration function for various optical oxygen sensors based on quenching of ruthenium fluorescence. A simple and flexible mathematical model, which was derived from the Stern-Volmer equation, and could calculate oxygen partial pressures ranging from 0 to 760 Torr in gaseous samples, and 0 to 200 Torr in aqueous samples, was proposed by Chuang and his co-workers (1998).

The influence of possible failure mechanisms on the poor *in vivo* performance of subcutaneously implanted glucose sensors was reviewed by Gerritsen *et al.* (1999). Most implanted glucose sensors showed a significant drift in sensitivity over the implantation period; and, this bio-instability was not to be expected from the *in vitro* performance of the sensors.

In 2000, Wolfbeis and his co-workers presented a planar thin-film glucose biosensor which was based on a fluorescent oxygen-sensitive ruthenium-ligand complex entrapped in a sol–gel along with sol–gel immobilised glucose oxidase (GOx). Three different configurations were tested and the sol–gel matrix of the oxygen sensor was

optimised in terms of entrapment of the fluorescent oxygen probe. A comparison among the sensors was carried out in terms of response time, enzyme activity, and operational and storage life time.

Tierney and his team (2001) demonstrated the GlucoWatch® biographer biosensor, which provided frequent, automatic, and, non-invasive, up to 3 per hour glucose measurements over a period of 12 hours, with high precision and accuracy. This device extracted glucose through intact skin via reverse iontophoresis where it was detected by an amperometric biosensor.

Rhemrev-Boom *et al.* (2002) proposed a portable lightweight measuring device, which comprised a sampling unit (MD probe), a miniaturised flow-through biosensor and a semi-vacuum pump. The biosensor utilised the amperometric detection of hydrogen peroxide which is produced after conversion of glucose by immobilised glucose oxidase. For detection and registration, a portable potentiostat equipped with data logging was utilised. The performance characteristics (precision, accuracy, linearity, selectivity and stability) that were defined during *in vitro* and *ex vivo* experiments, justified the implementation of the presented measuring system for the *in vivo* monitoring of glucose in subcutaneous sampled interstitium of diabetic patients.

Cost effective portable devices were constructed for field applications and point of care diagnosis by Albers and co-workers (2003) using electrical biochips made with Si-technology. These miniaturised amperometric biosensors made possible the evaluation of biomolecular interactions by measuring the redox recycling of ELISA products, and the monitoring of metabolites. The highly sensitive redox recycling was facilitated by interdigitated ultramicroelectrodes of high spatial resolution. The measurement procedure was demonstrated through the implementation of these electrical biochips as DNA microarrays for the molecular diagnosis of viral infections. Self-assembling of capture oligonucleotides via thiol-gold coupling was used to construct the DNA interface on-chip. Another practical application for this electrical detection principle was the continuous measurement with bead-based biosensors. A Si-micromachined glucose sensor for continuous monitoring in interstitial fluid *ex vivo* was presented.

Paramagnetic nanoparticles were used as carriers of the bioanalytical interface in ELISA format.

A method of preparing a polyaniline (PANI) glucose oxidase sensor, which was called template process, was presented (Pan *et al.*, 2004). Based on the process steps, a PANI glucose oxidase electrode was obtained using one-step process, i.e. enzymes were entrapped into a polymer film directly during electrochemical polymerisation of aniline. Then the electrode was hydrolysed in 6.0 mol/dm³ hydrochloric acid solution to remove the glucose oxidase from the PANI film, for part of the glucose oxidase affected by monomer of aniline were denatured and inactive. Finally, fresh glucose oxidase was immobilised into the PANI film again to obtain an active PANI glucose oxidase sensor. The response current of the biosensor prepared by template process reached to a maximum at the first 2 days, then decreased by only 4.6% for 30 days, while that of the sensor prepared by two-step process decreased by approximately 55.4%.

Piechotta *et al.* (2005) described a micromachined silicon sensor for continuous monitoring of glucose. The sensor used the conventional enzymatic conversion of glucose with amperometric detection of the produced hydrogen peroxide. The paper demonstrated the diffusion control of the analyte through a porous silicon membrane into a silicon etched cavity where the immobilised enzyme was placed.

A publication related to glucose oxidase characterisation for the fabrication of hybrid microelectronic devices was published by Fichera *et al.* (2007). Glucose oxidase (GOx) immobilisation on silicon oxide surfaces was studied and the protocol fulfilled requirements for both of enzyme preservation (measured by enzymatic activity) and VLSI compatibility. The immobilisation consisted of four steps: oxide activation, silanisation, linker molecule deposition and immobilisation of GOx. The formation of a uniform linker layer on the sample surface was crucial in order to maximise the sites available for enzyme bonding and deposition. X-ray Photoelectron Spectroscopy (XPS) was used to monitor the utilisation of glutaraldehyde as bifunctional reagent. The same protocol was used to anchor the enzyme in a porous silicon dioxide matrix. Electron diffraction X-ray (EDX) measurements coupled with scanning electron microscopy

(SEM) were utilised to monitor gold labelled GOx molecules. The enzymatic activity was also monitored to confirm the suitability of the proposed immobilisation method. The electrical characterisation of MOS capacitors, showing a shift of about 1 V in the flat band voltage, demonstrated the possibility to use this approach for electrical detection.

A chemically modified microelectrode was proposed for the direct measurement of cerebral glucose concentration, Ahmad *et al.* (2008). The effects of exogenous insulin, AIIRB (angiotensin II receptor blockers) and CCB (calcium channel blockers) on the glucose level in the striatum of the brain in diabetic and hyperglycemia rates, were investigated.

Wei Yan *et al.* (2008) developed an amperometric glucose biosensor by adsorption of glucose oxidase (GOx) on an AuNPs–AgCl@PANI modified glassy carbon (GC) electrode. AuNPs–AgCl@PANI could provide a biocompatible surface for high enzyme loading. The AuNPs in the hybrid material could act as a good catalyst for both oxidation and reduction of H₂O₂. The measurement of glucose concentration was based on the electrochemical detection of H₂O₂ generated by the enzymatic reaction of glucose oxidation, the biosensor exhibited a highly sensitive response to the analyte with a detection limit of 4 pM, a good reproducibility and an operation stability.

Li Shang and his colleagues (2008) reported the biocatalytic growth of gold nanoparticles (Au-NPs) in the design of new optical biosensors based on enhanced resonance light scattering (RLS) signals. Absorption spectroscopy and transmission electron microscopy (TEM) measurements showed that Au-NP seeds could be effectively enlarged upon the reaction with hydrogen peroxide which is an important metabolite that could be generated by many biocatalytic reactions. Combination of the biocatalytic glucose oxidase reaction with the enlargement of Au-NPs enabled the design of a sensitive glucose biosensor using the RLS technique.

The performance of a glucose biosensor based on the combination of biocatalytic activity of glucose oxidase with the electrocatalytic properties of CNTs and neutral red

(NR) for measuring glucose concentration, was described (Jeykumari & Narayanan, 2008). This sensor consisted of a multiwalled conduit of carbon nanotubes (MWNTs) functionalised with NR and Nafion (Nf) as a binder and glucose oxidase as a biocatalyst. Neutral red was covalently immobilised on carboxylic acid groups of the CNTs via carbodiimide reaction. The catalytic reduction of hydrogen peroxide liberated from the enzymatic reaction of glucose oxidase upon glucose with NR functionalised CNTs allowed the selective detection of glucose.

Patel and his co-workers (2008) presented a self-aligned and hybrid polymer fabrication process for the development of an electro-enzymatic glucose sensor. The self-aligned fabrication process was performed using polydimethylsiloxane (PDMS) as a substrate material, SU-8 as a sensor structural material, and gold as an electrode material. During microfabrication, SU-8 demonstrated good adhesion to the PDMS. However, the SU-8 easily peeled-off from the PDMS in the end of the process. The PDMS was prepared on a glass handle wafer and remained reusable and an SU-8 release technique from a PDMS substrate was proposed. The novel process was employed to realise a glucose sensor with active and reference gold electrodes that were sandwiched between two SU-8 layers with contact pad openings and the active area opening to the top SU-8 layer. Glucose oxidase was immobilised within the confined active area opening in order to provide an active electrode sensing surface. The authors reported a linear response for the glucose sensors.

2.4 BioMEMS / Biosensors Using SU-8 Polymer:

Recent Developments

In the last few years, the latest developments in the research fields of BioMEMS and biosensors have been combined with the utilisation of SU-8 polymer to develop a new generation of micro- nano-biosensors, such as biophotonic BioMEMS cell biosensors. Powers and co-workers (2005) presented a new platform for the optical analysis of biomolecules based upon the polysaccharide chitosan. The versatile, stable and compatible nature of chitosan makes it an ideal material for integrating biological

materials in microfabricated systems. Chitosan's pH-responsive solubility allows electrochemical deposition, while its chemical reactivity enables facile coupling of proteins, oligonucleotides and other biomolecules by covalent bonds. This work demonstrated the spatially selective assembly of a fluorescent molecule on chitosan and its applicability to microscale optical transducers. They defined multimode waveguides and fluidic channels on a Pyrex wafer using a single layer of SU-8. Their implementation of sidewall patterning of transparent electrodes (indium tin oxide) on SU-8 structures was demonstrated and can be beneficial to fluorescent signal transduction.

A new construction method of multifunctional biosensor using many kinds of biomaterials was described by Choi *et al.* (2006). A metal particle and an array were fabricated by photolithography. The metal particles were in a multilayer structure (Au, Ti, and Ni) whereas the biomaterials were immobilised on the metal particle. Thick negative photoresist (SU-8) was used to cover the sidewalls of patterned Ni dots on the array and the array was magnetised. The particles and the array were mixed in a buffer solution and were arranged by magnetic force interaction and random fluidic self-assembly. The particles were arranged on the array and the biomaterial activities were detected by electrochemical methods and chemiluminescence.

Gadre and Bari (2006) proposed a polymeric BioMEMS device for a qualitative test for Feline immunodeficiency virus (FIV) and Feline leukemia virus (FeLV). FIV and FeLV are both generally termed as retroviruses, which function by inserting their genes into the host's DNA. The BioMEMS device which utilised a non-invasive method, in order to obtain a complete result would require 60 seconds or less. The electrochemical deposition technique was integrated with a multilayer fabrication approach using various polymers such as SU-8, a conducting polymer polypyrrole (PPy) and a transparent elastomer polydimethylsiloxane (PDMS).

An injection micromixer for biochemical microfluidic systems, which was fabricated through SU-8 processing, was presented by Liu *et al.*, (2006). Firstly, a modular polymer-based (PMMA) injection micromixer prototype was designed, fabricated and

tested. Then an SU-8 injection mixer was designed and fabricated to run some biochemical sample liquids. Internal stress in patterned SU-8 structures was reduced and multi-layer SU-8 processing was developed to fabricate the SU-8 injection mixer.

The development of a silicon cell electrophysiology lab-on-a-chip device for measuring transcellular calcium currents in an advanced throughput format was carried out by Haque et al. (2006). The device consisted of 16 pyramidal pores on a silicon substrate with four Ag/AgCl electrodes leading into each pore on the four poles. As the structural and insulating layer, an SU-8 layer was used and a calcium ion selective membrane was employed to impart ion selectivity to the Ag/AgCl electrodes. The authors claimed that future applications could be based on incorporating multiple analyte detection, amperometry and biosensors into the device.

In 2007, Yun and his colleagues presented carbon nanotube-based biosensors which were used on-line in microfluidic channels using SU-8 and PDMS. Highly aligned double wall carbon nanotubes (DWCNT) and multi-wall carbon nanotubes (MWCNT) were synthesised in tower shapes and embedded into microchannels for use as biosensors. Based on the impedance results using the flowing cells and the cyclic voltammetry CV and differential pulse voltammetry (DPV) results, carbon nanotube microelectrodes appeared to be a promising candidate for cancer cell detection and neurotransmitter detection.

A micro-plane amperometric immunosensor for the detection of human immunoglobulin G was fabricated on silicon wafer based on MEMS technology (Chao *et al.*, 2007). The microsensor was an electrochemical system composed of a working and a counter electrode integrated with a micro-reaction cell made of SU-8 photoresist. The sensitive area of the working electrode was only 1mm^2 . A method for the orientation-controlled of antibody immobilisation was developed.

Pennell and his colleagues (2007) presented a high-speed microfluidic thermal stimulator for temperature-activated ion-channel studies. The thermal chip was designed to facilitate the patch clamp to study temperature dependent activities of ion channels. The device consisted of a fluid channel for perfusing solution which was linked to an

accessible reservoir for performing patch-clamp measurements on individual cells. A thin film platinum heater was used to cause rapid temperature changes and the temperature was measured with the use of a thin film resistor. The thermal chip was constructed using SU-8 on glass wafer to minimise the heat losses to the channel walls and the substrate.

In 2008, an SU-8 based fluidic immuno-spectroscopic lab-on-a-chip for rapid quantitative detection of biomolecules was developed (Jiang *et al.*, 2008). A 30mm-long multimode waveguide, 40 μm x 40 μm , was fabricated on a silicon wafer using SU-8 polymer as the core and liquid buffer as the cladding. The antibodies that were successfully immobilised on the SU-8 surface, were designated for binding target antigens which were dispersed in the buffer solution. Evanescent-wave spectroscopy was performed by exciting the fluorescently-labelled antigens, bound to the waveguide surface within its evanescence field, and measuring emission light intensity. This evanescent-wave biosensor detected specific molecular interaction; and, its output was proportional to antigen concentration.

It is well known that determining the lactose concentration in human breast milk (HBM) via standard assay techniques requires fat removal from the milk (defatting), followed by lactose detection in the remaining skim milk. Work focused on methods of defatting which can be subsequently integrated in the same Lab-on-Chip (LOC) as the lactose measurement was described by Meifang *et al.* (2008). Photolithography using SU-8 was applied for mould fabrication; however, hot-embossing using SU-8 mould was not successful due to the high stress resulting in the demoulding process. To improve mould strength, nickel moulds were fabricated by electroplating using different current densities. The deposition rates were found to have a linear relationship with applied current density, while the smaller features have a higher deposition rate than larger features.

Another publication presented a single-use fluid microvalve for Lab-on-Chip (LOC) applications that combined printed circuit board and SU-8 technologies (Moreno *et al.*, 2008). The main advantage of this device lay in the simplicity and low cost of the

fabrication process. The design was conceived to be integrated in an array composed by microneedles modules and biosensing devices.

A microcalorimeter based on a split-flow microchannel structure for biochemical applications was investigated by Yoon and co-workers (2008). It measured the heat of reaction between biotin and streptavidin. In order to enhance its sensitivity, the thermal components were fabricated on a high-thermal resistivity layer, the SU-8, which reduced the amount of parasitic heat transfer to the silicon substrate.

A wet release of multipolymeric structures with nanoscale release layer of SU-8 was explored (Pes *et al.*, 2008). A process using OmniCoat™ was developed for the release of the multilayer microsensor device for biomedical applications. OmniCoat™ has high thermal stability which makes it compatible with processes occurring at high temperature levels. A multilayer fabrication approach and OmniCoat™ release layer were successfully integrated for a microsensor device to be released from the substrate. The influence of OmniCoat™ development on the optical properties of SU-8 were analysed. The authors claimed that good adhesion between metals and cured polymer layers and highly aligned structures were accomplished. OmniCoat™ has great potential as a release layer in several other MEMS applications where SU-8 is used as a structural material.

In 2009, Lechuga *et al.* investigated the design, fabrication and packaging of microfluidic networks with photonic sensors for a Lab-on-Chip platforms which incorporate the on-chip biosensing detection. An integrated Mach-Zehnder interferometer (MZI) based on TIR waveguides (Si/SiO₂/Si₃N₄) of micro/nanodimensions for evanescent field detection of biomolecular interactions onto the sensing areas, was used as sensor. For the lab-on-a-chip development, the biosensors were integrated with a 3-D SU-8 polymer microfluidic network.

Another paper demonstrated a micro flow cytometry device fabricated using Ultra Violet (UV) lithography of the negative tone photo resist SU-8 (Shao & Wang, 2009). A diamond-shaped sample injection nozzle, a three-dimensional hydro-focusing unit,

and an optical detection unit with integrated out-of-plane microlens were fabricated using tilting lithography techniques. To improve detection efficiency, an out-of-plane microlens made of cured SU-8 polymer was imbedded in one of the outlet fluid channel walls.

Fabrication of three-dimensional microwell patterns and their integration with human neuroblastoma cells was reported by Wu et al. (2009). UV lithography, silicon etching and soft lithography were adopted to fabricate microwell patterns with SU-8 photoresist and poly(DL-lactide-co-glycolide) (PLGA). Patterns were integrated with SH-SY5Y human neuroblastoma cells.

2.5 BioMEMS / Biosensors Using SU-8 Polymer: Latest Immobilisation Techniques

Enzymes are generally immobilised onto supports by covalent attachment, passive adsorption, surface modification, entrapment within a polymeric film or encapsulation in order to construct biosensors that can be used to monitor the concentration of a target analyte inside a biological fluid.

It is well established that SU-8 has been primarily used as a material for the construction of structural elements and microfluidics components in MEMS. BioMEMS applications require immobilisation of biomolecules on the MEMS structures. In order to functionalise SU-8 for such purposes, its surface requires to be modified. In the paper presented by Joshi *et al.* (2007), the epoxy-groups of the SU-8 surface were hydrolysed in the presence of sulphochromic solution. Subsequently, the surface was treated with [3-(2-aminoethyl) aminopropyl]-trimethoxysilane (AEAPS). The silanised SU-8 surface was then utilised to incubate human immunoglobulin (HIgG). The immobilisation of HIgG was proved by allowing FITC tagged goat anti-human IgG to react with HIgG. This antibody immobilisation process was employed to immobilise HIgG on microfabricated SU-8 cantilevers.

Libertino *et al.* (2007) studied the possibility to use techniques that are traditionally employed in microelectronics to detect biological molecules immobilised on and into Si-based materials having, as final goal, the structural characterisation of a glucose biosensor. Bulk and porous silicon dioxide was used as inorganic immobilisation surfaces and GOx was used as the biological molecule to monitor. Bulk SiO₂ was used to optimise the immobilisation protocol and Atomic Force Microscopy measurements were used for the step-by-step characterisation. The enzyme monitoring was carried out by electron diffraction X-ray measurements coupled with scanning electron microscopy. The protein was previously labelled with gold nano particles, in order to ensure its presence.

A dry method of surface modification of SU-8 was reported by Joshi *et al.* (2007). The surface obtained by spin coating SU-8 (2002) on silicon wafer, was modified by grafting amine groups using pyrolytic dissociation of ammonia in a hotwire CVD setup. Fourier transform infrared spectroscopy was used to assess the presence of amine groups on the modified SU-8 surface and also the surface characteristics after modification. The surface morphology before and after modification was investigated using atomic force microscopy. SU-8 microcantilevers were fabricated and subjected to the same surface modification protocol in order to use the above process for application in BioMEMS.

Libertino *et al.* (2007) reported the study of biological molecules (glucose oxidase) immobilised in Si-based materials (porous silicon). An optimised immobilisation protocol was used to covalently bind GOx to an oxidised porous Si surface and the GOx presence was monitored on both bulk and porous SiO₂. They reported that such method could be implemented in microelectronics to monitor the presence of biological material in hybrid (organic-inorganic) devices.

Erkan and his colleagues (2007) demonstrated a rapid, simple one-step procedure for the high-yield immobilisation of cholesteryl-tetraethyleneglycol modified oligonucleotides (chol-DNA) at hydrophobic sites / surfaces made of SU-8 photoresist. Topographic structures of SU-8 were microfabricated on microscope glass coverslips

sputtered with a Ti/Au layer. Upon application, chol-DNA adsorbed to the SU-8 structures from solution, leaving the surrounding gold surface free of chol-DNA. chol-DNA immobilisation was complete within 15 min and it was stable and could be sustained despite rinsing, drying, dry storage for several hours and rehydration of chips. Furthermore, complementary DNA in solution hybridised efficiently to immobilised chol-DNA.

Due to its favourable optical properties and flexibility in process development, SU-8 photoresist has attracted attention for optical sensing applications (Amberkar *et al.*, 2008). Manipulation of the surface properties of SU-8 waveguides was critical in order to attach functional films such as chemically-sensitive layers. An integration process was followed to immobilise fluorescence molecules on SU-8 waveguide surface for application to intensity-based optical chemical sensors. Two polymers were used for this application. Spin-on, hydrophobic, photopatternable silicone was a convenient material to contain fluorophore molecules and to pattern a photolithographically defined thin layer on the SU-8 surface. The other material was polyethylene glycol diacrylate (PEGDA). The researchers demonstrated a novel photografting method for the surface modification of SU-8 using a surface bound initiator to control its wettability. The activated surface was then coated with a monomer precursor solution. Polymerisation followed when the sample was exposed to UV irradiation, resulting in a grafted PEGDA layer incorporating fluorophores within the hydrogel matrix.

Fabrication, characterisation and development of novel read-out methods using SU-8 cantilevers for bio/chemical sensing have been demonstrated by Nordstrom *et al.* (2008). Over the last five years, the above research group worked in the field of cantilevers fabricated in the polymer SU-8. They claimed that SU-8 is an interesting polymer for fabrication of cantilevers for bio/chemical sensing due to its simple processing and low Young's modulus. They demonstrated examples of different integrated read-out methods and their characterisation. In addition, they showed that SU-8 cantilevers have a reduced sensitivity to changes in the environmental temperature and pH of the buffer solution. The SU-8 cantilever surface functionalised directly with receptor molecules for analyte detection, thereby avoiding gold-thiol chemistry.

2.6 Outline Summary of the Literature Review

From the literature review that was carried out in the framework of the present project a number of important issues can be highlighted:

- a) During the last decade there has been significant progress in the research field of BioMEMS with a wide variety of important biomedical applications. Research and applications areas in BioMEMS range from diagnostics, such as biosensors, protein and DNA micro-arrays, to novel materials, microfluidics, surface modification, tissue engineering, implantable BioMEMS, drug delivery systems, etc.
- b) A significant amount of work has been carried out in the implementation of MEMS technologies to biosensor applications and the adaptation of various types of sensors to *in vivo* diagnostics. However, at the intersection of these fields there are formidable challenges faced in the more general field of implanted biosensors. The goal of short-term sensing of analytes, pH and pressure in blood, tissue, and body fluids has largely been accomplished. However, long-term *in vivo* sensing is still to be achieved as the issues of biocompatibility and biofouling must be addressed.
- c) Glucose biosensors, both *in vivo* and *in vitro*, represent the largest biosensor market with continuing accumulation of new research and development efforts for further improvement.
- d) The SU-8 polymer is one of the most commonly used materials in BioMEMS. SU-8 has found a significant number of applications not only as a structural material but as a biocompatible material. In addition, microfabrication techniques of SU-8 are well-advanced.
- e) There is little reported research work in the area of enzyme immobilization in SU-8 matrices for the development of novel microbiosensors. The use of SU-8 in BioMEMS applications is limited to surface modification of the polymer for immobilisation of biomolecules. To date, efforts to immobilise

biomolecules by entrapment inside and on the surface of an SU-8 matrix have not been reported in the literature.

Based on the above, there is very limited reported research on the performance of SU-8 photoepoxies as an immobilisation matrix in the field of biosensors. In order to fill this identified gap in the literature, the present project seeks to establish the concept of building a novel BioMEMS micro-biosensor using a simple one-step microfabrication process exploiting the widely used SU-8 polymer as a matrix for enzyme immobilisation carried out simultaneously with the micro-fabrication process.

CHAPTER 3

GENERAL MATERIALS AND INSTRUMENTATION

3.1 Materials

The following chemicals were mainly used for this work: Epon™ resin SU-8 (Epikote™ 157) granules from Hexion Specialty Chemicals, Columbus OH 43215 - USA (<http://www.hexion.com>); gamma-Butyrolactone (GBL), an organic solvent from Avocado Research Chemicals Ltd, Alfa Aesar – Johnson Matthey Co, Lancashire LA3 2XY, U.K. (<http://www.avocadochem.com>); triarylsulfonium hexafluoroantimonate salts mixed 50% in propylene carbonate, a curable photo-initiator from Sigma-Aldrich Company, Dorset, U.K. (<http://sigmaaldrich.com>); dextran clinical grade, average molecular weight 64,000-76,000, used as a solution 5% w/v in distilled water from Sigma-Aldrich (<http://sigmaaldrich.com>); glucose oxidase type X-S from *Aspergillus niger*, lyophilised powder, 100,000-250,000 units/g solid from Sigma-Aldrich (<http://sigmaaldrich.com>); D-(+)-Glucose ACS reagent from Sigma-Aldrich (<http://sigmaaldrich.com>); tris(4,7-diphenyl-1,10-phenanthroline) ruthenium(II) dichloride complex, a fluorescent indicator from Fluka, Sigma-Aldrich (<http://sigmaaldrich.com>); 8-Hydroxypyrene-1,3,6-trisulfonic acid trisodium salt (HPTS) 97% from Aldrich, Sigma-Aldrich (<http://sigmaaldrich.com>); cyclopentanone, cyclohexanone, polyethylene glycol 400 dimethyl ether,

tetrahydrofuran, ethanol, acetonitrile, 2-methoxy-1-methylethyl-acetate (PGMA), propylene carbonate, and 1-methoxy-2-propyl-acetate (PGMEA) from Fluka, Sigma-Aldrich (<http://sigmaaldrich.com>).

Plain silica nanoparticles with mean diameter of 30 nm in 5% aqueous suspension were purchased from Nanostructured & Amorphous Materials, Inc., Houston, USA (<http://www.nanoamor.com>). In addition, FITC (Fluorescein isothiocyanate) surface labeled microspheres with mean diameter of 0.21 μ m (green fluorescence: excitation 492nm; emission 519nm), PS FITC surface labeled microspheres with mean diameter of 0.96 μ m (green fluorescence: excitation 492nm; emission 519nm) and Rhodamine WT surface labeled microspheres with mean diameter 0.87 μ m (red fluorescence: excitation 550nm; Emission 590nm), with all of them solids content 1%, were obtained from Bangs Laboratories Inc., Fishers, USA (<http://bangslabs.com>).

All other chemicals were of the highest purity available and were purchased commercially. Water was doubly distilled in a quartz apparatus and stock solutions of glucose were left to mutarotate at room temperature for 24 hours before use, and were stored in a refrigerator. In all experiments, the buffer solution used was phosphate buffer 10mM, pH7.4 (Na_2HPO_4 , NaH_2PO_2).

3.2 Instrumentation

The main instruments that were used in this work were the following: a KLA-Tencor P-15 Profiler with its software which was used for calculating the average stress values of the samples (KLA-Tencor Corporation, California, USA) (www.kla-tencor.com). A Zygo interferometer with its software NewView 200 for film applications (Zygo Corporation, Middlefield, USA) (www.zygo.com). This instrument was used for obtaining the surface topology images of the stress experiments of the SU-8 films (Chapter 4). A Wyko NT9000 series optical interferometric profiler (Veeco Co.) for film applications (Veeco Instruments Inc., Tucson, USA) (www.veeco.com). This instrument was used for obtaining

the surface topology images during the biosensor experiments using SU-8 films (Chapter 5).

A UV aligner (Karl Suss MA 6) which was used for the exposure of the SU-8 films or structures (SUSS MicroTech AG, Waterbury Centre, USA) (www.suss.com). Amperometric measurements were performed using the Autolab PGSTAT-12 potentiostat in combination with the software GPES (General Purpose Electrochemical System) Version 4.9 (Metrohm Autolab, Westbury, USA) (www.metrohm-autolab.com). Scanning Electron Microscope images were obtained with an environmental scanning electron microscope, model Philips XL30 ESEM-FEG. (FEI Company, Oregon, USA) (www.fei.com). For the fluorescence measurements, the Coherent Innova 300 Laser at 490 nm was used as a source and the Andor Technology Model No SR-500i-B1 was used as a detector (Coherent Corporate, California, USA; Andor Technology Plc, Belfast, UK) (www.coherent.com) (www.andor.com).

Stress measurements and characterisation of the SU-8 films were performed in the Micro- and Nanotechnology Centre at Rutherford Appleton Laboratory in Didcot, UK. The rest of the experimental work was carried out in the Sensors, Actuators and Microsystems Laboratory (SAMPLAB) at IMT - EPFL in Neuchatel, Switzerland, except the fluorescence experiments that were performed in the Optics Laboratory of the Engineering Department of EPFL in Lausanne, Switzerland.

3.3 Properties of SU-8 Polymer

3.3.1 Commercially Available SU-8 Composition

As was described in Chapter 2, SU-8 is a negative-tone, epoxy-type, near-UV photoresist and it is commercially available from MicroChem Corporation (Newton, MA USA). It is prepared from commercially available components by dissolving an EPON® SU-8 resin (from Shell Chemical) in an organic solvent such as gamma-butyrolactone (GBL). The quantity of the solvent determines the viscosity which permits the range of the possible resist thicknesses to extend from tens of nm to mm. The resin is photosensitised with triaryl sulfonium salt which is a photoinitiator and is

responsible for the polymerisation of the SU-8 photoresist with UV-exposure. Subsequently, both parameters, the percentage of the solvent and the photoinitiator are responsible for the chemical and the physical properties of the final SU-8 structures.

3.3.2 Chemical Properties

Polymerisation is the process of reacting monomers to form polymers. Photopolymerisation is based on exposure of a liquid resin to light. Polymerisation of the SU-8 is based on chemical amplification. A single photo event, also known as protolysis, initiates a cascade of subsequent chemical reactions that induce the cross linking. The chemical reactions in SU-8 involve the use of a cationic photoinitiator (triaryl sulfonium salt), which generates a strong acid upon UV-exposure, as shown in Figure 3.1(a). This photoacid acts as a catalyst in the subsequent cross linking reaction by the cationic ring opening of epoxy groups by the acid (Figure 3.1(b)).

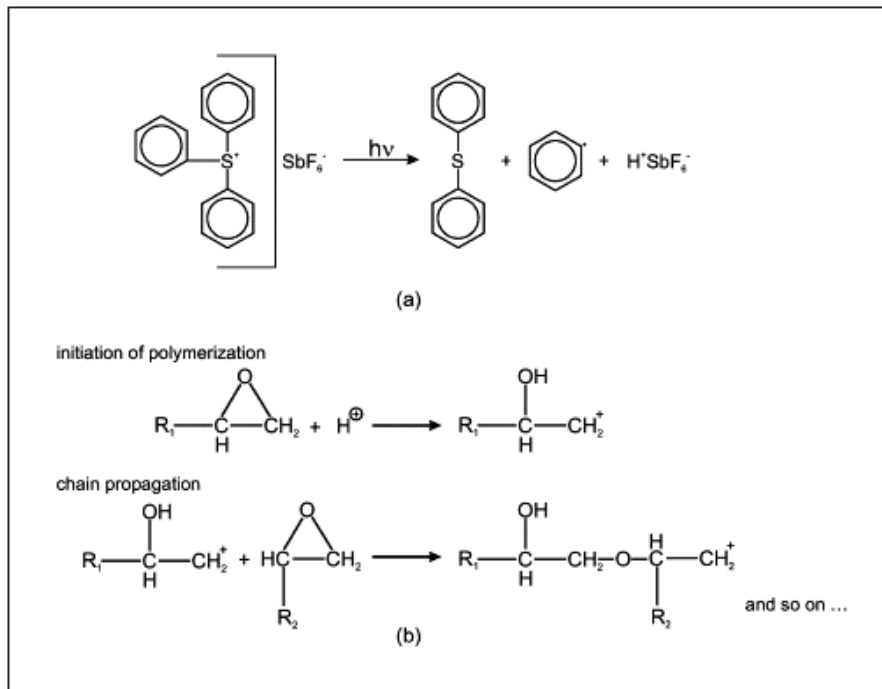


Figure 3.1 (a) Protolysis of the triaryl sulfonium hexafluoroantimonium which generates an acid that induces the cross-linking (Genolet, 2001).
(b) Opening of the epoxy group and reaction propagation.

The acid is not consumed in the initiation process and can function to initiate several chains. The cross linking process yields a dense, stable network where each epoxy monomer is connected to 7 others on average.

Photoinitiated polymerisation based on UV curing occurs between 225 and 550 nm. Free radical and cationic curing mechanisms may be used. When the photoinitiator is exposed to UV, they break down, leaving components with an unpaired electron, or free radicals. This highly cross linked structure induced by ultraviolet exposure offers SU-8 its high thermal stability and good chemical resistance.

3.3.3 Physical Properties

The mechanical, electrical, and optical properties, which are of high importance for a particular BioMEMS application, depend on the composition of the SU-8 polymer and the steps of the microfabrication process which will be addressed in the following chapter. Bulk and surface characteristics and the ability to modify them to induce specific functionality are important in biosensor applications. In addition, other properties such as thermodynamic, kinetic, and heat transfer are also important depending on the application. The most interesting mechanical and thermal properties for the fabrication of microstructures are summarised in Table 3.1.

3.3.3.1 Mechanical Properties

Polymers are *viscoelastic* and exhibit some of the properties of both *viscous liquids* and *elastic solids*. Mechanical properties are dependent on temperature according the diagram of the Young's modulus versus temperature for a model polymer, as can be seen in Figure 3.2. Elevation of the temperature above the glass transition temperature lowers Young's modulus with a change of material from brittle glass to elastic rubber consistency. In the transition, temperature ranges of mixed properties are displayed, including *creep*, or the change in shape under a constant load, and *stress-relaxation*, the lowering of stress required to maintain the strain. Actual polymers may undergo more than one transition, while amorphous and crystalline polymers behave differently.

Table 3.1 Physical Properties of SU-8 Photoresist

Property	Value	Reference
Young's Modulus E	4.02 GPa (Postbake at 95°C) 4.95±0.42 GPa (Hardbake at 200°C)	Lorenz <i>et al.</i> , 1997 Dellmann <i>et al.</i> , 1997
Bi-axial Modulus of Elasticity $E/(1-\nu)$	5.18 ± 0.89 GPa	Lorenz <i>et al.</i> , 1998
Film Stress	16-19 MPa (Postbake at 90°C)	Lorenz <i>et al.</i> , 1998
Maximum Stress	34 MPa (Hardbake at 200°C)	Dellmann <i>et al.</i> , 1997
Friction Coefficient μ	0.19 (Postbake at 95°C)	Lorenz <i>et al.</i> , 1997
Glass Temperature T_g	~50°C (unexposed)	LaBianca & Delorme, 1995
Glass Temperature T_g	>200°C (fully cross linked)	LaBianca & Delorme, 1995
Degradation Temperature T_d	~380°C (fully cross linked)	LaBianca & Delorme, 1995
Thermal Expansion Coefficient TEC	52±19 ppm/K (Postbake at 95°C)	Lorenz <i>et al.</i> , 1998
Polymer Shrinkage	7.5%	Guerin <i>et al.</i> , 1997

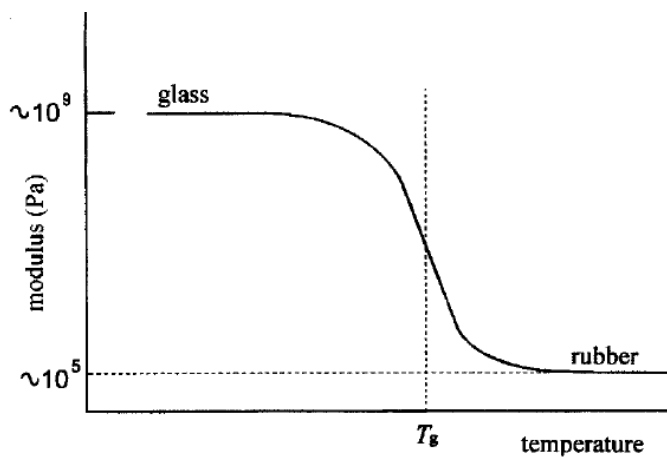


Figure 3.2 Young's modulus against temperature for a model polymer.

T_g is the glass transition temperature (Bower, 2002).

Hooke's law describes the behavior of an ideal elastic solid:

$$\sigma = Ee \quad (\text{Eq. 1})$$

where

σ is the tensile stress (force / unit cross section)

E is the Young's modulus of the material, and

e is the linear strain (Δ length / initial length).

3.3.3.2 Optical Properties

Optical properties of polymers for BioMEMS devices, and especially for optical biosensor applications, are of particular importance in detection schemes and in light-initiated reactions. Polymers generally absorb in the infrared and ultraviolet regions, allowing visible light to pass through. This occurs because the molecules consist of atoms linked together through single bonds, isolated double bonds, or benzene rings such as in the SU-8 polymer. There is increased absorption if the polymer contains significant lengths of adjacent double bonds. Scattering occurs if the polymer contains structures of a similar wavelength to the light passing through, and this is more likely to occur if it is appreciable crystalline. Scattering may make the material appear "milky". If there is a high degree of transparency, then the material is largely amorphous.

3.3.3.3 Electrical Properties

Polymers have dielectric, electrical conducting and ion-conducting properties. Their high electrical resistance makes them useful for insulators in electrical applications, and as dielectric materials for such devices as capacitors. Additional electrical properties include *ferroelectric* (the ability to acquire a permanent electric dipole), *piezoelectric* (the interaction between their states of stress or strain and the electric field across), and *photoelectric* (exposure to light can cause them to become conductors).

3.3.4 Preparation of “customised” SU-8 solutions

In the current research project, the SU-8 resist was prepared “in-house” as the straightforward utilisation of the commercially available SU-8 was not a satisfactory route for a number of reasons. First of all, the composition of the commercially available SU-8 is not provided and hence the amount of the photoinitiator used is not known and, as a result, it is not possible to control it depending on the particular requirements of every application, especially for stress control.

The commercially available SU-8 has a composition which mainly depends on the desired thickness of the resulted microstructures, and there is no consideration for the survival of any biomolecules which may be incorporated in the bulk material. This can be justified by the fact that there is no previous application of attempting to immobilise enzymes in bulk SU-8 polymer. The amount of contained solvent is also not known and thus it is not possible to modify for controlling the fluid’s viscosity.

The “customised” SU-8 resist was prepared by dissolving the resist Epon SU-8 (Epikote 157) in an organic solvent, the gamma-butyrolactone (GBL), and adding the curable photo-initiator triarylsulfonium hexafluoroantimonate salts.

In order to determine the final composition of the SU-8 resist, a large number of experiments were carried out aiming towards accomplishment of a number of objectives such as stress minimisation, acquired film thickness, survival capability of entrapped biomolecules and fluorescence indicator molecules, optical transparency etc.

The quantity of the solvent determines the viscosity and thereby the range of possible resist thicknesses to extend from tens of nm to μm or even mm. In all experiments, the composition of 40% SU-8 and 60% solvent (40/60) with different percentages of UV photoinitiator was used, as can be seen in Table 3.2. The amount of the added photoinitiator was subtracted from the solvent. The final product was left in the roller mixer for 96 hours and afterwards to mature for at least two weeks.

Table 3.2 Chemical compositions for preparing SU-8 resists with different percentages of photo-initiator.

<i>SU-8 Solutions</i>		<i>SU-8 granules (g)</i>	<i>GBL solvent (g)</i>	<i>UV photo-initiator (g)</i>
<i>Composition %SU-8 / % solvent</i>	<i>Photoinitiator concentration</i>			
40 / 60	1%	40	59	1
40 / 60	2.5%	40	57.5	2.5
40 / 60	5%	40	55	5
40 / 60	7.5%	40	52.5	7.5
40 / 60	10%	40	50	10

3.4 Outline of the Experimental Work

As described in Chapter 1, the main aim of the present project has been the investigation of new matrices for immobilisation of biomolecules and more specifically the suitability of SU-8 matrix which is of particular technological interest for micro-nano systems. The ultimate objective was the application of the above immobilised matrices in the field of micro-biosensors.

In order to accomplish the above aim, a number of specific aspects were experimentally investigated during the research project. Firstly, a comparison between utilising the commercially available SU-8 solutions against the “customised” SU-8 solutions was carried out. Solubility checks of the SU-8 pure resin and the enzyme glucose oxidase (GOx), in different organic solvents were performed. The chemicals were firstly tested separately and then in combination in the same solution. A thorough assessment of advantages and disadvantages of the above solutions followed and the optimum solution using specific solvent and photoinitiator percentage was obtained. Finally, a method for making SU-8 solutions was established with significant importance for the progress of the current research project. Measurements of the surface topography with optical microscope, optical interferometer (VEECO) and environmental scanning electron microscope (ESEM, XL-series PHILIPS) were performed. An electrochemical method

was used in order to check the activity of the immobilised enzyme in the SU-8 matrices. A detailed assessment of the suitability and biocompatibility of the SU-8 polymer as a matrix to encapsulate biomolecules such as enzymes was carried out. The optical indicators oxygen-sensitive ruthenium complex and pH sensitive HPTS were introduced in the matrices. The optical properties of the SU-8 materials were assessed using a fluorescence spectrophotometer. An investigation on the utilisation of microspheres entrapped in the established matrices was carried out.

All microfabrication processes presented in this thesis were performed in a clean room environment (CLASS 100) under strictly controlled conditions. It has to be mentioned, that all the detailed descriptions of the chemicals and the specific conditions involved in the aforementioned experiments will be presented in the following Chapters 4 and 5.

CHAPTER 4

INVESTIGATION INTO THE MICROFABRICATION PROCESS OF “CUSTOMISED” SU-8 FILMS

4.1 SU-8 Microfabrication Processing

4.1.1 Introduction

Microfabrication is a process used to construct objects with dimensions in the nanometer or micrometer to millimeter range. It utilises established semiconductor fabrication processes for integrated circuits, and augments these with processes especially developed for microfabrication. A sequence of process steps in a given order are used in order to produce a physical structure. The variety of process steps and materials leads to a large range of possible devices. Microfabricated objects or devices can be comprised of a range of miniature structures, including moving parts such as cantilevers and diaphragms, static structures such as flow channels and wells, chemically sensitive surfaces such as proteins and cells; and, electrical devices such as resistors and transistors.

The use of MEMS for biological purposes (BioMEMS) is growing rapidly providing with unique methods of producing devices on the same length scale as cells which can

interact with cells and biological molecules for both research and therapeutic applications including DNA sequencing, cell encapsulation, biosensors, chemical analysis systems and drug delivery.

Photolithographic processes are the cornerstone of microfabrication and resist patterning is crucial to the development of many microdevices. By using a thick photoresist, MEMS designers can often use the polymer itself as the structural material for mechanical, optical, and fluidic devices. Currently, the standard thick resist used by MEMS and BioMEMS engineers to develop microdevices using ultraviolet (UV) lithography is EPON SU-8 negative photoresist.

4.1.2 Microfabrication Steps

The standard soft microfabrication of UV-lithography processing steps of SU-8 are illustrated in Figure 4.1 and include:

- (1) pretreatment of the substrate and spin-coating of SU-8
- (2) prebake or pre-exposure bake,
- (3) UV exposure (usually between 320 to 450 nm)
- (3) post-exposure bake
- (4) development
- (5) hardbake (which is optional)

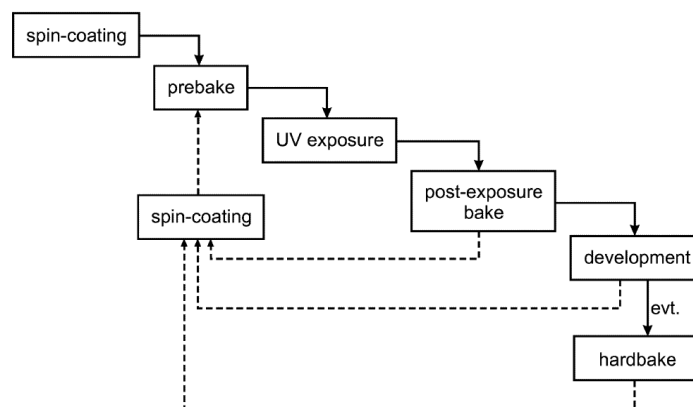


Figure 4.1 Schematic diagram of the processing steps for SU-8.

Dash lines show alternative steps for multi-layers spin-coating. Hardbaking is not a mandatory step.

The process parameters determine the final quality of the microstructures. The curing process of SU-8 is completed in two steps: formation of acid during optical exposure and thermal epoxy cross-linking during the post-exposure bake. A flood exposure or controlled hardbake is recommended to further cross-link the exposed SU-8 microstructures if they are going to be used as parts of the final products.

4.1.3 Pretreatment of the Silicon Wafers – Sacrificial Layers

In order to obtain good adhesion for SU-8 on a substrate, the substrate needs to be cleaned with acetone, isopropyl alcohol (IPA), and distilled water sequentially, and then dehydrated at 120°C for approximately 5 to 10 minutes on a hotplate. The substrate may also be primed using plasma oxygen immediately before spin-coating the resist in order to be cleaned for residual organic substances. In addition, an adhesion promoter may be used as required. In the present study, a 4 inch silicon wafer <100> was used as substrate. Since SU-8 is a highly cross-linked epoxy after UV-exposure and post-exposure bake, it is extremely difficult to release or remove it from the substrate, which is the silicon wafer. Subsequently, for the applications involving electroplating metals and alloys, and, stripping of cured SU-8, the vendor of SU-8, MicroChem company, recommends using OmniCoat before coating of SU-8. In addition, according to the literature other sacrificial layers could be utilised for releasing SU-8 structures, such as polystyrene, polymethyl methacrylate (PMMA), copper, chromium, gold etc. (Psoma & Jenkins, 2005; Hwang & Song, 2007; Wang *et al.*, 2009).

4.1.4 Spin-Coating of SU-8

SU-8 solution was used for spin coating in a range of different thicknesses, and the obtained thickness of the resulted film is dependent on several factors including: the viscosity of the resist used, the spin speed, and the total number of rotations. For thick layers, the final thickness also depends on the quantity of photoresist initially placed on the substrate. The vendor of SU-8, MicroChem, provides some spin-coating curves for different commercial SU-8 formulations, such as SU-8 5, SU-8 50, and SU-8 100. Some research laboratories have also developed their own spin-coat curves based on the

particular equipment used. Figure 4.2 presents some typical spin-coating curves of SU-8 from the commercial provider MicroChem company.

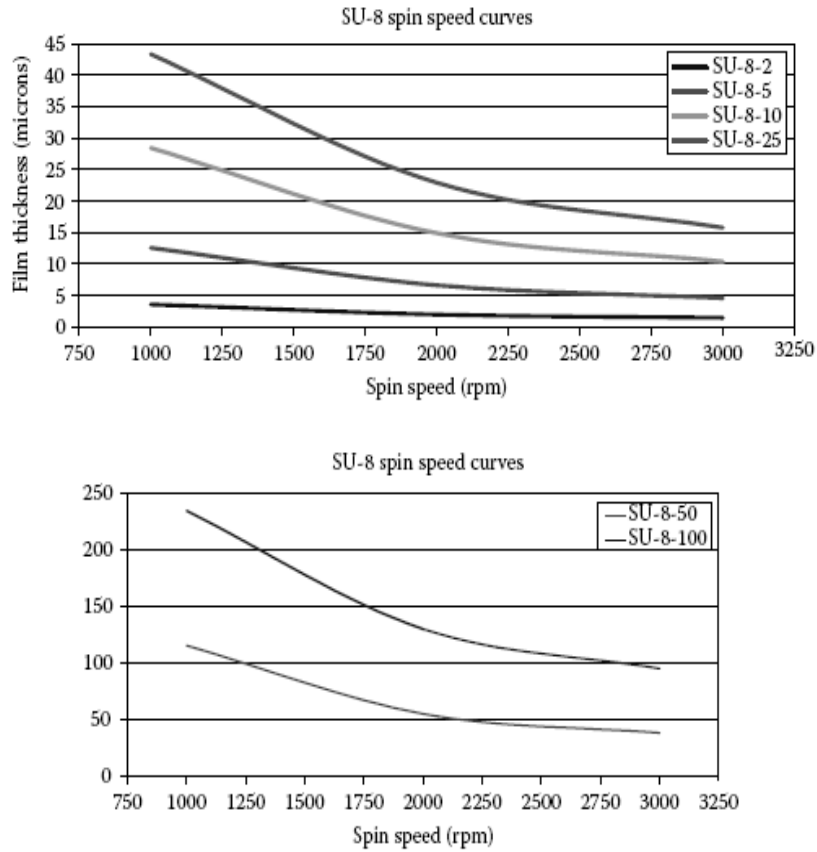


Figure 4.2 Selective SU-8 spin-speed versus film thickness curves.
(Source: MicroChem Corp., Newton, MA USA)

Bubbles formed during the spin-coating step may lead to reduced lithographic quality. In order to eliminate the bubbles in a resist film, the substrate should be placed on a flat and horizontal plate for approximately 2 to 10 hours before the prebake process. This is an especially critical step for accomplishing good quality of thick SU-8 film.

4.1.5 Soft Bake – Prebake

The spin-coated sample needs to be soft baked in order to cause evaporation of the solvent from the resist layer. The prebake is performed on a levelled hotplate usually at

a temperature of 95°C. Prebake time depends on the thickness of the SU-8 layer, for example, for 5 µm thick SU-8, a 6 min prebake time is sufficient, whereas a 200 µm thick layer, 3 hours are required. Ramping and stepping the soft bake temperature is often recommended for better lithography results. The glass temperature of the unexposed SU-8 photoresist is approximately between 50°C to 55°C. The prebake temperature of SU-8 must be higher than the glass transition temperature and usually a reflow of the resist occurs during the first minutes of the prebake step. This reflow is important for reducing the edge bead which appears in thick layer spin-coating SU-8 and degrades the contact conditions between mask and resist during UV-exposure. Hence, it is very critical to have a levelled hotplate in order to produce smooth, uniformly coated substrates.

4.1.6 UV - Exposure

A near UV (320 to 450 nm) light source is normally used for lithography of SU-8. As the wavelength of the light source increases, the absorbance of the light reduces and the transmission increases significantly. The transmission increases from 6% at $\lambda = 365\text{nm}$ to about 58% as the wavelength increases to 405nm. SU-8 has high actinic absorption for wavelengths less than 350nm, but is almost transparent and insensitive for wavelengths above 400nm. Because of the high absorption of SU-8 for light with shorter wavelengths, a light source dominated by shorter wavelength components often results in overexposure at the surface of the resist and underexposure at the bottom part of the resist layer. This is the main reason why UV-lithography of SU-8 using an *i*-line dominated light source, tends to produce microstructures with T-topping geometric distortions.

Another key parameter is the thickness of the resist that determines the required dosage of the exposure. Figure 4.3 shows two curves of required exposure dosage as function of the thickness of SU-8. MicroChem, the vendor of SU-8, advises that the user filters out the light with a wavelength lower than 350nm in order to improve lithography quality. For lithography of a very thick resist, multiple exposures are required to avoid overheating, scattering, and diffusion on the surface of the resist. Typically, exposures

need to be separated in 20 seconds (or less than $400\text{mJ}/\text{cm}^2$ per time) intervals with 60 seconds waiting periods in between. For a highly reflective substrate, the effect of the reflection needs to be taken into account in estimating the total exposure time. In the present research project the exposure time was calculated using the intensity value of the 365nm spectrum line of the mask aligner as it will be described below in the current chapter.

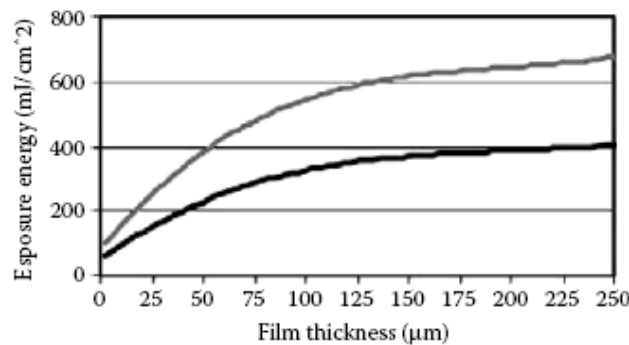


Figure 4.3 Calibration curves of exposure dosage versus film thickness of SU-8 films. (Source:MicroChem Corp.,Newton, MA.)

4.1.7 Post-exposure Bake (PEB)

SU-8 cross linking occurs during the post-exposure bake (PEB) only in regions that contain acid catalyst generated during the UV-exposure. The cross linking, or the curing step of SU-8, can be accomplished at room temperature. Post-exposure bake or postbake at a raised temperature facilitates the acceleration of the polymerisation process (Williams & Wang, 2004). The postbake is necessary because very little reaction can take place in the solid state where molecular motion is effectively frozen. In order to be effective, it must be carried out at temperatures greater than T_g (about 50°C in the solid resist film).

As cross linking occurs, the resist film properties may change in several ways: some shrinking may occur due to densification during cross linking formation and outgasing

of the solvent, and T_g will rise as the film becomes increasingly cross linked. As cross linking proceeds and the network gradually approaches completion, the crosslinking reaction will slow down and eventually stop. Subsequently, the final glass temperature of the material is dependent on the postbaking temperature. Typically, postbaking is performed on a levelled hotplate at a temperature of 95°C for a period of 15 to 20 minutes.

The cross-linking process of SU-8 may cause significant residual stress, which in turn may lead to cracks or de-bonding. In order to minimise possible residual stresses, wafer bowing, and cracking, rapid cooling from the postbake temperature should be avoided. For resist films with thicknesses more than 1000µm, ramping the postbake temperature down from 96°C should last for more than 8 hours. Another possible way of reducing the postbake stress is to use lower postbake temperatures, such as 55°C or 60°C, but longer baking times. This method would result in much lower thermal stress in comparison with using a postbake temperature of 96°C.

4.1.8 Development

After exposure and postbake, the sample is developed by SU-8 developer, which is propylene glycol methyl ether acetate (PGMEA). The development process can be optimised based on the experiment's agitation rate, development temperature, and SU-8 resist processing conditions. After the sample is developed by SU-8 developer, it is sometimes dipped into a fresh SU-8 developer to rinse, and afterwards it is rinsed with isopropyl alcohol (IPA) for 3 to 5 min. If white spots are present in the IPA, this is an indication that SU-8 is underdeveloped.

The sample needs to be immersed into SU-8 developer or rinsed with fresh SU-8 developer for further development. After the sample is completely developed, it needs to be rinsed using fresh IPA. If possible, avoiding a deionised water (DI) rinse is preferred. Finally, the sample is dried naturally or by nitrogen gas blow.

4.2 Influence of photoinitiator concentration on residual mechanical stress in SU-8 films

4.2.1 Introduction

Experiments were carried out in order to measure the residual mechanical stress generated during the different steps of the microfabrication process of SU-8 thin films using different photoinitiator concentrations in the resist composition. The main aim of this experimental work has been firstly to optimise the composition of the “customised” SU-8 resist which will be used in the following experiments, and, secondly to define the optimum microfabrication process steps of SU-8 in order to minimise the residual stresses which could cause serious problems during the encapsulation of the enzymes in the matrix with major problem the deactivation of the enzyme during the biosensor fabrication. In addition, the stress experiments can investigate and identify the causes for the generation of residual stresses. It was found that the major parameters that influence the generation of internal stresses were the exposure time, the postbake temperature and time, and, the concentration of the photoinitiator which was added in the SU-8 composition.

4.2.2 Experimental Setup

The 4 inch silicon wafers <100> were pretreated according to section 4.1.3 and at this stage a reference scan of the wafer for the stress measurements was taken using the profile-meter. Resist application was performed using a standard spinner (Karl Suss Gyrset) and constant dispense volume (4 ml) for a given thickness, and then it was allowed to relax for 15 min before baking. The soft-bake temperature was fixed at 75 °C for duration of 10 min on a hotplate. Subsequently, the resist film was exposed with a standard UV aligner (Karl Suss MA 6), and finally the cross-linked SU-8 was postbaked on a hotplate for 5 min.

In all microfabrication process steps, stress measurements were performed because stress was generated in the SU-8 films and wafers as a result of a thin film deposition from the beginning of the experiments. The deformation of the thin film has created

bending and compressing (compressive stress) or expansion (tensile stress) of the substrate surface. Careful monitoring of the thin film stress data was useful for reducing process variations.

The average stress was calculated according to the Stoney equation for stress in a thin-film layer deposited on a substrate, and it is as follows:

$$\sigma = \frac{1}{6R} \frac{E}{(1-\nu)} \frac{t_s^2}{t_f} \quad (\text{Eq. 2})$$

where

$$\frac{E}{(1-\nu)} = \text{wafer elastic constant}$$

σ = stress

t_s = wafer thickness

t_f = film thickness

R = radius of curvature

E = Young's Modulus for the wafer (substrate)

ν = Poisson's Ratio

The KLA-Tencor P-15 Profiler software was used for calculating the average stress values of the samples. In addition, the NewView 200 software for film applications of the interferometer Zygo (Zygo Corp.) was used for obtaining the surface topology images of the SU-8 films.

4.2.3 Influence on the SU-8 Films Due to Soft-bake Temperature

After coat-spinning the SU-8 thin films (from 1 μm to 15 μm) on the wafers, the softbake step on the stress effect was investigated. Different temperatures were used from 60°C to 160°C and also for different durations from 2 min to 30 min. Despite the high temperatures (up to 160°C) and the long duration (up to 30 min), only a small compressive stress in the range of 1 to 3.5 MPa was introduced for the film thickness of

1 μm to 15 μm on the wafer. The appearance of the stress is because of the difference between the thermal expansion coefficients (TECs) of the wafer and the SU-8 films.

However, this stress level is considered relatively low because during the cooling phase of the soft-bake, polymer chain re-arrangements take place in the resists that are not cross-linked. For this reason, in all experiments of this study a temperature of 75°C was used during soft-bake for a duration of 10 minutes.

4.2.4 Influence on the SU-8 Films due to UV-Exposure

It was observed that the main stress was generated as the cross-linked SU-8 started to cool down. Figure 4.4 shows the variation of the measured stress as a function of the exposure time for four different thicknesses of the 40/60 SU-8 that are equal to 1.2, 4, 7 and 11 μm . In this case, the concentration of the photo-initiator UV1 was set equal to 10%. A fast growth of the compressive stress level appears for all cases with the increase of the exposure time. At a given exposure time, the stress is found to be highest for the 1.2 μm film and reduces with the increase in thickness.

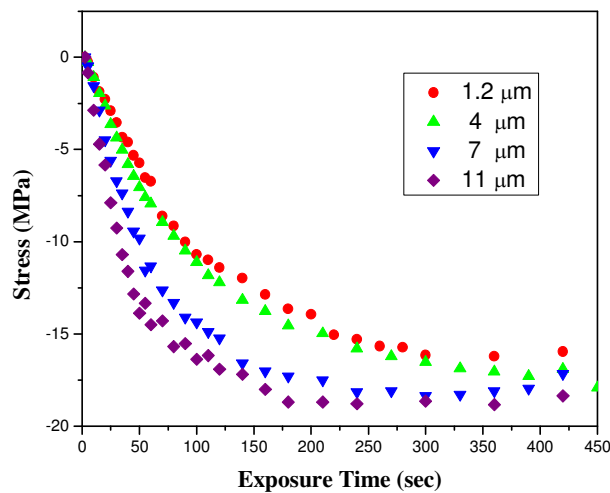


Figure 4.4 Variations of the measured stress as a function of the exposure time for different thickness of 40/60 SU-8 with 10% photoinitiator UV1.

Similar trends in the dependence of the residual stress on exposure time have been produced when using a 5% concentration of the photo-initiator. The experimental results from this investigation are presented in Figure 4.5 where four different thicknesses of the SU-8 film, equal to 1.4, 6.2, 8.3 and 11 μm , were considered. The increase in the compressive stress with exposure time is apparent and in addition the thickness variation has a considerable effect on stress levels.

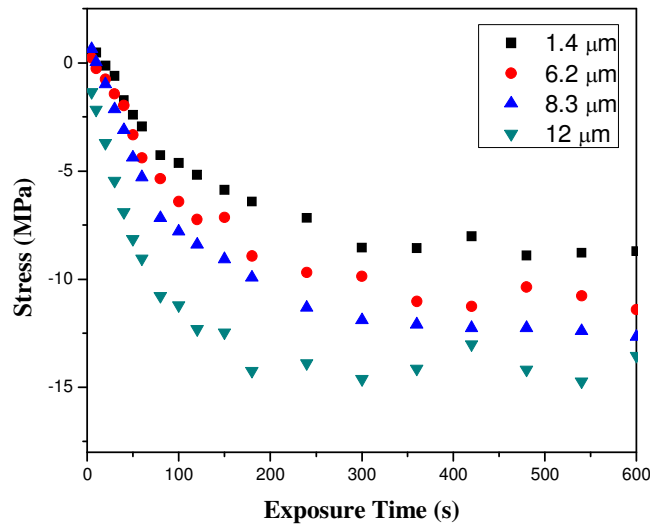


Figure 4.5 Variations of the measured stress as a function of the exposure time for different thickness of 40/60 SU-8 with 5% photoinitiator UV1.

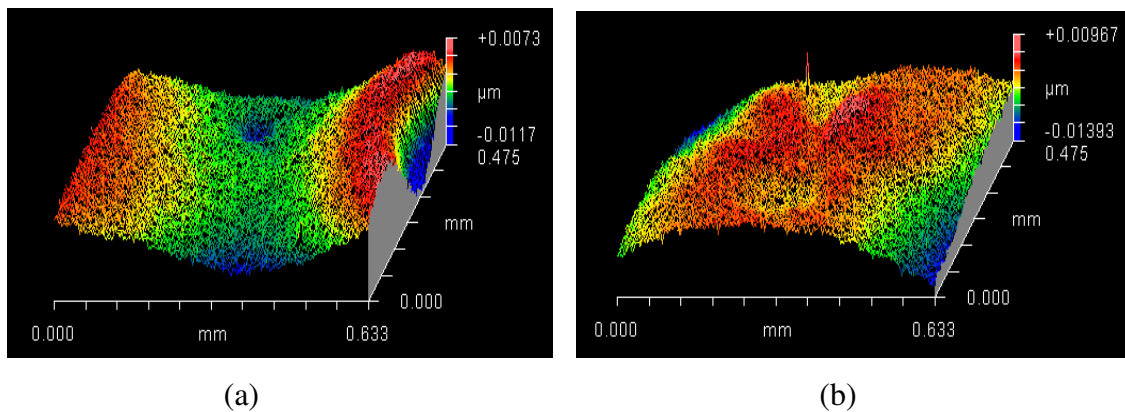


Figure 4.6 Interferometer images of the surface topology for 40/60 SU-8 film with 2.5% photo-initiator. (a) after the softbake at 75 °C (compressive stress) and (b) after the exposure time of 40s (tensile stress).

Figure 4.6(a) illustrates the surface topology of the SU-8 film with 2.5% photo-initiator after the soft baking process. As it can be observed, there is a deepening in the middle section and this is associated with a tensile stress at a low level (approximately 2MPa). In Figure 4.6(b), the morphology of the SU-8 film surface exhibits an opposite behaviour and the existence of a compressive stress after an exposure time of 40 sec. The stress levels increase significantly after the post-baking phase and they change rapidly becoming tensile (approximately 25MPa).

4.2.5 Influence of the percentage of the photo-initiator on the SU-8 films

Figure 4.7 presents the variation of the measured stress as a function of the exposure time for three different concentrations of the photo-initiator. The concentration of the photoinitiator appears to have a significant influence in the SU-8 thin films (with an approximate film thickness of 6.5 μ m) and its reduction from 10% to 1% is associated with a significant drop in the level of the residual stresses. However, by reducing this concentration, the exposure time has to be increased in order to accomplish the crosslinking of the resist. It was found that an SU-8 resist with at least 2.5% photo-initiator must be used in order to have reliable and repeatable structures in the UV-lithography.

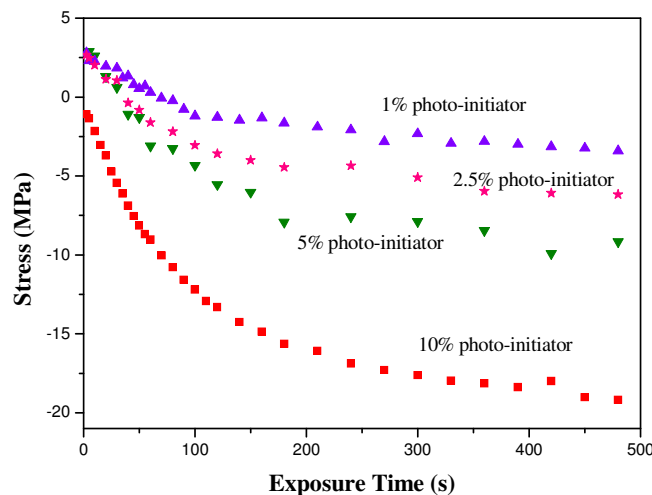


Figure 4.7 Variations of the measured stress as a function of the exposure time for three different concentrations photo-initiator UV1 of the 40/60 SU-8 resist.

4.2.6 Influence on the SU-8 films due to post-baking process

The influence of the duration of the postbake process on the measured residual stress is illustrated in Figure 4.8 where in all cases a tensile stress has been found to be present. The concentration of the photoinitiator has a significant influence on the stress levels and an increase in this concentration causes a marked increase in stress levels. The stress results of the different postbake temperatures were processed in such a way that all curves start from the same initial value of zero for the stress.

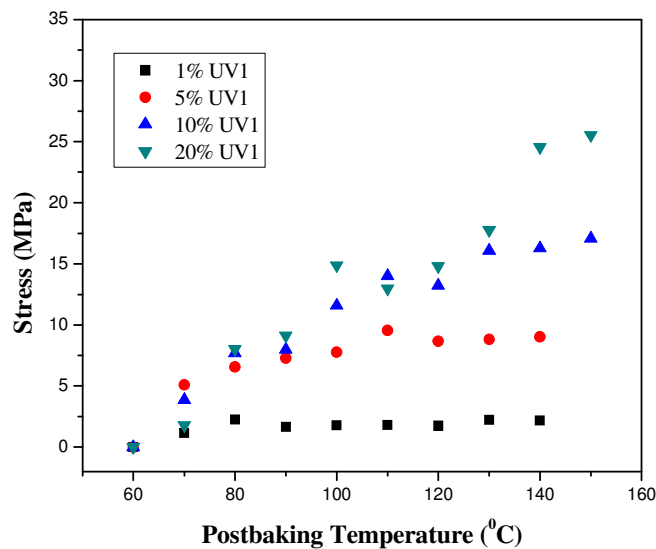


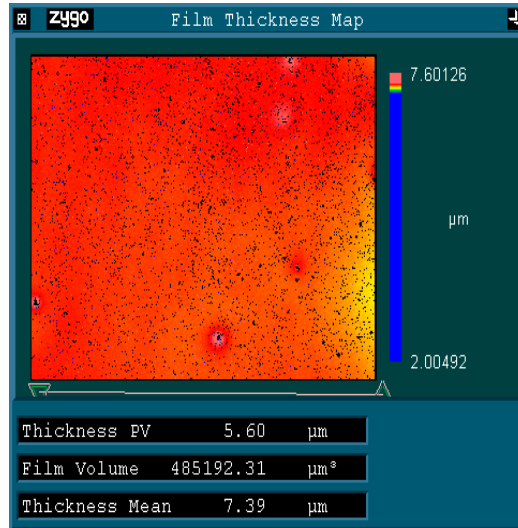
Figure 4.8 Variations of the measured stress as a function of the postbaking temperature for four different concentrations of the photo-initiator UV1 of the 40/60 SU-8 resist.

It was found that using a ramping hotplate during the postbake step the tensile stress was considerably reduced. This was significantly improved by adding relaxation times between all process steps.

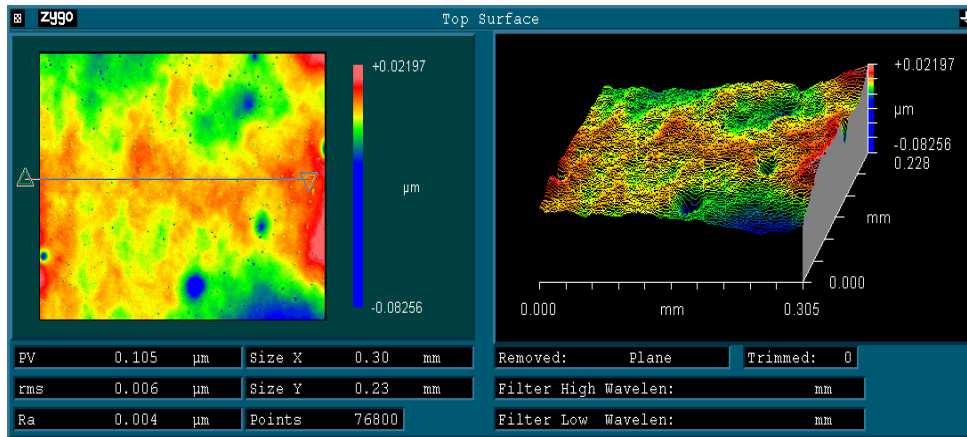
4.2.7 Influence of the addition of nanoparticles on the SU-8 films

Experiments were carried out in order to investigate the stress effect of SU-8 thin films with entrapped nanoparticles using different concentrations of photo-initiator. Figure 4.9 illustrates the surface topology of the SU-8 film with 2.5% photo-initiator after the

encapsulation of nanoparticles with a diameter of around 10nm. The softbake temperature was 75°C and the exposure time 40s. As it can be observed, there is a homogenous distribution of the nanoparticles inside the film.



(a)



(b)

Figure 4.9 Interferometer images of surface topology of the 40/60 SU-8 film.
 (a) Film thickness map, (b) planar and 3-D surface topology

The stress levels were found to be significantly reduced in comparison with the same SU-8 films without using nanoparticles. Finally, it was found that the new uniform SU-8 nanocomposite material/film had significantly reduced stress in comparison with the pure SU-8 film by a factor of 3 when using 5% and 2.5% photo-initiator UV1.

4.2.8 Sacrificial Layers for Releasing SU-8 Films

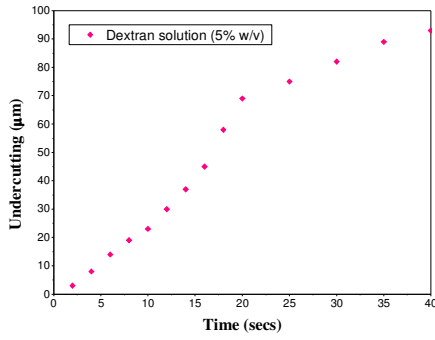
A range of materials were tested and compared as sacrificial layers for releasing SU-8 structures from the substrate, the silicon wafer. A dextran solution (5% w/v in distilled water), two polymers (polymethylmethacrylate (PMMA), and polystyrene), and, three metals (chromium, copper and aluminium) were investigated. The dextran solution and the polymers were deposited and the appropriate film thickness was achieved using a spin-coating process. Subsequently the films were baked at 90°C for 15 minutes. Deposition of the Cr, Al and Cu to different thickness on the silicon wafers was performed using a Nordiko plasma sputtering system. After the sacrificial layers were cured, the SU-8 was applied thus:

- (i) 4 ml of a SU-8 solution (50/50 SU-8/GBL with 2.5% photo-promoter) was placed onto the sacrificial layer and spun at 600 rpm for 150 seconds.
- (ii) Soft bake was carried out at 75 °C for a duration of 7 minutes.
- (iii) Exposure was applied using hard contact on Karl Suss MA6 mask aligner for 50 seconds.
- (iv) Post-exposure bake duration was 5 minutes.
- (v) Development time was 30 seconds in EC (Ethyl Lactate) solvent.

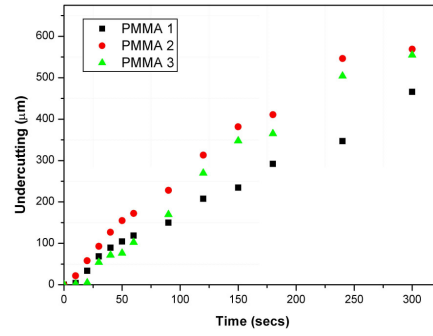
Finally, the samples were immersed in their appropriate etchant for measured units of time, and the level of undercut around the structures was measured (Figure 4.10).

Table 4.1 Sacrificial materials used and their etchants.

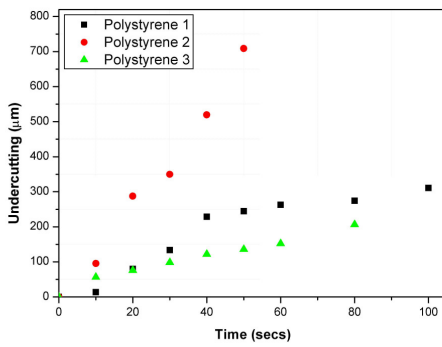
Sacrificial Materials	Dextran solution (5%)	PMMA	Poly-styrene	Al	Cr	Cu
Etchant Solutions	<i>Distilled water (DI)</i>	Acetone	Acetone	Al Etchant (<i>Rookwood Electronic Materials Ltd.</i>)	Cr Etchant 18 (<i>Rohmand Haas Electronic Mater.Ltd.</i>)	Cu Etchant (<i>Rookwood Electronic Materials Ltd.</i>)



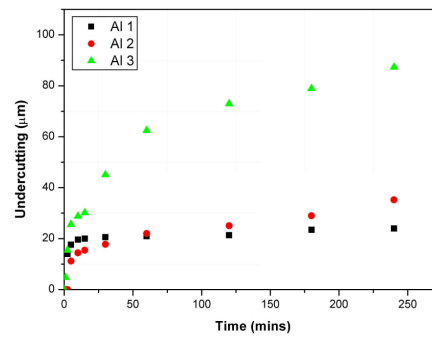
(a)



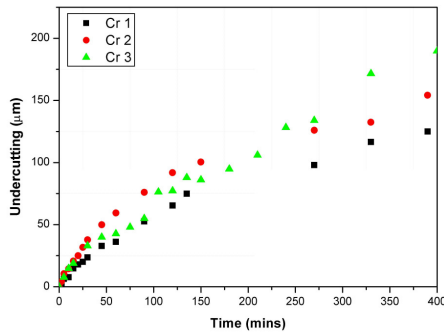
(b)



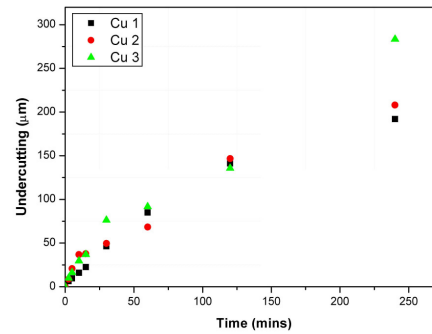
(c)



(d)



(e)



(f)

Figure 4.10 Undercutting of SU-8 structures using as sacrificial layer with: (a) dextran solution 5% ($5.3\mu\text{m}$), (b) PMMA (PMMA1:100nm, PMMA2:250nm, PMMA3:420nm), (c) Polystyrene (Poly1:1.2 μm , Poly2:1.6 μm , Poly3:5.8 μm), (d) Al (Al1=25nm, Al2=65nm, Al3=100nm), (e) Cr (Cr1:100nm, Cr2:225nm, Cr3:410nm) and (f). Cu (Cu1:150nm, Cu2:350nm, Cu3:600nm).

Measurements were made using an optical microscope with an integral digital camera. The system was calibrated using and NPL (National Physical Laboratories, UK) - standard grid pattern. Two structure-types were measured; large block (600 μm x 600 μm) and smaller lines (18 μm x 100 μm). The complete list of materials and their etchants are shown in Table 4.1. The factors were assessed included the quality of the SU-8 structures (by SEM examination before and after release), effect of changing etchant concentrations, monitoring of the undercutting process (through depth measurement with time), and the time taken for the successful release process. Overall, from the complete set of experimental investigations that were carried out and the assessment of the obtained results, it was found that dextran solution (5%w/v) and metals were the best choice as sacrificial layers under SU-8 for structures up to 200 μm in length, whereas polymers were a better option for larger structures (up to 600 μm in length).

4.2.9 Conclusions from the SU-8 Stress Experiments

Internal residual stress occurs in negative tone photoresist SU-8 caused by the difference between the coefficients of thermal expansion of the resist layer and the substrate. The network density of the exposed and postbaked photoresist also influences the value of stress. Stress reduction can be attained by optimising the process parameters as well as by a modification of the chemical composition of the photoresist. This stress can be significantly reduced by lowering the concentration of the photoinitiator both during the exposure and the postbake process. The minimum photoinitiator concentration must be at 2.5% in order to accomplish proper lithography.

In addition, during the process steps of the softbake and the postbake a slow warming up and also cooling down procedure using a ramping hotplate, with long relaxation times after post exposure bake and maybe special mask design can be implemented in order to improve the stress behavior of the photoresist. In addition, low stress thin films of SU-8 can be used for encapsulating nanoparticles or to improve the biocompatibility of materials used in the field of biosensors. In addition, the low stress new SU-8 nanocomposite films can be used in coating for moving parts or micro- nano structures

and also in other MEMS applications. Finally, the sacrificial layer which was selected for the current project was the dextran solution (5% w/v) due to its etchant which is distilled water and its simplicity, its fast release time and the most importantly its inertness with the enzyme glucose oxidase (GOx). The sacrificial layer, OmniCoat, which is recommended by the company MicroChem for releasing the commercially available SU-8 resist was not employed in the present project because of its unknown chemical composition and its uncertain effect on the final SU-8 structures which incorporates the immobilised glucose oxidase enzyme.

4.3 Experimental Procedures for the Preparation and Microfabrication of SU-8 Films for Glucose Biosensor Application

4.3.1 Specific SU-8 Composition

As described above, SU-8 is one of the most widely used polymers in the field of MEMS and in combination with its high biocompatibility it becomes very attractive for BioMEMS applications. In the majority of the reported applications, the commercially available SU-8 solutions are used, however, taking into consideration the findings from the stress experiments of the SU-8 films and the importance of the percentage of photoinitiator used in the photoresist composition, in combination with the specific biosensor application (see details in section 3.2.4) of the current research project, a “customised” SU-8 solution was definitely necessary to be defined and optimised. For this reason, it was decided to control and customise the composition of SU-8 solutions, which included the solid SU-8 granules, the solvent and the photoinitiator.

In the previous sections of the current chapter, a detailed analysis was presented and one of the outcomes was that a 2.5% of the photoinitiator could be used with obvious advantages for the preparation of the optimum SU-8 composition. The next experiment involved the solvent investigation. A number of organic solvents were tested such as cyclohexanone, polyethylene glycol, gamma-butyrolactone (GBL), tetrahydrofuran, ethanol, acetonitrile, 2-methoxy-1-methylethyl-acetate (PGMA) and propylene carbonate. These chemicals were mainly tested in terms of solubility with the

commercially available solid SU-8 granules and, simultaneously, the solubility and compatibility with the enzyme glucose oxidase (GOx) regarding the remaining activity and functionality of the enzyme. It was found that the best solvent candidates for the dilution of the solid SU-8 were GBL, propylene carbonate, PGMA, tetrahydrofuran, cyclohexane and polyethylene glycol. Unfortunately, the enzyme glucose oxidase was not directly diluted in the above organic solvents. This problem was solved by the initial dilution of the enzyme in very small amounts of distilled water or phosphate buffer in the range of few hundreds of μl , and, then the resulted solution was mixed with the solvent. From the number of solvents tested, it was found that the best solvents were GBL and ethanol. It is also reported in the literature that the best way to dilute the glucose oxidase in alcoholic solvents such as ethanol, methanol and isopropanol, it is to dissolve the enzyme firstly in phosphate buffer and then to mix it with the solvent (Kröger *et al.*, 1998; Cosnier *et al.*, 1998). As a result, the chosen solvent for the optimum SU-8 composition was GBL, because the solid SU-8 was not dissolved in ethanol as was mentioned earlier.

Subsequently, the preparation of the optimum SU-8 photoresist composition (total volume 100ml, with 40% SU-8 and 60% solvent (40/60) and 2,5% photoinitiator) was performed as follows:

- (a) Firstly, the commercially available solid uneven beads of the SU-8 resist were smashed to a very fine powder (40 g), and
- (b) it was mixed with GBL solvent (57.5g) and
- (c) the final solution was placed in an ultrasonic bath for an hour time.
- (d) Then the solution was left on a chemical shaker with smooth movements at 37°C for 96 hours.
- (e) In a cleanroom environment, an amount of 2.5g of the photoinitiator was added in the solution and then was left in ultrasound bath for a period of one hour.
- (f) The final solution was left to mature for at least two weeks (Figure 4.11).

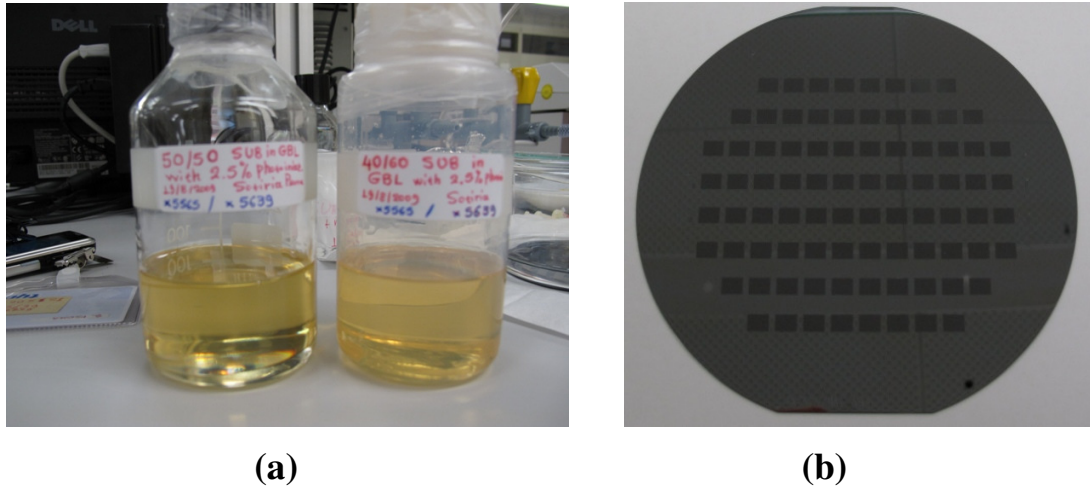


Figure 4.11 (a) “Customised” SU-8 solutions without adding the photoinitiator, (b) resulted SU-8 films/structures.

4.3.2 Specific Microfabrication process of Optimum SU-8 Films

Firstly, the silicon wafers were pretreated and cleaned according to section 4.1.3, in order to remove dirt and residual organics. A layer of dextran solution (5% w/v in distilled water) was added on the surface of the clean wafers. More specifically, 3 ml of this dextran solution was dispensed onto each wafer and spun at a speed of 500 rpm for 5 seconds which afterwards was immediately increased to 1000 rpm for 30 seconds, and, then it was soft baked on a hotplate at 150°C for 2 minutes.

The resulting uniform layer of the dextran solution served as sacrificial material in order to release the SU-8 structures. Then the standard microfabrication process steps for SU-8 resist, which have been described in details in the beginning of this chapter, took place. A basic schematic diagram of the microfabrication process steps of the SU-8 photoresist can be observed in Figure 4.12.

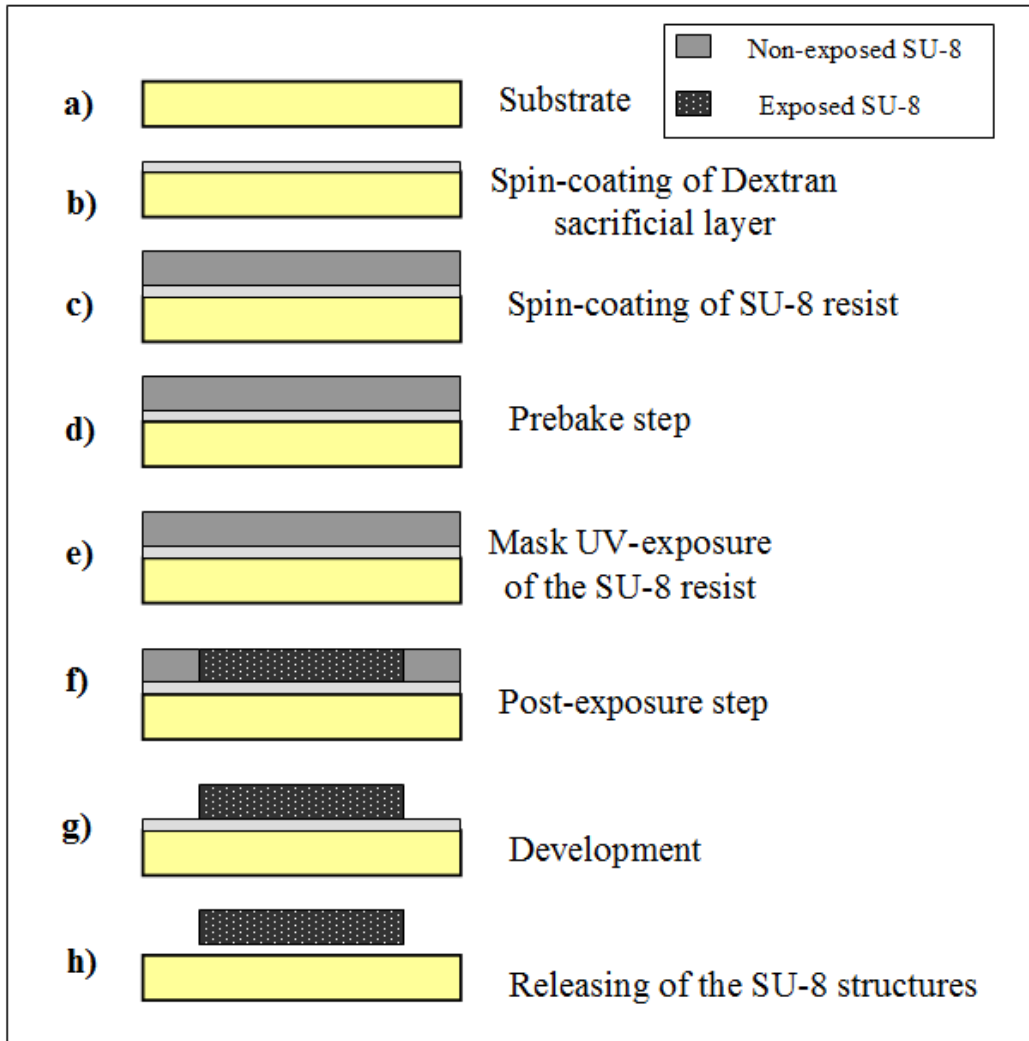


Figure 4.12 Basic microfabrication process of “customised” SU-8.

More specifically, 4ml of the “customised” SU-8 resist was spin-coated on the wafer with a spin speed 500rpm for 5 seconds and then immediately increased to 1000rpm for 30 seconds and allowed to relax for 15 minutes before soft-bake. The details of the soft-bake step, which is similar to that used and for the postbake step, are described in Figure 4.13, and were implemented through a programmable ramping hotplate. Subsequently, the resist film was exposed ($250\text{mJ}/\text{cm}^2$) with a standard UV aligner (Karl Suss MA6) using a quartz mask. The design of the mask was chosen to be a repeated pattern of a simple rectangular shape with dimensions of 5mm x 4mm.

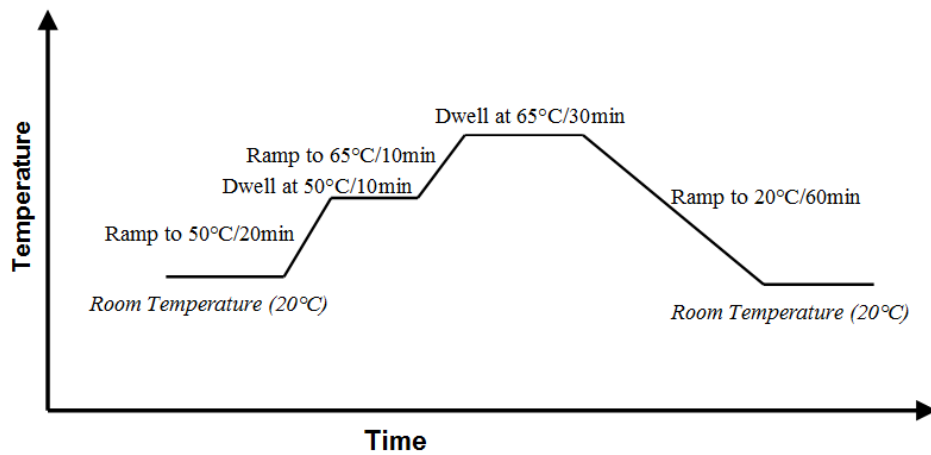


Figure 4.13 Temperature profile of prebake and post-exposure microfabrication steps of SU-8 films (aprox. $5.5\mu\text{m}$) (40/60 SU-8 film with 2.5% photo-initiator).

The resulted SU-8 structures after the end of the microfabrication process steps can be observed in Figure 4.11(b). The exposed cross-linked structures were followed the postbake step according to Figure 4.12. Afterwards, they were developed in PGMEA (aprox. 60 sec) and were rinsed in isopropanol following the details in section 4.1.8.

After processing, the resulted SU-8 films were highly transparent, without any evidence of cracks, easy to handle and separate, and, with an approximate thickness of $5.4\mu\text{m}$. Eventually, the structures were released in distilled water and collected and stored in 10mM phosphate buffer solution in the fridge (Figure 4.14).



Figure 4.14 Final SU-8 films/structures.

4.3.3 Enzyme and Fluorescent Indicator Immobilisation in SU-8 Films

For the experiments which required enzyme (glucose oxidase) immobilisation and / or the encapsulation of fluorescent indicator (tris(4,7-diphenyl-1,10-phenanthroline) ruthenium(II) dichloride complex) or HPTS in the bulk SU-8 films, the same microfabrication process as described in the previous section was followed, with the main difference being in the composition of the SU-8 solution. More specifically, the glucose oxidase solution and / or the indicator solution was added to the “customised” SU-8 solution (4ml) and was shaken gently trying to avoid generation of bubbles before the spin-coating step (details about specific quantities of the enzyme and the fluorescent indicator are given in Chapter 5).

As mentioned above, the enzyme was dissolved in a 10mM phosphate buffer solution pH 7.4. A number of experiments were performed in order to establish the optimum added enzyme quantity in a 4ml SU-8 solution. This standard enzyme added quantity was 10mg of glucose oxidase (141,200 units/g) diluted in 300 μ l of phosphate buffer 10mM, pH7.4. The main problem appeared to be that the solution became opaque with bad quality UV-exposure when the amount of the enzyme solution exceeded a certain quantity, usually 200 μ l. In addition, it was important for the fluorescent indicator to be dissolved in the same solvent as SU-8, which was GBL.

The oxygen-sensitive fluorescent indicator tris(4,7-diphenyl-1,10-phenanthroline) ruthenium(II) dichloride complex was possible to be dissolved in GBL. However, the pH-sensitive fluorescent indicator HPTS did not dissolve in GBL but in a phosphate buffer and this produced opaque structures with little transparency which had disappointing results during the fluorescence spectroscopy measurements (very low and noisy signal).

Consequently, the SU-8 structures used in the following Chapter, for the biosensor investigations, were:

- (i) plain “customised” SU-8 films/structures as a reference,

- (ii) “customised” SU-8 films/structures with glucose oxidase immobilisation with different concentration/activity in bulk structure,
- (iii) “customised” SU-8 films/structures with fluorescent indicator encapsulation,
- (iv) “customised” SU-8 structures with simultaneously enzyme and fluorescent indicator encapsulation in bulk structures.

CHAPTER 5

EXPERIMENTAL INVESTIGATION FOR THE PROOF OF CONCEPT OF THE SU-8 GLUCOSE BIOSENSOR

5.1 Introduction

This chapter describes the experimental results which were carried out in order to assess the SU-8 glucose biosensor after the completed microfabrication process and is divided into three main sections.

- In the first part, the surface topology measurements, which were obtained for surface characterisation of the SU-8 films without and with encapsulated enzyme, are presented.
- In the second part, the SU-8 film with and without encapsulated enzyme is used in order to act as a catalyst for the enzymatic oxidation of glucose and the amount of hydrogen peroxide that is produced is measured through an amperometric method.
- In the third part, the same enzymatic reaction is used and the amount of consumed oxygen is measured with fluorescence spectroscopy through the utilisation of an oxygen sensitive fluorescent indicator. This may form the basis for the development of an optical glucose micro-biosensor.

5.2 Characterisation of SU-8 Films with Immobilised Enzyme GOx

As it was described in the previous Chapter, a method for preparing the SU-8 solutions was established which had a significant impact on the progress of the research project. The next step was to find the most appropriate type of microstructure for the SU-8 matrix and the microfabrication process which was required in order to achieve this. A rectangular film with dimensions of 5mm x 4mm and with a thickness of around 5 μ m was eventually utilised. This shape was quite easy to be lifted from the wafer using a sacrificial layer of dextran solution. An already existing mask with a pattern of 84 rectangular shapes with the aforementioned dimensions was utilised.

The encapsulation of the enzyme GOx in the SU-8 solution was accomplished according to section 4.3.3. This technique was finally selected and tested regarding the activity of the enzyme, glucose oxidase, after the microfabrication process. The resulted structures with and without encapsulated enzyme were observed under an optical microscope. In addition, the distribution of enzyme molecules on the film's surface was observed in an optical interferometer (VEECO) and an environmental scanning electron microscope (ESEM, XL-series PHILIPS).

During the work for identifying the optimum microfabrication process it was found that it is necessary to leave the "customised" SU-8 solution for a period of at least two weeks (as it was mentioned in the previous chapter) in order to mature allowing all the SU-8 crystals to fully dissolve themselves in the solvent. In Figure 5.1, a 3-D and a planar image taken from the optical interferometer are presented for a film which was left to mature for only one week. As it can be observed, there is a distribution of surface cracks which made the film very fragile and difficult to handle. The observation of these films under the optical microscope, showed the existence of randomly distribution of crystalline structures on the whole film.

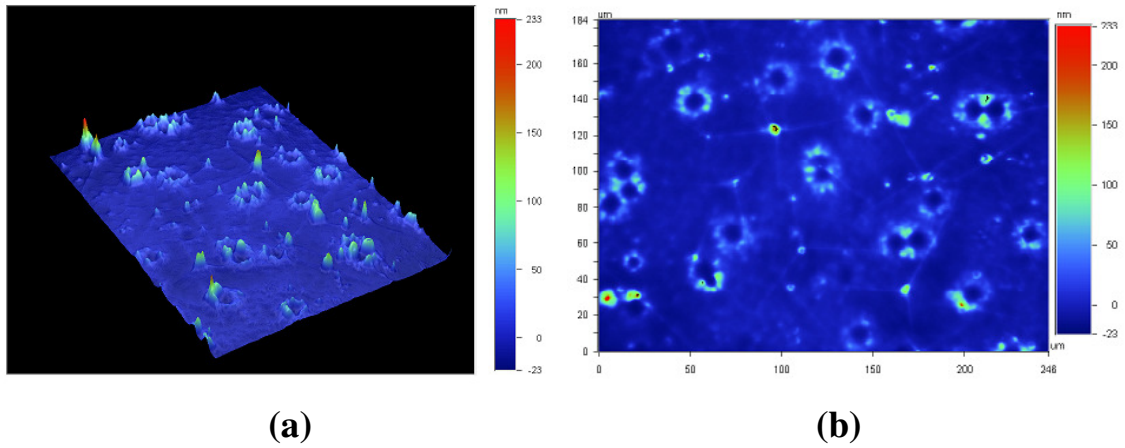


Figure 5.1 Interferometer images of plain SU-8 films (prepared from one week matured solution prior to film microfabrication) (a) 3-D image, and (b) planar image.

In Figure 5.2, the illustrated surface topology images from the optical interferometer were taken from SU-8 films that were left for a period of two weeks to mature. A smooth surface is shown and there is no presence of cracks and the structure attained very good strength properties.

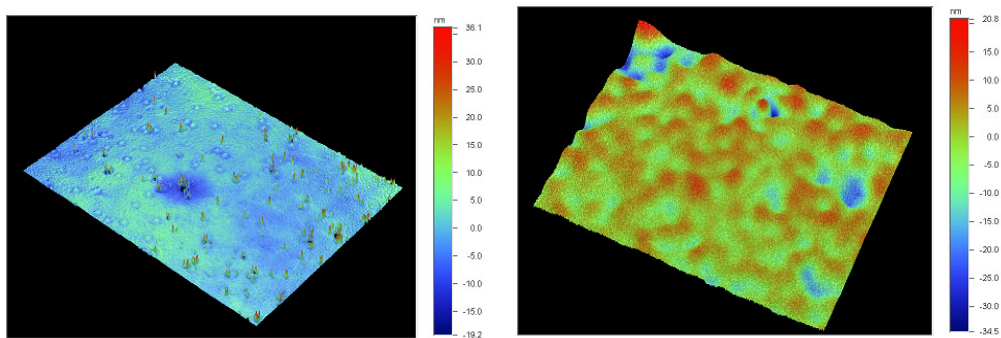


Figure 5.2 Interferometer 3-D images of two different plain SU-8 films (prepared from two weeks matured solution prior to film microfabrication)

Following the GOx encapsulation in the SU-8 microstructure, a number of surface topology images were obtained in order to assess the effect of the enzyme presence on the topological characteristics. These pictures are illustrated in Figure 5.3 in terms of 3-D and planar representations.

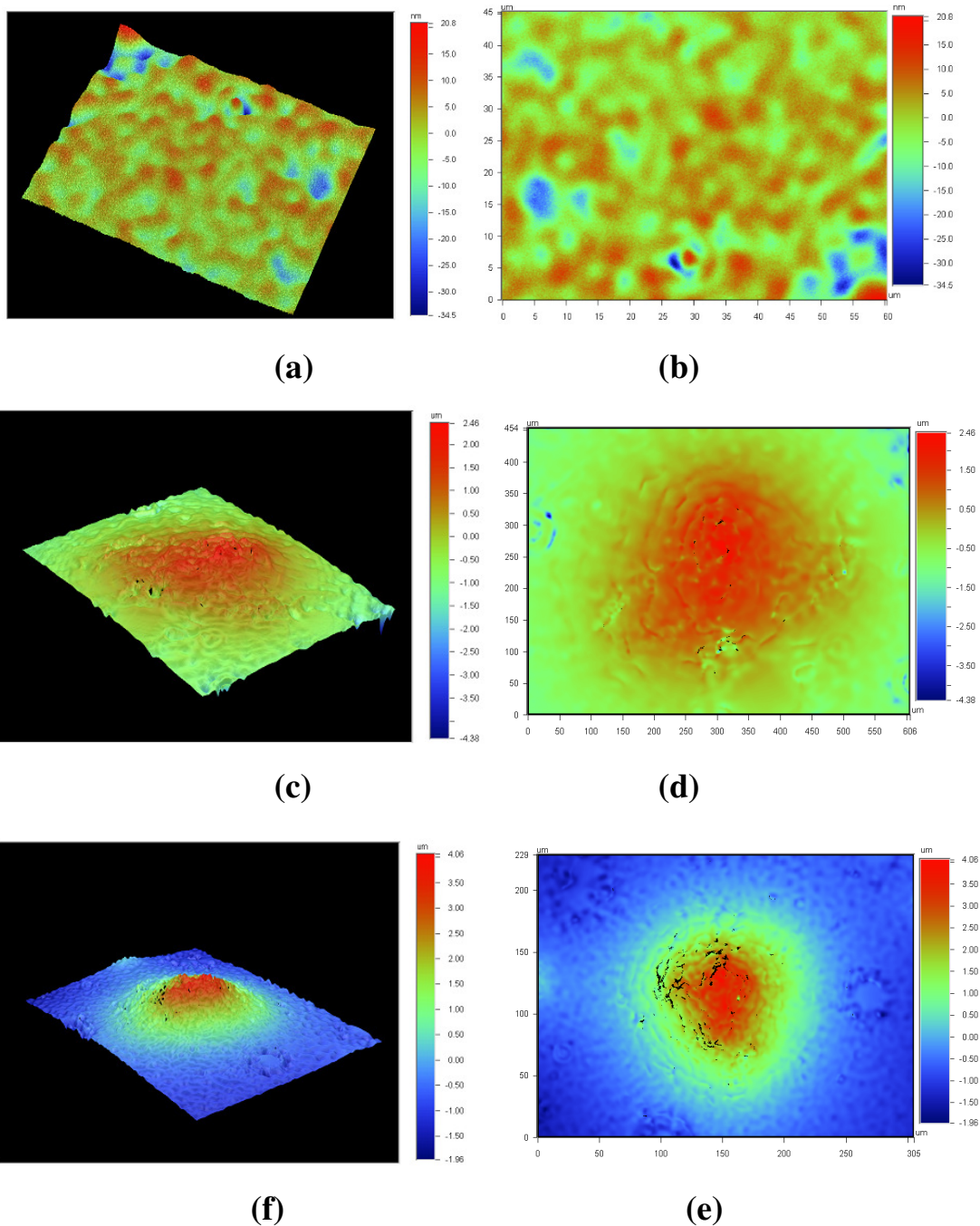


Figure 5.3 Interferometer images of surface topography of SU-8 films: (a) 3-D view, and (b) planar view of plain SU-8 film; (c) 3-D view, and (d) planar view of GOx (5mg) loaded SU-8 film; (f) 3-D view, and (e) planar view of GOx (10mg) loaded SU-8 film.

The central red-coloured region of the surface is elevated by a few (2 to 4) micrometers and is the area where bulk enzyme molecules are concentrated. This pattern was found

to be uniformly distributed on the whole film surface which was scanned and was not present in the plain SU-8 films, where the mean elevation varied in the range of few nanometers.

In Figure 5.4, surface images obtained with a Scanning Electron Microscope (SEM) from a plain SU-8 film and from a film with immobilized enzyme. The plain SU-8 film presents a very uniform, clear and smooth surface. The spot which appears on the surface is due to the presence of dirt. From a careful observation of the film with enzyme, it can be found that clusters of enzyme molecules are formed on the film's surface whereas the remaining surface remains uninterrupted and uniform. The red marked region of Figure 5.4 (b) indicates the GOx molecules cluster. This observation agrees with the patterns identified in the scan images from the optical interferometer.

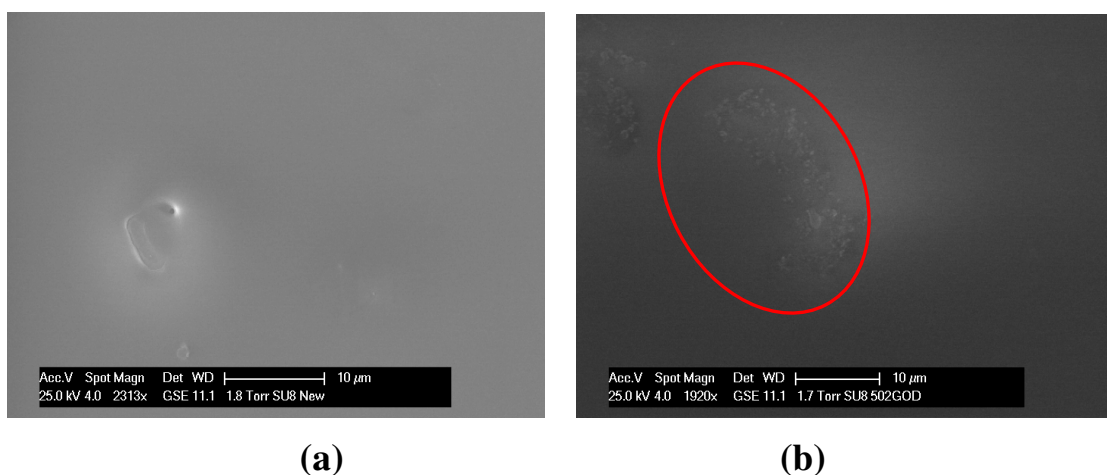


Figure 5.4 Comparison of SEM pictures of surface topography of (a) plain SU-8 films (magnification: 2313x) and (b) SU-8 films with immobilised enzyme (magnification: 1920x).

Higher resolution SEM images are presented in Figure 5.5 where the magnification is approximately 10 to 15 times larger than the one used in the previous images of Figure 5.4. The presence of the clusters of GOx molecules modifies the surface morphology as

it is apparent in Figure 5.4(b). The reported diameter size of GOx molecules in the literature is the region of 8 to 15nm (Lvov *et al.*, 1996; Ram *et al.*, 2000). The white patches that are present in this image are due to the remaining salt from the evaporated phosphate buffer used to keep the SU-8 films. Images from different regions of the same SU-8 film are illustrated in Figure 5.6 where the same patters of bulk enzyme distributions on the surface are discerned.

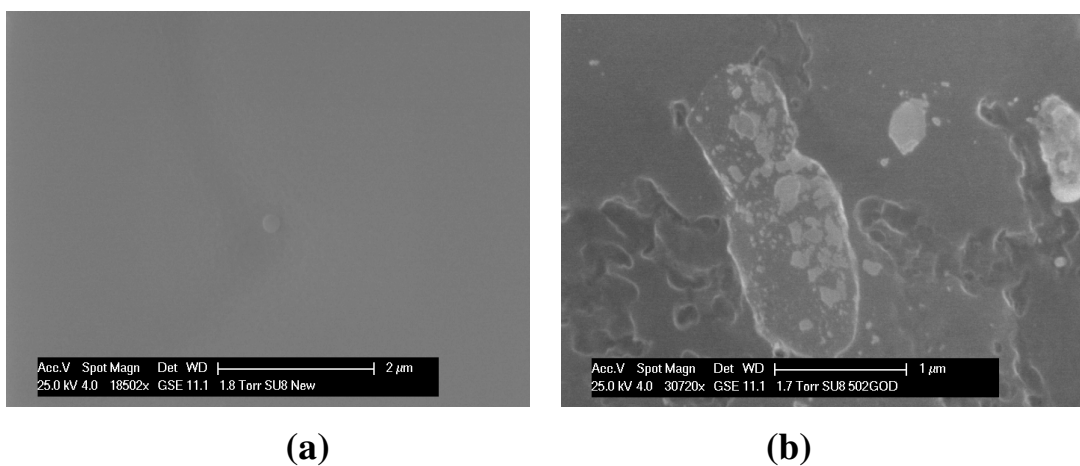


Figure 5.5 SEM pictures of surface topography of (a) plain SU-8 films (magnification: 18502x); (b) SU-8 films with immobilised enzyme (magnification: 30720x).

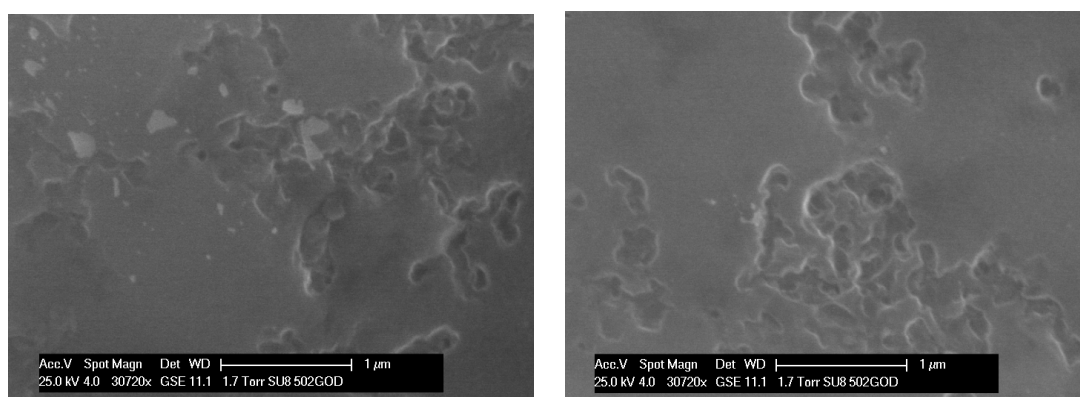


Figure 5.6 SEM pictures of surface topography of SU-8 film with immobilised GOx in two different regions (magnification: 30720x).

5.3 Amperometric Measurements of SU-8 Films with Immobilised Enzyme

5.3.1 Enzymatic Reaction

In order to assess whether the immobilised enzyme remained active inside the SU-8 matrix, an experimental investigation was carried out using an electrochemical method (amperometric detection of hydrogen peroxide) to check the activity of the enzyme.

The most widely used method for detecting and measuring glucose in biosensor applications is the enzymatic oxidation of glucose in the presence of oxygen which produces gluconic acid and hydrogen peroxide.



In order to define the glucose concentration, the used methods usually measure the oxygen consumption or the production of either hydrogen peroxide or gluconic acid which is related to pH changes. In the present study, the above reaction was utilised to detect different levels of glucose concentration in a solution through the further oxidation of the produced hydrogen peroxide and the measurement of the associated electric current. Consequently, the present method is an indirect method of glucose measurement.

Two different experimental set-up arrangements with different glass cells are utilised for carrying out the amperometric measurements. In both cases, the experimental set-up consisted of a measurement glass cell, the electrodes and the computerised data acquisition system. The viability of the enzyme was tested by measuring its ability to produce hydrogen peroxide upon exposure to glucose. The first experimental set-up was simpler and was used for a preliminary assessment and the second one was more complicated and provided with a better control of the experimental conditions. Both experimental arrangements are described below.

5.3.2 First Experimental Set-up

The first experimental set-up is depicted in Figure 5.7 and consists of a measurement glass cell, the electrodes and the computerised data acquisition system. The measurement cell used is illustrated in Figure 5.8. 40 ml of PBS was introduced in a thermostatted titration vessel (Metrohm 6.1418.110), a number of SU-8 platelets were added, ensuring that they remained in the proximity of the bottom of the vessel.

Electrochemical measurements were performed using a 3-electrode set-up with platinum working and counter electrode (Metrohm 6.0301.100, resp. 6.305.100) and a Ag/AgCl reference electrode (Metrohm 6.0733.100). The working electrode was polarised at +650 mV with respect to the reference electrode. In every experiment, 5 films were used to offer a larger surface area and hence provide higher volume of reaction products allowing an easier detection.

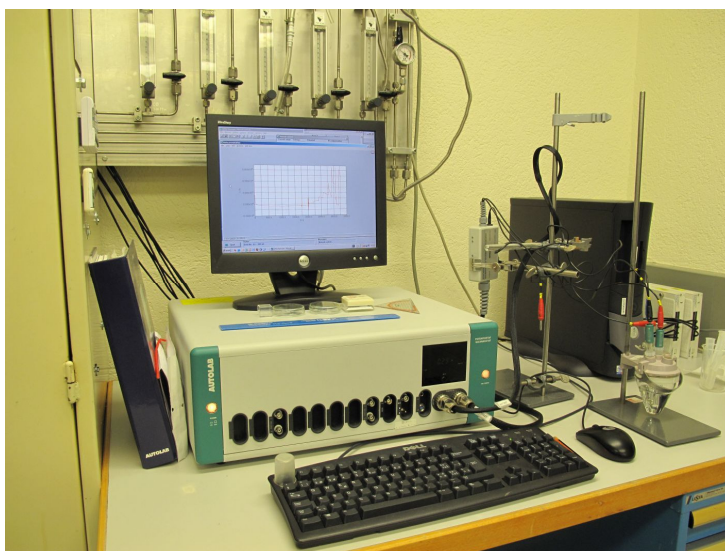


Figure 5.7 Amperometric experimental set-up.

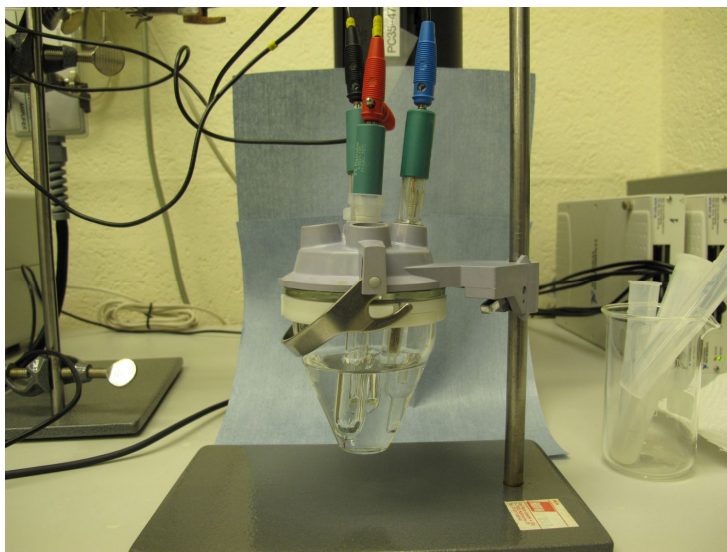


Figure 5.8 Measurement glass cell for the first experimental set-up.

SU-8 films without enzyme were used as reference at the outset and they showed negligible variation in the observed electric current during the addition of glucose in the measurement cell which occurred at a time of approximately 625 seconds after the initiation of the experiment (Figure 5.9). After the completion of the experimental set-up, the produced electric current was monitored in a continuous manner. When the level of the detected current was stabilised, a controlled amount of glucose was added in the solution (0.25 mM) and the response in the level of the measured electric current was observed despite the poor conditions of mixing through stirring. The presence of the enzyme causes the enzymatic reaction of glucose to gluconic acid and hydrogen peroxide, as described above, and the produced electric current is proportional to the glucose concentration.

SU-8 films without enzyme were used as reference at the outset and they showed negligible variation in the observed electric current during the addition of glucose in the measurement cell which occurred at a time of approximately 625 seconds after the initiation of the experiment, as it is illustrated in Figure 5.9.

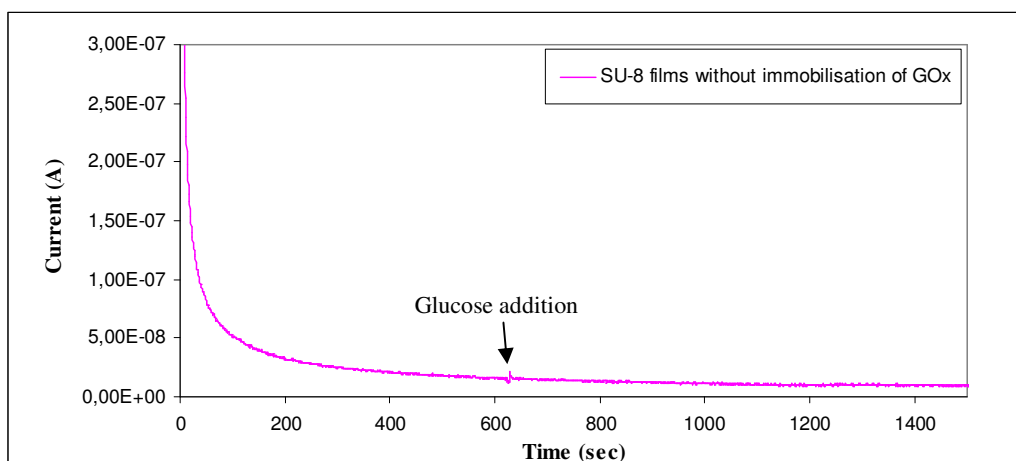


Figure 5.9 *SU-8 films without immobilised GOx with added glucose.*

In more details, standard SU-8 platelets with GOx immobilised were placed close at the bottom of a glass cell. Approximately 20 to 25 minutes after initiating the measurement, the current had stabilised and 40 μl of a 1 M glucose solution was added to the buffer solution. The signal was immediately increased and stabilised after a few minutes. Subsequent additions showed an increase in the signal. In Figure 5.10 an example of a raw measurement graph is presented.

It has to be mentioned that the solution was not stirred during this experiment and consequently the exact concentration is not known. In a proof of principle, the electrode was retracted from the surface of the platelets, during which the signal decreased to virtually zero current at large distance and increased upon re-approaching the platelets. The same films used in the previous experiment, were tested again one week after and showed similar behaviour, as it is depicted in Figure 5.11 proving that the enzyme remains active inside the SU-8 matrix. Similar results were acquired two months later.

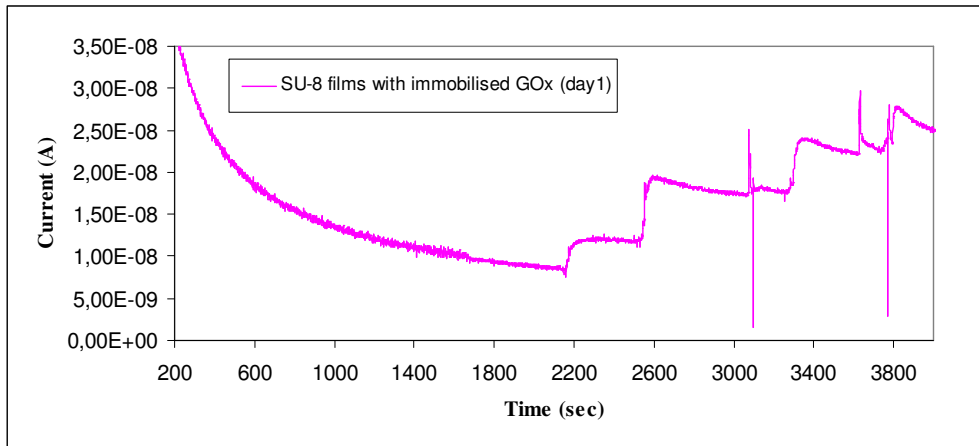


Figure 5.10 *SU-8 films with immobilised GOx during oxidation (average film thickness 5.7 μ m).*

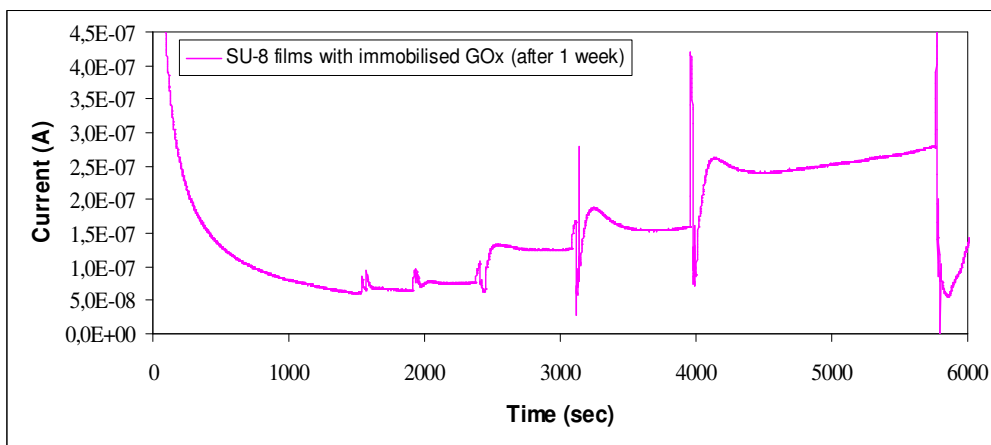


Figure 5.11 *SU-8 films with immobilised GOx during oxidation after 1 week from the first measurement (average film thickness 5.7 μ m).*

A different set of experiments were also carried out, using films with immobilised enzyme, of the same standard dimensions but of three different average thicknesses equal to approximately 2.4 μ m, 4.2 μ m and 8.8 μ m. All other remaining parameters of the microfabrication process remained unchanged. Figures 5.12 to 5.14 present the electric current variation with time where it is obvious that there is an increase in the current in response to successive additions of the same glucose quantity (0.25mM) in the solution.

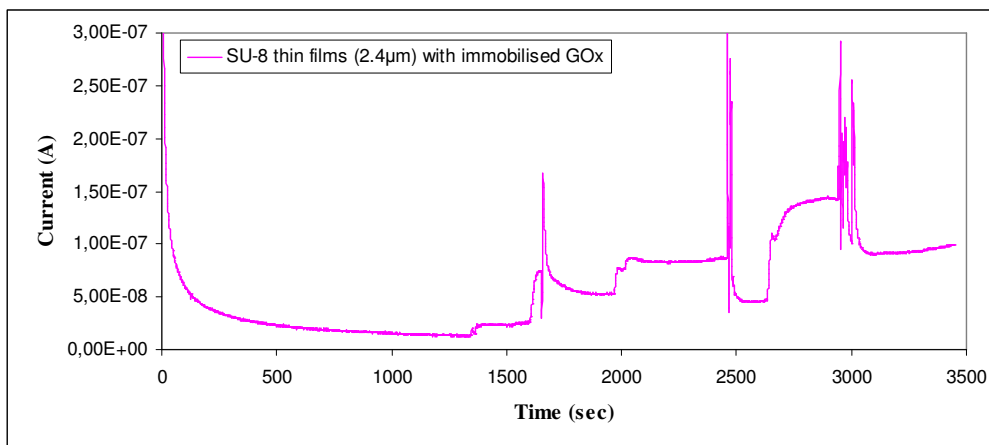


Figure 5.12 *SU-8 films (2.4 μm) with immobilised GOx.*

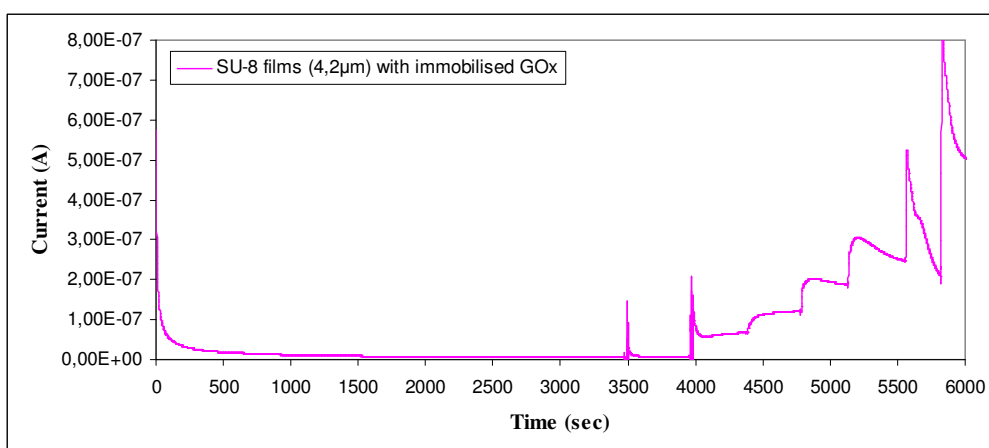


Figure 5.13 *SU-8 films (4.2 μm) with immobilised GOx.*

In addition, the response time reduces and the process becomes slower as the film thickness increases, which indicates that the encapsulated enzyme in the interior matrix of the film also plays a significant role in the process as the reaction products (hydrogen peroxide) inside the porous material move more slowly towards the surface and in the outer region.

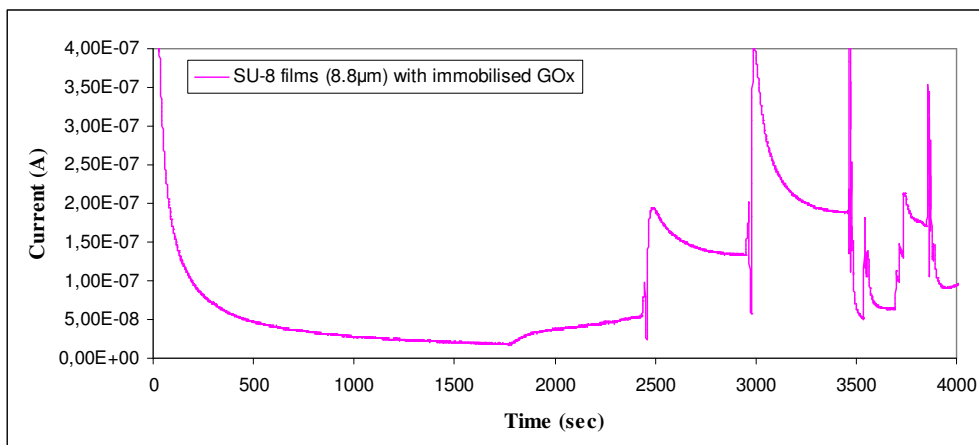


Figure 5.14 *SU-8 films (8.8µm) with immobilised GOx.*

This experimental analysis step proved that the enzyme remains active on the surface and inside the matrix of the SU-8 microfabricated films and the process steps that were followed during the manufacturing process did not deactivate it. Nevertheless, a limited influence on its activity is expected, but it is extremely difficult to be quantified at this stage because of the limited scope of the present research study. In addition, the proposed sensing method can be used in combination with an electrochemical measurement technique and can be combined with the infrastructure of an already existing electrochemical sensor.

5.3.3 Second Experimental Set-up

A second series of tests were performed in a thermostatted vessel at 37°C, in this case with only 500 µl of PBS solution and only one platelet of SU-8 (special care had to be taken in order not to float). The vessel was equipped with a small stirrer bar. A custom made miniaturised 3 electrode cell was immersed in the electrolyte. The cell consisted of a double sided Kapton substrate with 3 electrodes as it is illustrated in Figure 5.15. The total length of the substrate is 23 mm, to the contact pads of the upper part, wires were soldered for further connecting, the electrodes are located at the tip (last mm) of the long lower part (16 mm long and 125 µm wide). The original metal lines were made of gilded copper, passivated with Kapton, platinum was electrodeposited on all 3 electrodes in a post process and the reference electrode was additionally coated with

Ag/AgCl by a galvanostatic method. The dimensions of the working electrode were approximately $300 \times 50 \mu\text{m}$. The working electrode was polarised at +650 mV vs the on-chip Ag/AgCl pseudo-reference electrode.

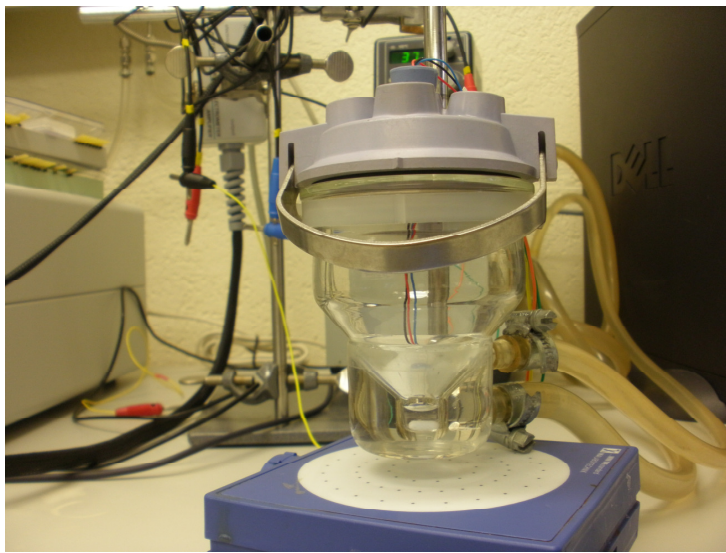


Figure 5.15 Measurement glass cell for the second experimental set-up.

Measurements were performed under constant stirring with intermittent stopping of the stirrer. After approximately 5 to 10 minutes a stable current was established and $5\mu\text{l}$ of a 1M glucose solution was added, resulting in a concentration of approximately 10mM. In case of the enzyme containing platelets, a continuously increasing current was observed. The increase showed a constant slope, during the duration of the measurements (2 hours). Obviously the enzyme is continuously producing hydrogen peroxide that is accumulated in the solution. As measurements are dependent upon stirring speed, stirring was stopped with 6 minute intervals for 2 minutes for taking stir-independent measurements. In Figure 5.16, the variation of electric current with time is presented. The signal was found to decrease and stabilise during these 2 minutes intervals. Restarting of the stirrer (same speed as before) resulted in a signal that could be extrapolated without the turning off of the stirrer.

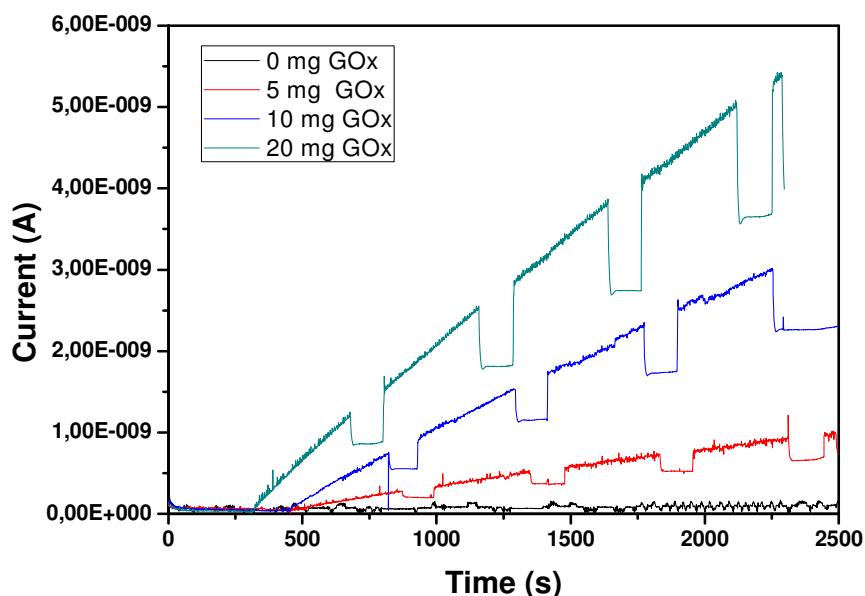


Figure 5.16 Amperometric measurements using SU-8 films with similar thickness and different GOx concentrations. Glucose concentration is increased from 0 to 10 mM in the first part of the graph. Stirring is stopped every 6 minutes.

A different set of experiments were also carried out, using films with immobilised enzyme, of the same standard dimensions but of two different average thicknesses equal to approximately $6\mu\text{m}$ and $9\mu\text{m}$. All other remaining parameters of the microfabrication process remained unchanged. Figure 5.17 presents the electric current variation with time where it is obvious that there is an increase in the current in response to one addition of the same glucose quantity (10mM) in the solution.

In addition, the response time reduces and the process becomes slower as the film thickness increases, which indicates that the encapsulated enzyme in the interior matrix of the film also plays a significant role in the process as the reaction products (hydrogen peroxide) inside the SU-8 matrix move more slowly towards the surface and in the outer region.

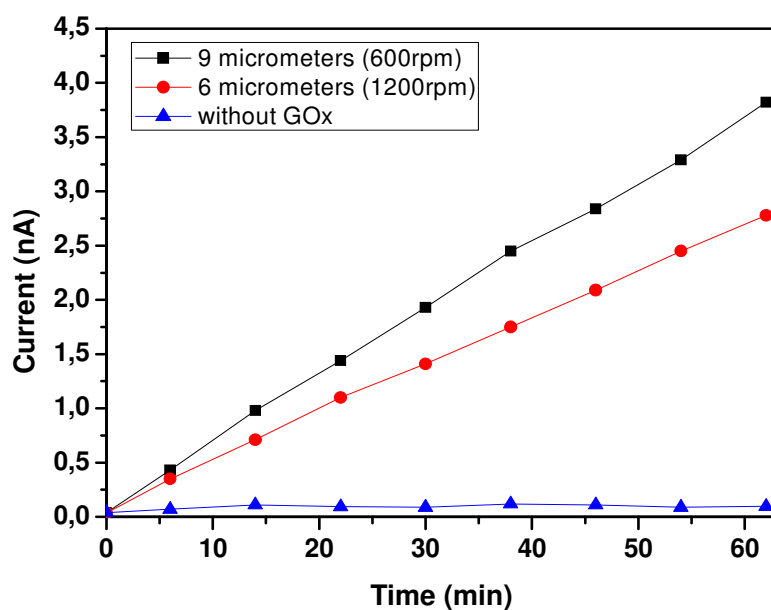


Figure 5.17 Amperometric measurements using SU-8 films with stirring-independent values, effect of SU-8 film's thickness (similar GOx). At $t=0$, 10mM glucose is added.

This experimental analysis step proved that the enzyme remains active not only on the surface but also inside the matrix of the SU-8 microfabricated films and the process steps that were followed during the manufacturing process did not deactivate it. Nevertheless, a limited influence on its activity is expected, but it is extremely difficult to be quantified.

5.4 Fluorescence Intensity Measurements of SU-8 Films with Immobilised Enzyme and Fluorescent Indicator

Fluorescence spectroscopy is used in the field of biosensors as a highly-sensitive optical method using fluorescent indicators dependent in pH changes or oxygen consumption. Specifically, glucose can be measured by monitoring oxygen consumption through the increase in the fluorescence intensity of the oxygen-sensitive fluorescent indicator tris(4,7-diphenyl-1,10-phenanthroline) ruthenium(II) dichloride, and/or by changes in

pH due to gluconic acid with the pH-sensitive fluorescent indicator HPTS. When the ionic strength of the buffer solution is increased then its corresponding fluorescence intensity increases as well, and the opposite take places also. In addition, most optical oxygen biosensors are based on dynamic fluorescence quenching of a suitable indicator resulting in a decrease in luminescence intensity of the biosensor material as a function of the oxygen tension, which means that fluorescence quenching by molecular oxygen reduces the fluorescence intensity (Psoma, 1996).

Specifically, fluorescence spectroscopy experiments were carried out using the SU-8 film matrices in order to assess their suitability as sensing elements for the development of an optical micro-biosensor. Based on the enzymatic oxidation of glucose and the measurement of either the oxygen consumption using an oxygen sensitive indicator or the changes in pH due to the production of gluconic acid with the use of a pH sensitive fluorescence indicator. In the present work, both approaches were attempted. The high transparency of the SU-8 films is a significant advantage when used as a sensing element of an optical detection method.

Two different methods were used in order to entrap the oxygen indicator inside the polymer matrix. The first one involved the use of three different types of surface labelled microspheres with an oxygen sensitive fluorescein indicator (Kurner *et al.*, 2002). More specifically, the following microspheres were used: FITC (fluorescein isothiocyanate) surface labelled microspheres with a mean diameter of 0.21 μ m (green fluorescence: excitation 492nm; emission 519nm), PS FITC surface labelled microspheres with a mean diameter of 0.96 μ m (green fluorescence: excitation 492nm; emission 519nm); and, Rhodamine WT surface labelled microspheres with a mean diameter of 0.87 μ m (red fluorescence: excitation 550nm; emission 590nm). All the aforementioned microspheres were provided in an aqueous solution with a solids concentration of 1% and were added in the SU-8 composition before the microfabrication process. The microspheres were left in ultrasound bath for 15min in order to be separated and then a quantity of 200 μ l was added in the 4ml SU-8 solution.

The second method involved the utilisation of the tris(4,7-diphenyl-1,10-phenanthroline) ruthenium(II) dichloride oxygen sensitive fluorescent indicator

included in the initial SU-8 solution and then the standard microfabrication process carried out (Gillanders *et al.*, 2005; Wencel *et al.*, 2007). The concentration of the oxygen indicator was 10mM in the GBL organic solvent, which was subsequently added in a quantity of 100 μ l to the initial SU-8 solution (4ml).

The results from the experimental work using a fluorescence spectrophotometer showed that only the second method proved to be sensitive to glucose concentration changes during the oxidation reaction whereas the presence of microspheres did not produce any tangible variation in fluorescence intensity other than excessively noisy signals.

In Figure 5.18, the fluorescence spectra of solutions with different added glucose concentrations are presented. In these experiments, a number of 5 standard SU-8 films with encapsulated enzyme were placed in a 1ml quartz cuvette containing phosphate buffer. The enzyme quantity that was added in the 4ml SU-8 solution before the microfabrication process was equal to 10mg of glucose oxidase (141,200 units/g) diluted in 300 μ l of phosphate buffer 10mM, pH7.4. No oxygen indicator was added during the preparation of the microfabricated SU-8 films that were used in the present experiment. From the obtained fluorescence spectra, it is impossible to discern the effect of glucose concentration on the obtained spectra. Although the glucose oxidation takes place, there is no fluorescence detected due to the absence of any fluorescent sensitive indicator. Similar experiments using SU-8 films without immobilised GOx but with the presence of either the oxygen sensitive or the pH indicator inside the microfabricated film, were also carried out. In this case the addition of glucose did not cause any change in the level of the emitted fluorescence intensity proving that there was not any enzymatic activity to cause changes in the oxygen concentration or in the pH of the solution in the cuvette. Blank films without GOx or any indicator were utilised and there was negligible fluorescence which remained unchanged during the addition of glucose in the solution.

The effect of the addition of the oxygen indicator is shown in Figure 5.19 where a clear difference among the spectra can be observed with different glucose concentration. As the reaction takes place, the consumption of available oxygen during the reaction is

proportional to the added glucose concentration and hence it causes an increase in fluorescence intensity of the oxygen sensitive indicator.

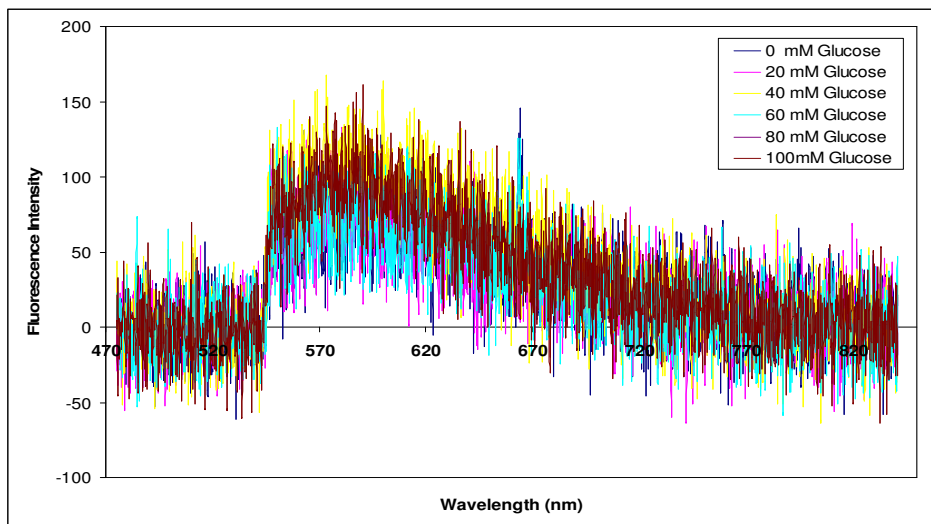


Figure 5.18 Fluorescence spectra using SU-8 films with immobilised GOx only.

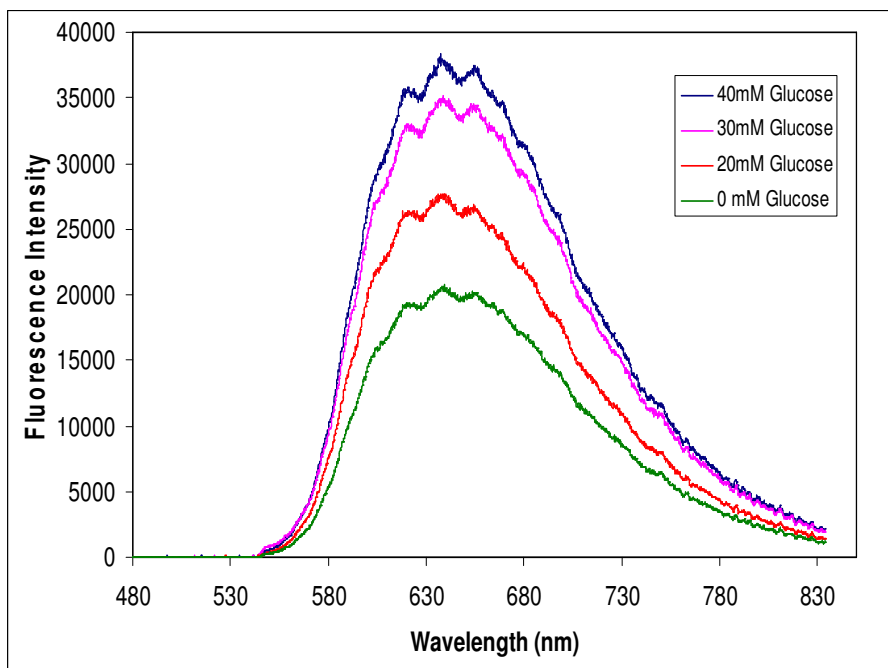


Figure 5.19 Fluorescence spectra using SU-8 films with immobilised GOx and oxygen sensitive fluorescent indicator.

Using an alternative approach to measure glucose concentration through the effect of the produced gluconic acid on pH, the 8-Hydroxypyrene-1,3,6-trisulfonic acid trisodium salt (HPTS) pH sensitive fluorescent indicator was utilized (Schulman *et al.*, 1995; Borisov *et al.*, 2007). The concentration of the added pH sensitive fluorescent indicator was 100 μ M in phosphate buffer 10mM, pH7.4, which was subsequently added in a quantity of 60 μ l to the initial SU-8 solution (4ml).

During the microfabrication process, it was found that the quantity of the phosphate buffer with the HPTS indicator was very critical and any small excess amount above this caused an opaque SU-8 solution with consequent bad lithography results. In Figure 5.20, the effect of adding the above pH indicator is shown. A number of four different concentrations of glucose were used and fluorescence spectra were obtained. With increase in glucose concentration, the produced gluconic acid concentration increases proportionally and this causes an increase in the solution's pH which is reflected in a higher fluorescence intensity from the pH indicator in its acidic form (excitation wavelength 401nm, emission wavelength 510nm).

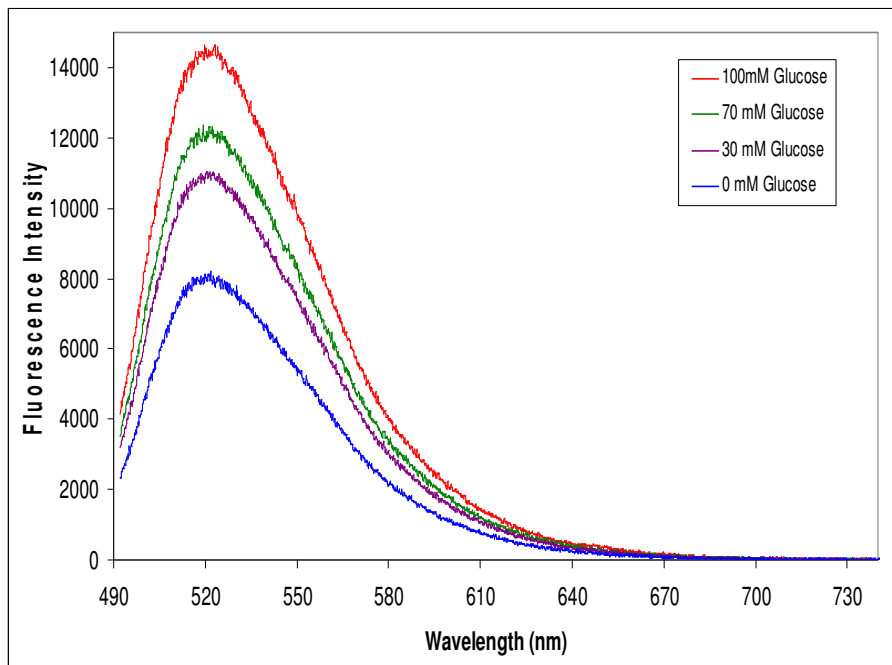


Figure 5.20 Fluorescence spectra using SU-8 films with immobilised GOx and pH indicator.

A set of experiments was performed and fluorescence spectra were obtained from samples including SU-8 films of variable thickness. The SU-8 films were prepared with the standard microfabrication process and included the simultaneous encapsulation of the GOx enzyme and the ruthenium complex as an oxygen sensitive fluorescent indicator. The thicknesses studied are 2.4 μm , 5.5 μm and 8.8 μm and the corresponding fluorescence spectra are presented in Figures 5.21, 5.22 and 5.23 respectively. In all thicknesses used, the added glucose quantity causes a higher oxygen consumption which is indicated by the increase in the fluorescence intensity of the indicator.

The effect of thickness appears to be very important as it is inversely proportional to the level of fluorescence intensity measured; the thinner the film used, the higher the fluorescence intensity measured. This can be attributed to the enzymatic activity caused by the enzyme molecules which are entrapped inside the volume of the film and not only by the ones that are located on its outer surfaces.

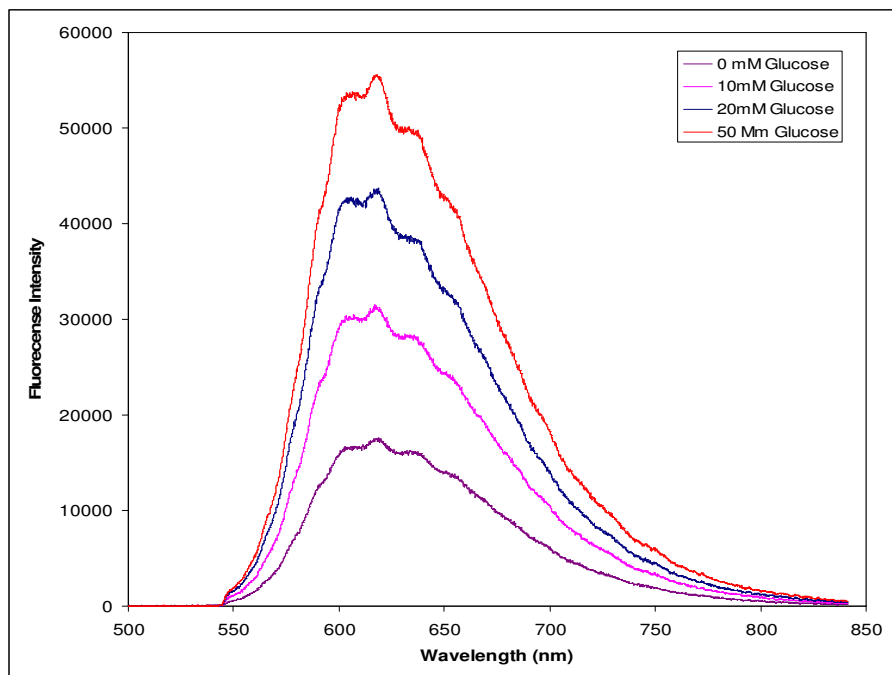


Figure 5.21 Fluorescence spectra using SU-8 films (thickness: 2.4 μm) with immobilised GOx and Oxygen indicator.

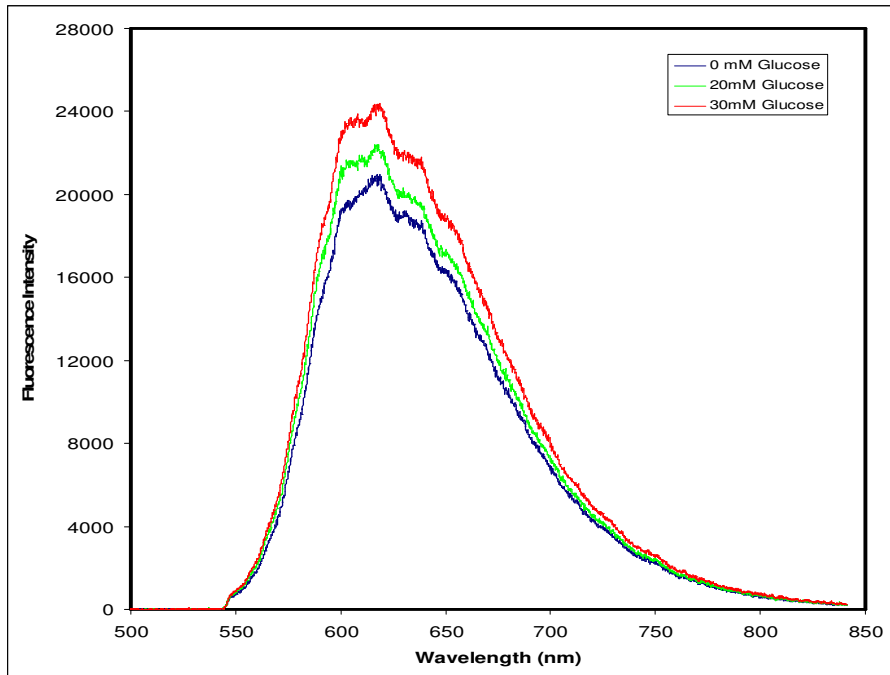


Figure 5.22 Fluorescence spectra using SU-8 films (thickness: 5.5 μm) with immobilised GOx and Oxygen indicator.

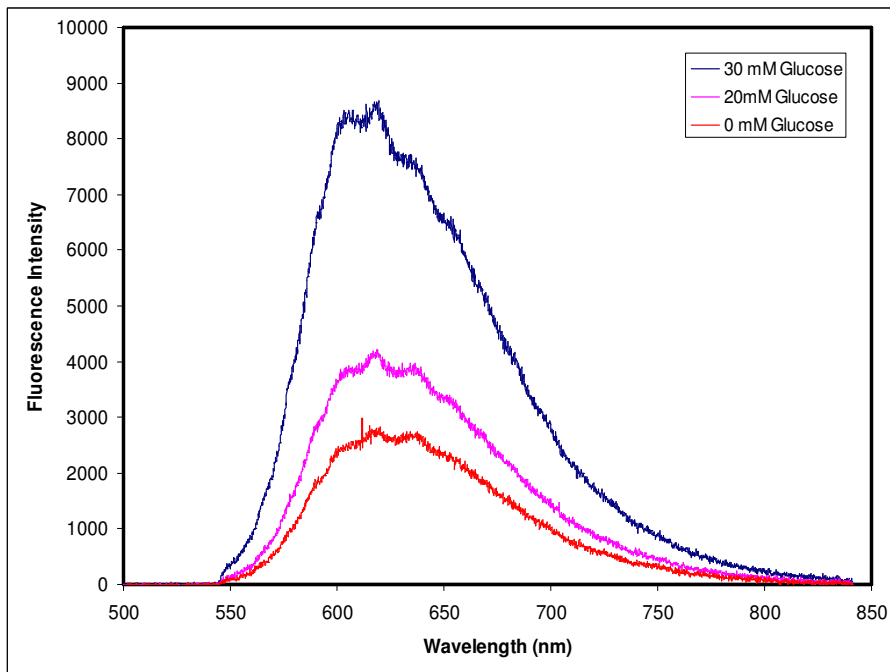


Figure 5.23 Fluorescence spectra using SU-8 films (thickness: 8.8 μm) with immobilised GOx and Oxygen indicator.

From the results presented above, a general conclusion is that the optical measurements proved that the enzyme remains active inside the transparent SU-8 film and the proposed microfabrication process did not damage it. In addition, the oxygen and the pH indicators did not degrade during the microfabrication process and are present inside the SU-8 microfilms.

CHAPTER 6

CONCLUSIONS AND SUGGESTIONS FOR FUTURE WORK

6.1 Conclusions

The present project investigated and proved the concept of developing a novel BioMEMS micro-biosensor using a simple one-step microfabrication process of new polymer matrices with immobilised biomolecules. More specifically, the study focused on the investigation of the suitability of the widely used SU-8 polymer as a matrix for the immobilisation of the enzyme glucose oxidase. The ultimate objective is the utilisation of the above immobilised matrices for the development of an integrated glucose micro-biosensor.

From the literature review that was carried out, it can be concluded that there has been a significant progress in the research field of BioMEMS, which is now a heavily researched area with a wide variety of important biomedical applications. A significant amount of work has been carried out in the application of MEMS technology to biosensors and the adaptation of various types of sensors to *in vivo* diagnostics. Glucose

biosensors, both *in vivo* and *in vitro*, represent the largest biosensor market with continuing research and development efforts for further improvement. One of the most commonly used materials in BioMEMS is the SU-8 polymer which has found a significant number of applications not only as a structural material but as a biocompatible material; and, microfabrication techniques of SU-8 are well-advanced. There is little reported research work in the area of enzyme immobilisation in SU-8 matrices for the development of novel microbiosensors. The use of SU-8 in BioMEMS applications is limited to surface modification of the polymer for immobilisation of biomolecules and efforts of immobilisation of biomolecules entrapped inside and on the surface of SU-8 matrix have not been reported in the current literature.

During this research project, it was identified that it is not possible to utilise the commercially available SU-8 solutions because there is no control of their composition. More specifically, the comparative study between commercially available SU-8 and “customised” SU-8 solutions showed that the optimum percentage of photo-initiator in the solution can be achieved more easily with “customised” SU-8 solutions. Detailed experiments were carried out for the definition of the optimum composition of the SU-8 films.

A study for the control and reduction of the internal mechanical stresses through modification of the chemical composition of the “customised” SU-8 resist, without deterioration of its lithographic properties as compared to conventional SU-8, was carried out. Internal residual stresses occur in SU-8 due to the difference between the thermal expansion coefficients of the resist layer and the substrate. Stress reduction can be obtained by optimising the process parameters as well as by a modification of the chemical composition of the photoresist. The influence of different concentrations of photo-initiator on the residual stresses during the exposure and the post-bake process was studied. The minimum photo-initiator concentration must be at least 2.5% in order to accomplish proper lithography. In addition, during softbake and postbake, a slow warming up and also cooling down procedure using a ramping hot plate, with long relaxation times after post exposure bake was applied in order to improve the stress behaviour of the photoresist.

The investigation for the selection of a sacrificial layer for the removal of the final SU-8 structures from the silicon wafers at the end of the microfabrication process led to the conclusion that the most appropriate sacrificial layer was a dextran solution. The most appropriate type of microstructure for the SU-8 matrix and the corresponding required micro-fabrication process were established through the experimental investigation.

The suitability of the SU-8 polymer as a biocompatible matrix capable of encapsulating biomolecules such as enzymes was proven through the encapsulation of the enzyme GOx in the SU-8 solution. The electrochemical and optical measurements showed that the entrapped enzyme remained active after the micro-fabrication process. In addition, optical fluorescent indicators, such as the oxygen-sensitive ruthenium complex and the pH sensitive HPTS, were included in the matrices. A novel aspect of the present work is that the immobilisation is carried out in parallel with the microfabrication process and not afterwards as a surface modification process.

A detailed investigation was carried out using an electrochemical method in order to check the activity of the enzyme. Testing of immobilised enzyme activity inside the SU-8 matrix, was carried out using amperometric detection of hydrogen peroxide in a 3-electrode setup. SU-8 films were immersed in buffer solutions and the platinum working electrode was brought in close contact with the film. Films without enzyme showed negligible variation in current during the addition of glucose, whereas when films with encapsulated enzyme were utilised, a very clear increase in electric current was consistently observed when glucose was introduced. A significant conclusion from this experiment is that the enzyme remains active not only on the film's surface but inside the matrix as well. A possible explanation could be that the SU-8 film is likely to be porous allowing glucose to diffuse to the interior and approach the immobilised enzyme where oxidation occurs. In addition, hydrogen peroxide is released and diffuses to the surrounding aqueous environment where they are detected with the platinum electrode which is in close proximity to the film surface. A test which was carried out two months after production of the SU-8 films, showed that the enzyme maintained similar levels of activity with the first test which took place the first day.

In the experiments carried out using fluorescence spectroscopy, it was found that the utilisation of the tris(4,7-diphenyl-1,10-phenanthroline)ruthenium(II) dichloride oxygen indicator, which was also captured in the polymer matrix during the microfabrication process, proved to be very sensitive to glucose concentration changes during the oxidation of glucose and did not present any photobleaching. A general conclusion is that the optical measurements proved that the enzyme remains active inside the transparent SU-8 film and the proposed microfabrication process did not damage it. In addition, the oxygen and the pH indicators did not degrade during the microfabrication process and are present inside the SU-8 microfilms.

The effect of thickness appears to be very important as it is inversely proportional to the level of fluorescence intensity measured; the thinner the film used, the higher the fluorescence intensity measured. This can be attributed to the enzymatic activity caused by the enzyme molecules which are entrapped inside the volume of the film and not only by the ones that are located on its outer surfaces.

The above experimental investigations proved that the proposed concept of using SU-8 matrices for the immobilisation of biomolecules, is a valid proposal for the construction, using one-step microfabrication process, of disposable low-cost biosensing elements for the measurement of glucose concentration.

6.2 Suggestions for Future Work

During the research project, different aspects were investigated such as microfabrication process, surface and mechanical properties of SU-8, enzyme immobilisation, electrochemical characterisation, fluorescence spectroscopy analysis etc. As a first step for future work, a number of improvements are proposed in the framework of the above processes in order to improve the functionality of the sensing element and the accuracy of the measurements for assessing its quality.

Regarding the electrochemical measurements, it is proposed to design and construct an electrode where the combination of the SU-8 matrix with the immobilised enzyme will be attached and fixed on the electrode surface. This is expected to provide a more reliable and repeatable measurement system. The main problem with the surface measurement method used in the present study, where loose and very light micro-films were employed in a large solution volume, was the localised effect of the enzyme and the difficulty to touch the electrode on the film's surface which gave rise to repeatability problems. In addition to this, a more uniform environment needs to be guaranteed in the solution through the use of stirring.

As far as the fluorescence spectroscopy measurements are concerned, further investigation is required to include additional reaction kinetics measurements in order to assess the effect of glucose concentration on the reaction rate which can be calculated through the slope of the intensity versus time curve. This consists a much more reliable way forward in order to produce calibration curves.

Further material characterisation measurements are required in order to address an uncertainty that exists related to the level of porosity, the nanostructure and the enzyme distribution in the interior domain of the produced SU-8 films. In the present study, the surface characterisation measurements did not resolve this issue.

The current investigation can form the basis for investigations of other enzymes such as lactate oxidase, polyphenol oxidase etc for different biosensor applications. In addition, other materials such as copolymers could be used instead of SU-8. Copolymers contain more than one type of repeating unit, for example, cyclic olefin copolymers (COCs) are amorphous highly transparent thermoplastics.

The integration of the developed glucose micro-biosensor offers a promising first step for the integration with organic electronics (organic LED and photodetectors) in order to produce an integrated system which can be micromanufactured in the same polymer matrix and can form a basis for the development of the next generation BioMEMS biosensors.

REFERENCES

Abel, PU, von Woedtke, T (2002) Biosensors for in vivo glucose measurement: can we cross the experimental stage. *Biosensors and Bioelectronics* **17**(11-12): 1059-1070.

Abgrall, P, Charlot, S, Fulcrand, R, Paul, L, Boukabache, A, Gue, AM (2008) Low-stress fabrication of 3D polymer free standing structures using lamination of photosensitive films. *Microsystem Technologies-Micro-and Nanosystems-Information Storage and Processing Systems* **14**(8): 1205-1214.

Abgrall, P, Conedera, V, Camon, H, Gue, AM, Nam-Trung, N (2007) SU-8 as a structural material for labs-on-chips and microelectromechanical systems. *Electrophoresis* **28**(24): 4539-4551.

Abgrall, P, Gue, AM (2007) Lab-on-Chip technologies: making a microfluidic network and coupling it into a complete microsystem - a review. *Journal of Micromechanics and Microengineering* **17**(5): R15-R49.

Abgrall, P, Lattes, C, Conederal, V, Dollat, X, Colin, S, Gue, AM (2006) A novel fabrication method of flexible and monolithic 3D microfluidic structures using lamination of SU-8 films. *Journal of Micromechanics and Microengineering* **16**(1): 113-121.

Addae-Mensah, KA, Reiserer, RS, Wikswo, JP (2007) Poly(vinyl alcohol) as a structure release layer for the microfabrication of polymer composite structures. *Journal of Micromechanics and Microengineering* **17**(7): N41-N46.

Ahmad, F, Yusof, APM, Bainbridge, M, Ab Ghani, S (2008) The application of glucose biosensor in studying the effects of insulin and anti-hypertensive drugs towards glucose level in brain striatum. *Biosensors and Bioelectronics* **23**(12): 1862-1868.

Ainslie, KM, Desai, TA (2008) Microfabricated implants for applications in therapeutic delivery, tissue engineering, and biosensing. *Lab on a Chip* **8**(11): 1864-1878.

Albers, J, Grunwald, T, Nebling, E, Piechotta, G, Hintsche, R (2003) Electrical biochip technology - A tool for microarrays and continuous monitoring. *Analytical and Bioanalytical Chemistry* **377**(3): 521-527.

Amberkar, R, Gao, Z, Park, J, Henthorn, D. B., Kim CS (2008) Process development for waveguide chemical sensors with integrated polymeric sensitive layers; USA. SPIE - The International Society for Optical Engineering. pp 68860-68861.

Bashir, R (2004) BioMEMS: State-of-the-art in detection, opportunities and prospects. *Advanced Drug Delivery Reviews* **56**(11): 1565-1586.

Behringer, UFW, Uttamchandani, DG (eds) (2001) Profile control of SU-8 photoresist using different radiation sources. *Conference on MEMS Design, Fabrication, Characterization, and Packaging*; May 30-Jun 01; Edinburgh, Scotland. SPIE-Int Soc Optical Engineering. pp 119-125.

Borisov, SM, Waldhier, MC, Klimant, I, Wolfbeis, OS (2007) Optical carbon dioxide sensors based on silicone-encapsulated room-temperature ionic liquids. *Chemistry of Materials* **19**(25): 6187-6194.

Bower DI (2002) *An Introduction to Polymer Physics*. Cambridge, U.K.: Cambridge University Press.

Byfield, MP, Abuknesha, RA (1994) BIOCHEMICAL ASPECTS OF BIOSENSORS. *Biosensors & Bioelectronics* **9**(4-5): 373-400.

Chang, H-K, Kim, Y-K (2000) UV-LIGA process for high aspect ratio structure using stress barrier and C-shaped etch hole. *Sensors and Actuators A: Physical* **84**(3): 342-350.

Changgeng, Liu, Ling ZG, Lian, K, Goettert, J, Hormes, J (2006) An injection micromixer fabricated by improved SU-8 processing for biochemical microfluidic systems; USA. SPIE - The International Society for Optical Engineering. pp 61120-61121.

Chao, Bian, Sun, J, Qu, L, Xia S (2007) Micro amperometric immunosensor by antibody immobilizing with electropolymerized protein A; USA. SPIE - The International Society for Optical Engineering. pp 68360-68361.

Choi, Y, Choi, SO, Shafer, RH, Allen, MG (2005) Highly inclined electrodeposited metal lines using an excimer laser patterning technique. *Transducers '05, Digest of Technical Papers, Vols 1 and 2*: 1469-1472.

Chuang, H, Arnold, MA (1998) Linear calibration function for optical oxygen sensors based on quenching of ruthenium fluorescence. *Analytica Chimica Acta* **368**(1-2): 83-89.

- Cohen, B, Gadre, A, Kaloyeros, AE (2007) Design, fabrication, and characterization of polymeric BioMEMS for the detection of Feline Immunodeficiency Virus (FIV) - art. no. 643012. *Advanced Biomedical and Clinical Diagnostic Systems V* **6430**: 43012-43012.
- Cosnier, S, Lepellec, A, Guidetti, B, Rico-Lattes, I (1998) Enhancement of biosensor sensitivity in aqueous and organic solvents using a combination of poly(pyrrole-ammonium) and poly(pyrrole-lactobionamide) films as host matrices. *Journal of Electroanalytical Chemistry* **449**(1-2): 165-171.
- Cremers, C, Bouamrane, F, Singleton, L, Schenk, R (2001) SU-8 as resist material for deep X-ray lithography. *Microsystem Technologies* **7**(1): 11-16.
- Dellmann, L, Roth, S, Beuret, C, Paratte, L, Racine, GA, Lorenz, H, Despont, M, Renaud, P, Vettiger, P, de Rooij, N (1998) Two steps micromoulding and photopolymer high-aspect ratio structuring for applications in piezoelectric motor components. *Microsystem Technologies* **4**: 147-150.
- Dellmann, L, Roth, S, Beuret, C, Racine, GA, Lorenz, H, Despont, M, Renaud, P, Vettiger, P, De Rooij, NF (1997) Fabrication process of high aspect ratio elastic structures for piezoelectric motor applications. *Proceedings of the IEEE International Conference on Solid-State Sensors and Actuators (Transducers '97)*; June 1997; Chicago, USA. pp 641-644.
- Dentinger, PM, Clift, WM, Goods, SH (2002) Removal of SU-8 photoresist for thick film applications. *Microelectronic Engineering* **61-62**: 993-1000.
- Dentinger, PM, Krafcik, KL, Simison, KL, Janek, RP, Hachman, J (2002) High aspect ratio patterning with a proximity ultraviolet source. *Microelectronic Engineering* **61-62**: 1001-1007.
- Desai, SP, Taff, BA, Voldman, J (2008) A photopatternable silicone for biological applications. *Langmuir* **24**(2): 575-581.
- Elbuken, C, Gui, L, Ren, CL, Yavuz, M, Kharnese, MB (2008) Design and analysis of a polymeric photo-thermal microactuator. *Sensors and Actuators a-Physical* **147**(1): 292-299.
- Erkan, Y, Czolkos, I, Jesorka, A, Wilhelmsson, LM, Orwar, O (2007) Direct immobilization of cholesteryl-TEG-modified oligonucleotides onto hydrophobic SU-8 surfaces. *Langmuir* **23**(10): 5259-5263.
- Fan, XD, White, IM, Shopoua, SI, Zhu, HY, Suter, JD, Sun, YZ (2008) Sensitive optical biosensors for unlabeled targets: A review. *Analytica Chimica Acta* **620**(1-2): 8-26.
- Feng, XJ, Szaro, BG, Gracias, A, Baselmans, S, Tokranova, N, Xu, B, Castracane, J (2005) Microfabricated devices for bio-applications. *Microfluidics, BioMEMS, and*

Medical Microsystems III **5718**: 13-21.

Fichera, M, Libertino, S, Aiello, V, Scandurra, A, Sinatra, F, Renis, M, Lombardo, S (2007) Glucose oxidase characterization for the fabrication of hybrid microelectronic devices - art. no. 65920T. *Bioengineered and Bioinspired Systems III* **6592**: T5920-T5920.

Gad-el-Hak, M (2006) MEMS applications, ed. Gad-el-Hak, M, CRC Press Taylor and Francis Group, Boca Raton, USA, pp 1-10.

Gadre, A, Di Bari, J (2006) Design and fabrication of a polymeric BioMEMS device for sensing FIV P24 antibodies and FELV P27 antigens in Feline saliva; Piscataway, NJ, USA. IEEE. pp 7-16.

Gelorme JD, Cox RJ, Gutierrez SAR (1989) Photoresist composition and printed circuit boards and packages made therewith. In *United States Patent*, US Patent 4882245. U.S.A.: International Business Machines Corporation (Armonk, NY).

Genolet, G New photoplastic fabrication techniques and devices based on high aspect ratio photoresist. Ph.D. Thesis, Ecole Polytechnique Federale de Lausanne (EPFL), Lausanne, 2001.

Gerritsen, M, Jansen, JA, Lutterman, JA (1999) Performance of subcutaneously implanted glucose sensors for continuous monitoring. *The Netherlands Journal of Medicine* **54**(4): 167-179.

Gillanders, RN, Tedford, MC, Crilly, PJ, Bailey, RT (2005) A composite thin film optical sensor for dissolved oxygen in contaminated aqueous environments. *Analytica Chimica Acta* **545**(2): 189-194.

Giouroudi, I, Kosel, J, Scheffer, C (2008) BioMEMS in diagnostics: A review and recent developments. *Recent Patents on Engineering* **2**(2): 114-121.

Griscom, L, Degenaar, P, LePioufle, B, Tamiya, E, Fujita, H (2001) Cell placement and neural guidance using a three-dimensional microfluidic array. *Japanese Journal of Applied Physics Part 1-Regular Papers Short Notes & Review Papers* **40**(9A): 5485-5490.

Guerin, L, Bossel, M, Demierre, M, Calmes, S, Renaud, P (1997) Simple and low cost fabrication of embedded microchannels by using a new thick-film photoplastic. *Proceedings of the IEEE International Conference on Solid-State Sensors and Actuators (Transducers '97)*; Chicago, USA. pp 1419-1422.

Haque, A, Rokkam, M, De Carlo, AR, Wereley, ST, Wells, HW, McLamb, WT, Roux, SJ, Irazoqui, PP, Porterfield, DM (2006) In silico cell electrophysiology for measuring transcellular calcium currents; USA. SPIE - The International Society for Optical Engineering. pp 638007-638001.

- Henry, C (1998) Getting under the skin: Implantable electrochemical glucose sensors are moving closer to commercialization. *Anal Chem News Features*(SEPT. 1): 594A-598A.
- Hillberg, AL, Brain, KR, Allender, CJ (2005) Molecular imprinted polymer sensors: Implications for therapeutics. *Advanced Drug Delivery Reviews* **57**(12): 1875-1889.
- Hsieh, BY, Chang, YF, Ng, MY, Liu, WC, Lin, CH, Wu, HT, Chou, C (2007) Localized Surface Plasmon Coupled Fluorescence Fiber-Optic Biosensor with Gold Nanoparticles. *Analytical Chemistry* **79**(9): 3487-3493.
- Hulanicki, A, Glab, S, Ingman, F (1991) Chemical sensors: definitions and clasifications. *Pure & Appl.Chem.* **63**(9): 1247-1250.
- Hwang, HS, Song, JT (2007) An effective method to prevent stiction problems using a photoresist sacrificial layer. *Journal of Micromechanics and Microengineering* **17**(2): 245-249.
- Jeykumari, DRS, Narayanan, SS (2008) A novel nanobiocomposite based glucose biosensor using neutral red functionalized carbon nanotubes. *Biosensors & Bioelectronics* **23**(9): 1404-1411.
- Jiang, LN, Gerhardt, KP, Myer, B, Zohar, Y, Pau, S (2008) Evanescent-Wave Spectroscopy Using an SU-8 Waveguide for Rapid Quantitative Detection of Biomolecules. *Journal of Microelectromechanical Systems* **17**(6): 1495-1500.
- Joshi, M, Kale, N, Lal, R, Rao, VR, Mukherji, S (2007) A novel dry method for surface modification of SU-8 for immobilization of biomolecules in Bio-MEMS. *Biosensors & Bioelectronics* **22**(11): 2429-2435.
- Joshi, M, Pinto, R, Rao, VR, Mukherji, S (2007) Silanization and antibody immobilization on SU-8. *Applied Surface Science* **253**(6): 3127-3132.
- Kentsch, J, Breisch, S, Stezle, M (2006) Low temperature adhesion bonding for BioMEMS. *Journal of Micromechanics and Microengineering* **16**(4): 802-807.
- Kim, SJ, Yang, H, Kim, K, Lim, YT, Pyo, HB (2006) Study of SU-8 to make a Ni master-mould: adhesion, sidewall profile, and removal. *Electrophoresis* **27**(16): 3284-3296.
- Konaka, Y, Allen, MG (1996) Single and multi-layer electroplated microaccelerometers. *Proceedings of the IEEE Micro Electro Mechanical Systems (MEMS)*. pp 168-173.
- Kotzar, G, Freas, M, Abel, P, Fleischman, A, Roy, S, Zorman, C, Moran, JM, Melzak, J (2002) Evaluation of MEMS materials of construction for implantable medical devices. *Biomaterials* **23**(13): 2737-2750.

- Kröger, S, Setford, SJ, Turner, APF (1998) Assessment of glucose oxidase behaviour in alcoholic solutions using disposable electrodes. *Analytica Chimica Acta* **368**(3): 219-231.
- Kurner, JM, Wolfbeis, OS, Klimant, I (2002) Homogeneous luminescence decay time-based assay using energy transfer from nanospheres. *Analytical Chemistry* **74**(9): 2151-2156.
- LaBianca, N, Delorme, J (1995) High aspect ratio resist for thick film applications. Allen, R (ed) *Proceedings in SPIE - Advances in Resist Technology and Processing XII*; Bellingham, WA USA. pp 846-852.
- Lechuga, LM, Zinoviev, K, Fernandez, L, Elizalde, J, Hidalgo, OE, Dominguez, C (2009) Biosensing microsystem platforms based on the integration of Si Mach-Zehnder interferometer, microfluidics and grating couplers; USA, SPIE - The International Society for Optical Engineering. pp 7220-7228.
- Lee, DE, Chen, HP, Soper, S, Wang, W (2003) An electrochemical micropump and its application in a DNA mixing and analysis system; Micromachining and Microfabrication. Photonics West, San Jose, California.
- Lee, KY, LaBianca, N, Rishton, SA, Zolgharnain, S, Gelorme, JD, Shaw, J, Chang, THP (1995) Micromachining applications of a high resolution ultrathick photoresist. *Journal of Vacuum Science and Technology B: Microelectronics and Nanometer Structures* **13**(6): 3012-3016.
- Lian, K, Ling, ZG, Liu, CG (2003) Thermal stability of SU-8 fabricated microstructures as a function of photo initiator and exposure doses. *Reliability, Testing, and Characterization of Mems/Moems II* **4980**: 208-212.
- Libertino, S, Fichera, M, Aiello, V, Statello, G, Fiorenza, P, Sinatra, F (2007) Experimental characterization of proteins immobilized on Si-based materials. *Microelectronic Engineering* **84**(3): 468-473.
- Libertino, S, Scandurra, A, Aiello, V, Giannazzo, F, Sinatra, F, Renis, M, Fichera, M (2007) Layer uniformity in glucose oxidase immobilization on SiO₂ surfaces. *Applied Surface Science* **253**: 9116-9123.
- Lin, C, Lee, G, Chang, B, Chang, G (2002) A new fabrication process for ultrathick microfluidic microstructures utilizing SU-8 photoresist. *Journal of Micromechanics and Microengineering* **12**: 590-597.
- Ling, Z, Lian, K, Jian, L (2000) Improved patterning quality of SU-8 microstructures by optimizing the exposure parameters. *Proceedings of the International Society for Optical Engineering (SPIE)*. pp 1019-1027.
- Liu CG (2007) Recent developments in polymer MEMS. *Advanced Materials* **19**: 3783-3790.

- Liu, CG, Ling, ZG, Lian, K, Goettert, J, Hormes, J (2006) An injection micromixer fabricated by improved SU-8 processing for biochemical microfluidic systems - art. no. 61120G. *Microfluidics, BioMEMs, and Medical Microsystems IV* **6112**: G1120-G1120.
- Lorenz, H, Despont, M, Fahrni, N, LaBianca, N, Renaud, P, Vettiger, P (1997) SU-8: A low-cost negative resist for MEMS. *Journal of Micromechanics and Microengineering* **7**(3): 121-124.
- Lorenz, H, Despont, M, Fahrni, N, LaBianca, N, Vettiger, P, Renaud, P (1996) EPON SU-8: A low-cost negative resist for MEMS. *Proceedings of Micro Mechanics Europe'96*; Barcelona. pp 32-35.
- Lorenz, H, Despont, M, Vettiger, P, Renaud, P (1998) Fabrication of photoplastic high-aspect ratio microparts and micromoulds using SU-8 UV resist. *Microsystem Technologies* **4**: 143-146.
- Lorenz, H, Laudon, M, Renaud, P (1998) Mechanical characterization of a new high-aspect-ratio near UV-photoresist. *Microelectronic Engineering* **41-42**: 371-374.
- Lvov, Y, Ariga, K, Ichinose, I, Kunitake, T (1996) Molecular film assembly via layer-by-layer adsorption of oppositely charged macromolecules (linear polymer, protein and clay) and concanavalin A and glycogen. *Thin Solid Films* **284**: 797-801.
- Mata, A, Kim, EJ, Boehm, CA, Fleischman, AJ, Muschler, GF, Roy, S (2009) A three-dimensional scaffold with precise micro-architecture and surface micro-textures. *Biomaterials* **30**(27): 4610-4617.
- McDonagh, C, Burke, CS, MacCraith, BD (2008) Optical chemical sensors. *Chemical Reviews* **108**(2): 400-422.
- Mehrvar, M, Bis, C, Scharer, JM, Moo-Young, M, Luong, JH (2000) Fiber-optic biosensors - Trends and advances. *Analytical Sciences* **16**(7): 677-692.
- Meifang, Lai, Ching Tat, Lai, Keating, A, Dell, J, Yinong, Liu (2008) Cross-flow microfiltration for Lab-on-Chip defatting of human breast milk; USA. SPIE - The International Society for Optical Engineering. pp 72700-72711.
- Moreno, M, Aracil, C, Quero, JM (2008) High-integrated microvalve for Lab-on-Chip biomedical applications; Piscataway, NJ, USA. IEEE. pp 313-316.
- Moser, I (2003) BioMEMs for multi-parameter clinical monitoring. *Microfluidics, Biomems, and Medical Microsystems* **4982**: 144-155.
- Moser, I, Jobst, G, Urban, GA (2002) Biosensor arrays for simultaneous measurement of glucose, lactate, glutamate, and glutamine. *Biosensors and Bioelectronics* **17**(4): 297-302.

- Nakamura, H, Karube, I (2003) Current research activity in biosensors. *Anal. Bioanal. Chem.* **377**: 446-468.
- Nan-Chyuan, T, Chung-Yang, S (2007) Thermal trajectory control for micro RT-PCR biochips. *Microsystem Technologies* **13**(1): 109-115.
- Newman, JD, Turner, APF (eds) (2008) *Historical perspective of biosensor and biochip development*. John Wiley & Sons.
- Newman, JD, Turner, APF (2005) Home blood glucose biosensors: a commercial perspective. *Biosensors & Bioelectronics* **20**(12): 2435-2453.
- Nordstrom, M, Keller, S, Lillemose, M, Johansson, A, Dohn, S, Haefliger, D, Blagoi, G, Havsteen-Jakobsen, M, Boisen, A (2008) SU-8 cantilevers for bio/chemical sensing; Fabrication, characterisation and development of novel read-out methods. *Sensors* **8**(3): 1595-1612.
- O'Brien, J, Hughes, PJ, Brunet, M, O'Neill, B, Alderman, J, Lane, B, O'Riordan, A, O'Driscoll, C (2001) Advanced photoresist technologies for microsystems. *Journal of Micromechanics and Microengineering* **11**(4): 353-358.
- Ozkan, M, Erhan, E, Terzi, O, Tan, I, Ozoner, SK (2009) Thermostable amperometric lactate biosensor with *Clostridium thermocellum* L-LDH for the measurement of blood lactate. *Talanta* **79**(5): 1412-1417.
- Pai, JH, Wang, Y, Salazar, GT, Sims, CE, Bachman, M, Li, GP, Allbritton, NL (2007) Photoresist with low fluorescence for bioanalytical applications. *Analytical Chemistry* **79**: 8774-8780.
- Pan, X, Kan, J, Yuan, L (2004) Polyaniline glucose oxidase biosensor prepared with template process. *Sensors and Actuators B: Chemical* **102**(2): 325-330.
- Patel, JN, Kaminska, B, Gray, BL, Gates, BD (2008) Hybrid polymer fabrication process for electro-enzymatic glucose sensor; USA. SPIE - The International Society for Optical Engineering. pp 68860-68861.
- Perera, M, Nikolau, BJ (2007) *Metabolomics of cuticular waxes: A system for metabolomics analysis of a single tissue-type in a multicellular organism*. Ed. by Nikolau, B. J. Wurtele, E. S Springer: Dordrecht, pp 111-123.
- Pes, DE, Amponsah, EK, Gadre, AP (2008) Wet release of multipolymeric structures with a nanoscale release layer. *Sensors and Actuators B (Chemical)* **132**(2): 426-430.
- Petrou, PS, Moser, I, Jobst, G (2003) Microdevice with integrated dialysis probe and biosensor array for continuous multi-analyte monitoring. *Biosensors and Bioelectronics* **18**(5-6): 613-619.

Piechotta, G, Albers, J, Hintsche, R (2005) Novel micromachined silicon sensor for continuous glucose monitoring. *Biosensors and Bioelectronics* **21**(5): 802-808.

Powers, MA, Koev, ST, Schleunitz, A, Hyunmin, Y, Hodzic, V, Bentley, WE, Payne, GF, Rubloff, GW, Ghodssi, R (2005) Toward a biophotonic MEMS cell sensor; USA. SPIE-Int. Soc. Opt. Eng. pp 119-126.

Powers, MA, Koev, ST, Schleunitz, A, Yi, HM, Hodzic, V, Bentley, WE, Payne, GF, Rubloff, GW, Ghodssi, R (2005) Toward a biophotonic MEMS cell sensor. *Bioengineered and Bioinspired Systems II* **5839**: 119-126.

Psoma SD. Fluorescence-based optical biosensors for clinical and environmental applications. Ph.D. Thesis, Cranfield University, Cranfield, U.K., 1996.

Psoma, SD, Jenkins, DWK (2005) Comparative assessment of different sacrificial materials for releasing SU-8 structures. *Reviews on Advanced Materials Science* **10**(2): 149-155.

Rabarot, M, Bablet, J, Ruty, M, Kipp, M, Chartier, I, Dubarry, C (2003) Thick SU-8 photolithography for BioMEMS. *Micromachining and Microfabrication Process Technology VIII* **4979**: 382-393.

Rahman, AR, Justin, G, Guiseppi-Elie, A (2009) Towards an implantable biochip for glucose and lactate monitoring using microdisc electrode arrays (MDEAs). *Biomedical Microdevices* **11**(1): 75-85.

Rahman, ARA, Justin, G, Guiseppi-Wilson, A, Guiseppi-Elie, A (2009) Fabrication and Packaging of a Dual Sensing Electrochemical Biotransducer for Glucose and Lactate Useful in Intramuscular Physiologic Status Monitoring. *Ieee Sensors Journal* **9**(12): 1856-1863.

Ram, MK, Adami, M, Paddeu, S, Nicolini, C (2000) Nano-assembly of glucose oxidase on the in situ self-assembled films of polypyrrole and its optical, surface and electrochemical characterizations. *Nanotechnology* **11**(2): 112-119.

Reach, G, Wilson, GS (1992) Can continuous glucose monitoring be used for the treatment of diabetes. *Analytical Chemistry* **64**(6): A381-A386.

Rhemrev-Boom, RM, Tiessen, RG, Jonker, AA, Venema, K, Vadgama, P, Korf, J (2002) A lightweight measuring device for the continuous in vivo monitoring of glucose by means of ultraslow microdialysis in combination with a miniaturised flow-through biosensor. *Clinica Chimica Acta* **316**(1-2): 1-10.

Rogers, KR, Mascini, M (1998) Biosensors for field analytical monitoring. *Field Analytical Chemistry and Technology* **2**(6): 317-331.

Rowe, L, Choi, Y, Ross, J, Lee, K, Fogleman, N, Brewer, GJ, Vukasinovic, J, Glezer, A, DeWeerth, SP, Frazier, AB (2007) A fully functional, packaged active microsccaffold

system with fluid perfusion and electrical stimulation/recording functionalities for 3-D neuronal culture studies. *Transducers '07 & Eurosensors Xxi, Digest of Technical Papers, Vols 1 and 2*: U703-U704.

Saliterman, SS (2006) *Fundamentals of BioMEMS and medical microdevices*. Published by SPIE – The International Society for Optical Engineering, Washington, USA, pp107-118.

Schaffar, BPH, Wolfbeis, OS (1990) A fast responding fibre optic glucose biosensor based on an oxygen optrode. *Biosensors and Bioelectronics* **5**(2): 137-148.

Schulman, SG, Chen, SX, Bai, FL, Leiner, MJP, Weis, L, Wolfbeis, OS (1995) Dependence of the fluorescence of immobilised 1-hydroxypyrene-3,6,8-trisulfonate on solution pH – extension of the range of applicability of a pH fluorosensor. *Analytica Chimica Acta* **304**(2): 165-170.

Shang, L, Chen, H, Deng, L, Dong, S (2008) Enhanced resonance light scattering based on biocatalytic growth of gold nanoparticles for biosensors design. *Biosensors and Bioelectronics* **23**(7): 1180-1184.

Shao, G, Wang W (2009) A MEMS flow cytometer with integrated out-of-plane microlens and 3-D hydro-focus unit; USA. SPIE - The International Society for Optical Engineering. p 72070P (72077 pp.).

Shaw, JM, Gelorme, JD, LaBianca, NC, Conley, WE, Holmes, SJ (1997) Negative photoresists for optical lithography. *IBM Journal of Research and Development* **41**(1-2): 81-94.

Tierney, MJ, Tamada, JA, Potts, RO, Jovanovic, L, Garg, S (2001) Clinical evaluation of the GlucoWatch® biographer: a continual, non-invasive glucose monitor for patients with diabetes. *Biosensors and Bioelectronics* **16**(9-12): 621-629.

Turner, APF, (2005) Biosensors and Bioelectronics 20 years on. *Biosensors & Bioelectronics* **20**(12): 2387.

Turner APF, Karube I, Wilson GS (1990) *Biosensors: Fundamentals and Applications*. Oxford, U.K.: Oxford University Press.

Velten, T, Ruf, HH, Barrow, D, Aspragathos, N, Lazarou, P, Jung, E, Malek, CK, Richter, M, Kruckow, J (2005) Packaging of bio-MEMS: Strategies, technologies, and applications. *Ieee Transactions on Advanced Packaging* **28**(4): 533-546.

Vernekar, VN, Cullen, DK, Fogleman, N, Choi, Y, Garcia, AJ, Allen, MG, Brewer, GJ, LaPlaca, MC (2009) SU-8 2000 rendered cytocompatible for neuronal bioMEMS applications. *Journal of Biomedical Materials Research Part A* **89A**(1): 138-151.

Vora, KD, Shew, BY, Harvey, EC, Hayes, JP, Peele, AG (2007) Effect of process parameters and packing density on dimensional errors for densely packed high-aspect-

ratio SU-8 microstructures in x-ray lithography. *Journal of Micro-Nanolithography Mems and Moems* **6**(1) Article Number: 013003.

Vora, KD, Shew, DY, Harvey, EC, Hayes, JP, Peele, AG (2006) Process optimisation for compact, high aspect ratio SU-8 microstructures using x-ray lithography - art. no. 603701. *Device and Process Technologies for Microelectronics, Mems, and Photonics Iv* **6037**: 3701-3701.

Vora, KD, Holland, AS, Ghantasala, MK, Mitchell, A (2004) Patterning of SU-8 resist structures using CF₄. *Device and Process Technologies for Mems, Microelectronics, and Photonics Iii*: 162-172.

Voskerician, G, Shive, MS, Shawgo, RS, von Recum, H, Anderson, JM, Cima, MJ, Langer, R (2003) Biocompatibility and biofouling of MEMS drug delivery devices. *Biomaterials* **24**(11): 1959-1967.

Wang, J (1999) Electroanalysis and biosensors. *Analytical Chemistry* **71**(12).

Wang, P, Tanaka, K, Sugiyama, S, Dai, X, Zhao, X (2009) Wet releasing and stripping SU-8 structures with a nanoscale sacrificial layer. *Microelectronic Engineering* **86**(11): 2232-2235.

Wang, W, Soper, S (eds) (2007) *Bio-MEMS: Technologies and Applications*. CRC Press, Taylor & Francis Group: Boca Raton USA, pp11-42.

Weigl, BH, Holobar, A, Trettnak, W, Klimant, I, Kraus, H, O'Leary, P, Wolfbeis, OS (1994) Optical triple sensor for measuring pH, oxygen and carbon dioxide. *Journal of Biotechnology* **32**(2): 127-138.

Weisenberg, BA, Mooradian, DL (2002) Hemocompatibility of materials used in microelectromechanical systems: Platelet adhesion and morphology in vitro. *Journal of Biomedical Materials Research* **60**(2): 283-291.

Wencel, D, Higgins, C, Klukowska, A, MacCraith, BD, McDonagh, C (2007) Novel sol-gel derived films for luminescence-based oxygen and pH sensing. *Materials Science-Poland* **25**(3): 767-779.

Williams, JD, Wang, W (2004) Study on the postbaking process and the effects on UV lithography of high aspect ratio SU-8 microstructures. *Journal of Microlithography, Microfabrication and Microsystems* **3**(4): 563-568.

Wolfbeis, OS, Oehme, I, Papkovskaya, N, Klimant, I (2000) Sol-gel based glucose biosensors employing optical oxygen transducers, and a method for compensating for variable oxygen background. *Biosensors and Bioelectronics* **15**(1-2): 69-76.

Wu, MH, Huang, SB, Cui, Z, Cui, Z, Lee, GB (2008) Development of perfusion-based micro 3-D cell culture platform and its application for high throughput drug testing. *Sensors & Actuators: B. Chemical* **129**(1): 231-240.

Wu, Z-z, Kisaalita, WS, Zhao, YP, Wang, L, Zhang, L-g (2009) Fabrication of three-dimensional microwell patterns and their integration with human neuroblastoma cells. *Chinese Journal of Sensors and Actuators* **22**(3): 297-302.

Yan, W, Feng, X, Chen, X, Hou, W, Zhu, J-J (2008) A super highly sensitive glucose biosensor based on Au nanoparticles-AgCl@polyaniline hybrid material. *Biosensors and Bioelectronics* **23**(7): 925-931.

Yang, R, Wang, W (2005) Application of optical refractive index liquid and wavelength selection for ultra-high-aspect-ratio UV-lithography of thick SU-8 resist. *Sensor and Actuator B: Chemical* **110**(2): 279-288.

Yun, YH, Dong, Z, Shanov, VN, Bange, A, Heineman, WR, Halsall, HB, Conforti, L, Bhattacharya, A, Schulz, MJ (2007) On-line carbon nanotube-based biosensors in microfluidic channels; USA. SPIE - The International Society for Optical Engineering. pp 65210-65215.

Yoon, SI, Park, SC, Kim, YJ (2008) A micromachined microcalorimeter with split-flow microchannel for biochemical sensing applications. *Sensors and Actuators B (Chemical)* **134**(1): 158-165.

Zhang, J, Tan, KL, Hong, GD, Yang, LJ, Gong, HQ (2001) Polymerization optimization of SU-8 photoresist and its applications in microfluidic systems and MEMS. *Journal of Micromechanics and Microengineering* **11**(1): 20-26.

Zhong, ZW, Wang, ZF, Zirajutheen, BMP, Tan, YS, Tan, YH (2005) CMP of PC, PMMA and SU-8 polymers. *Polytronic 2005, Proceedings*: 58-62.

******* END OF THESIS *******

